DOI: 10.1002/anie.201100944

Mixed-Valence Compounds

Organic Mixed-Valence Compounds: A Playground for Electrons and Holes

*Alexander Heckmann and Christoph Lambert**

Keywords:
electron transfer · Marcus theory · mixed valence · redox processes · π systems

Dedicated to Professor Siegfried Hünig on the occasion of his 90th birthday

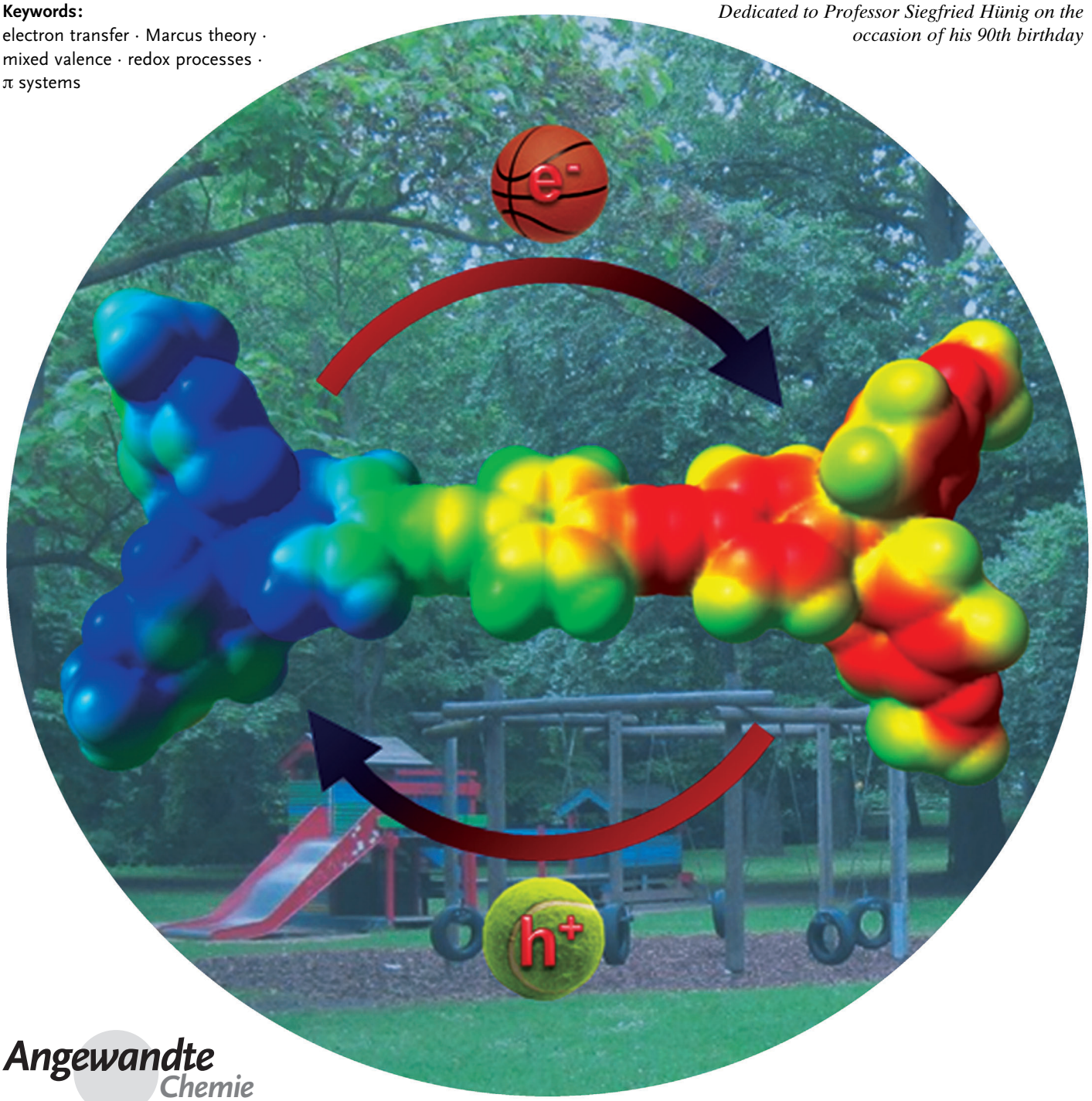

Mixed-valence (MV) compounds are excellent model systems for the investigation of basic electron-transfer (ET) or charge-transfer (CT) phenomena. These issues are important in complex biophysical processes such as photosynthesis as well as in artificial electronic devices that are based on organic conjugated materials. Organic MV compounds are effective hole-transporting materials in organic light emitting diodes (OLEDs), solar cells, and photochromic windows. However, the importance of organic mixed-valence chemistry should not be seen in terms of the direct applicability of these species but the wealth of knowledge about ET phenomena that has been gained through their study. The great variety of organic redox centers and spacer moieties that may be combined in MV systems as well as the ongoing refinement of ET theories and methods of investigation prompted enormous interest in organic MV compounds in the last decades and show the huge potential of this class of compounds. The goal of this Review is to give an overview of the last decade in organic mixed valence chemistry and to elucidate its impact on modern functional materials chemistry.

From the Contents

1. Introduction

What is a mixed-valence (MV) compound? Are MV compounds synonymous with donor–acceptor (D-A) compounds? These questions seem to be trivial as they are fundamental, but in fact it is not easy to give a straightforward answer, not least because no clear definition for MV compounds can be found in the literature, particularly not with regard to a differentiation to the term donor–acceptor compound. To solve this problem we have to consider the similarities of these two classes of systems: both consist of two or more redox centers, with one acting as an electron donor and the other one as an electron acceptor. In both MV compounds and donor–acceptor compounds an electron (ET) or charge transfer (CT; here defined as a partial electron transfer which gives rise to an optical absorption band)[1] can take place between the donor and acceptor moieties. This charge transfer can be induced optically, that is, by direct excitation into a CT band. The only distinguishing feature is that organic MV compounds are always open-shell systems, while donor–acceptor compounds are closed-shell systems in the ground state. Three examples of organic MV compounds **A**,[2] **B**,[3] and **C**[4] and two typical organic donor–acceptor compounds **D**[5] and **E**[6] are shown in Scheme 1 to illustrate the similarities and differences. All the compounds **A**–**E** consist of a donor (blue) and an acceptor moiety (red) as well as a bridging unit (green) connecting the redox centers. The issue of how to discriminate between the redox centers and bridge will be addressed below. In all of the compounds an ET can take place (black arrow), which may either result in another electronic ground-state structure (**A**, **B**, and possibly **C**) with altered charge (and spin) distribution or in an electronically excited state (right-hand side) in **D** and **E**. However, MV systems **A**, **B**, and **C** are open-shell systems, both in the ground state and in any other electronically excited state: radical cations **A**, radical anions **B**, or neutral open shell systems **C**. In contrast, donor–acceptor compounds are neutral (**D**) or charged (**E**) closed-shell systems in the ground state. Those electronically excited states that are accessible by optical excitation are then singlet states (although configuration mixing with other states induced by, for example, spin–orbit coupling may blur the spin multiplicity in some cases). Thus, it appears to us to be useful to define MV compounds as being a subclass of donor–acceptor compounds that possess an open-shell ground state. It is noteworthy that both classes can only rigorously be distinguished in terms of the spin multiplicity of the ground state but not in terms of the excited state, which can be open shell in both classes. However, we have to keep in mind that this definition is only strictly applicable to purely organic MV compounds. A general definition of MV compounds, including those containing metal centers cannot be based on the presence of unpaired electrons because transition-metal complexes may adopt high-spin states irrespective of whether the total number of electrons is even or odd and the oxidation state. Thus, these inorganic compounds are termed MV systems when they are built up of two or more metal redox centers in different formal oxidation states. The metals may then differ by ≥ 1 in their oxidation numbers as in, for example, low-spin Fe^{II}-Co^{III} complexes, although such complexes may be closed shell.[7] Hence, a clear differentiation of inorganic MV compounds to inorganic donor–acceptor compounds is not possible in the same way as given above for organic MV compounds. While we have now found a working definition for organic MV systems, it remains to be determined whether the discrimination between MV

[*] Dipl.-Chem. A. Heckmann, Prof. Dr. C. Lambert
Institut für Organische Chemie, Universität Würzburg
Am Hubland, 97074 Würzburg (Germany)
and
Wilhelm-Conrad-Röntgen Research Center for Complex Material Systems (RCCM) Würzburg (Germany)
E-mail: christoph.Lambert@uni-wuerzburg.de

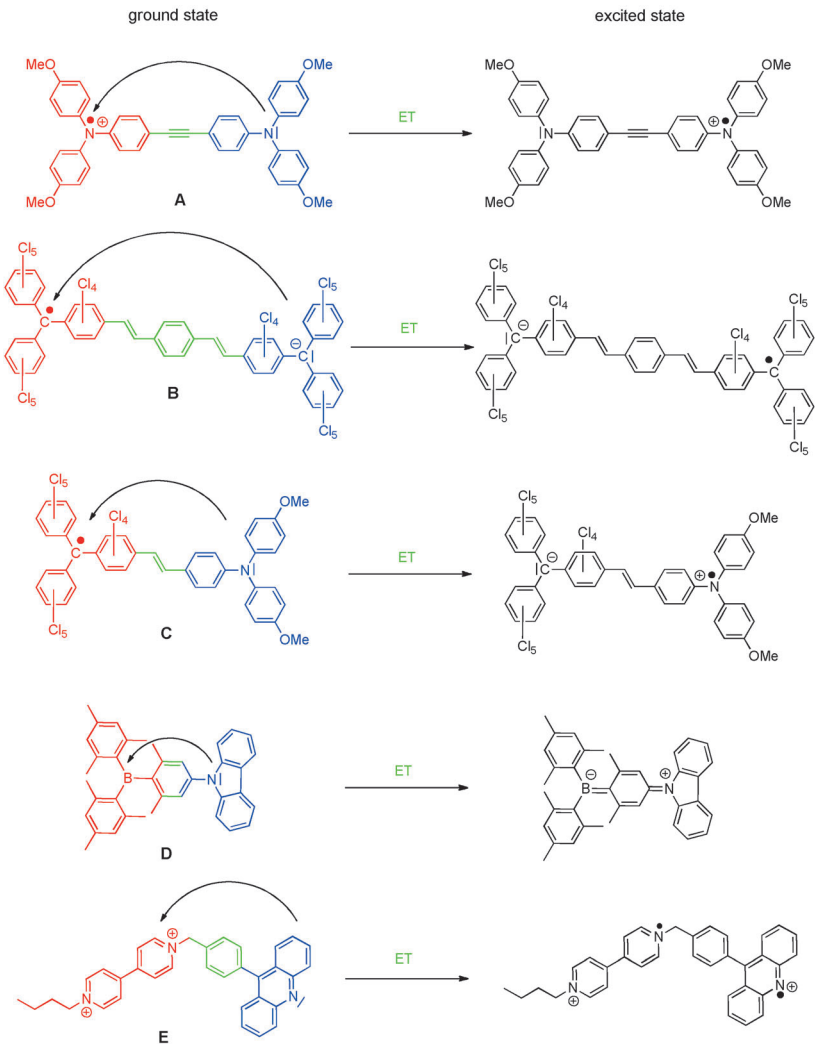

Scheme 1. Examples demonstrating the key difference between organic MV compounds **A**–**C** and organic donor–acceptor compounds **D** and **E**. The former are always open-shell systems in the electronic ground state (left-hand side), while the latter ones are closed-shell systems. Donor moieties are shown in blue, acceptors in red, and bridge units in green.

and donor–acceptor compounds will be of any help for a better understanding of their physical and chemical properties.

The term "mixed-valence" compound is closely related to its most-prominent representative, the inorganic Creutz–Taube ion **F**, which was first

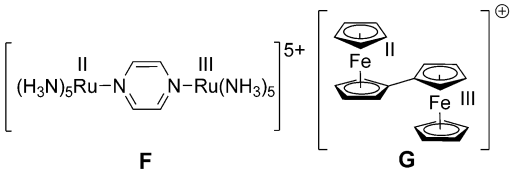

reported in 1969,[8,9] although much earlier examples of MV systems were known. In fact, it was in 1958 when the term "mixed-valence complex" was used for the first time by Klotz et al.[10] to describe a Cu^{I}/Cu^{II} complex. MV solid-state pigments such as Prussian Blue ($Fe^{III}[Fe^{III}Fe^{II}(CN)_6]_3$) were known since 1704.[11] In the Creutz–Taube complex, two ruthenium centers with different oxidation states are connected by a pyrazine bridge. While it is clear that this complex may be used to investigate the ET of the "extra" charge (= the charge difference between both metal centers) between the two ruthenium centers, there is evidence from later investigations that in fact the oxidation number of the ruthenium centers are averaged, and the "extra" charge is "almost" or fully delocalized over the two centers and the bridge.[12–17] Nearly concurrently, Cowan et al. synthesized the first of a series of organometallic MV compounds **G**, where ferrocene redox centers were directly linked at the cyclopentadienyl moieties.[18–20] The Creutz–Taube ion initiated both the syntheses and the physicochemical investigations of thousands of inorganic MV compounds, as well as the development of suitable ET theories.[21–29] In 1990, Reimers and Hush showed that by replacing the pyrazine ligand by vinylogues in **F** leads to the "extra" charge being localized at one ruthenium center.[30] Thus, the question of "localized" versus "delocalized" is an issue of general and utmost importance for MV compounds. As outlined in more detail in Section 2.4, one can classify MV compounds according to the delocalization/localization of charge into three classes:[31] Class I, in which the redox centers do not interact with each other. In

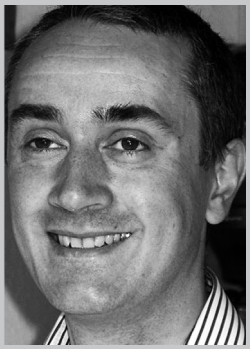

Christoph Lambert obtained his PhD with P. von R. Schleyer at the University of Erlangen-Nürnberg (Germany) in 1993. After postdoctoral research with R. Snaith at the University of Cambridge (UK) he moved to the University of Regensburg in 1994 and completed his habilitation in organic chemisty in 1998. In 1999 he became Associate Professor at the Institute of Organic Chemistry, Würzburg, and since 2010 he has been Full Professor of physical organic chemistry. His interests cover—besides mixed-valence chemistry—all kinds of electron-transfer phenomena at interfaces, in molecules, in covalently bound aggregates, and in polymers.

Alexander Heckmann studied chemistry at the University of Würzburg. He obtained his diploma in 2004 and worked in the group of C. Lambert until 2009 on neutral mixed-valence compounds.

practice, this class refers to species where the interaction of redox centers is too small to be measurable. Class II refers to weakly interacting redox centers and with the "extra" charge localized at one of the redox centers. Finally, in class III the interaction is so strong that the charge is delocalized over the whole system. In a strict sense, the term "mixed valence" only makes sense for class II systems. This will be more apparent if we consider organic MV compounds.

By definition, in organic MV compounds the metal redox centers are replaced by purely organic (nonmetal) redox centers. The first compounds directly synthesized on this basis and compared to their inorganic and organometallic analogues were radical cations of the tetrathiafulvalene type. In the literature, radical cation **H**—synthesized by Wudl et al.[32–34] in 1970—is sometimes regarded as the first purely organic MV compound, although the positive charge is delocalized over the whole system. However, in fact many earlier examples of organic radical ions are known that may

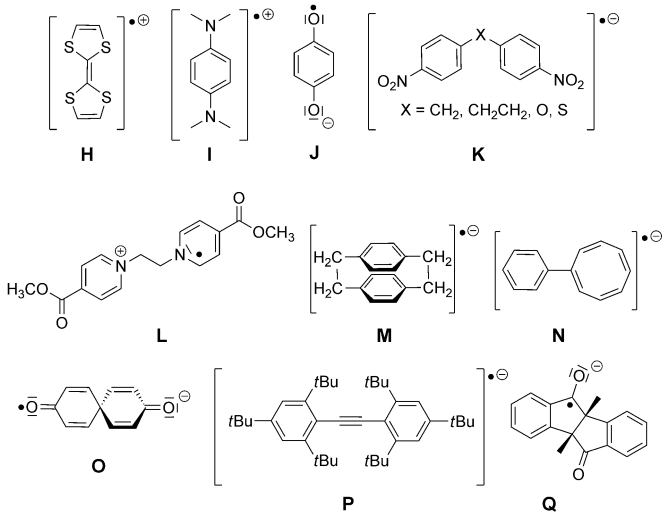

be mixed valent.[35] In 1879, Wurster already described *N*,*N*,*N*′,*N*′-tetramethyl-*para*-phenylenediamine **I**, but this also forms a delocalized radical cation.[36–38] Clearly, the temptation to consider these radical cations as MV systems stems from the fact that we can identify two moieties (dithiacyclopentenylidene and dimethylamine, respectively) which may act as redox centers in these systems. It is even harder to do this with *para*-quinone radical anions (e.g. **J**), and most chemists will hesitate to name the oxygen atoms as being the redox centers. It is thus apparent that for small delocalized systems, where it is arbitrary or even impossible to identify redox centers, it is in many cases not useful to talk about MV compounds. In fact the term "charge-resonance" compound is sometimes used to describe these systems.[39] We leave it to the reader to come to his own opinion about this semantic problem. In this Review, we will simply treat delocalized systems which are borderline cases as "delocalized MV compounds".

This topic brings us now to the problem of discerning between "redox centers" and "bridges" in MV systems. While in **A** it seems clear to assign the triarylamine moiety as the "redox center" and the triple bond as the bridge, it is difficult to do that in, for example, **H**, **I**, or **J**. In fact, strong electronic interaction (such as in systems at the boundary between classes II and III or even in purely class III systems) between the redox centers and the bridge will obscure this discrimination. At least we can define the "redox center" in class II systems to be the moiety within a MV compound that shows spectroscopic properties closely resembling those of the isolated redox moiety in either redox state. By this definition, we anticipate that class II compounds will show spectroscopic properties (mostly electronic absorption) as the sum of those of the isolated redox centers (oxidized and reduced) plus that of the bridge as well as those features that arise from the interaction of these moieties.

The earliest studies on organic MV radical ions date back to the 1950s when organic radical cations and anions were mainly investigated in detail by electron-spin resonance (ESR) measurements. However, the compounds studied in those days were not termed MV compounds, even though these early studies focused on the question of delocalization or localization of spin density and, consequently, on the extent of charge delocalization in these radical ions. In this regard, the ESR investigations of bis(*p*-nitrophenyl) radical anions of type **K**[40] and the studies of pyridyl radical cations (e.g. **L**) by Itoh[41] and of tetraalkylhydrazines by Nelsen et al.[42] should be mentioned in particular. Furthermore, ESR investigations on the spin-density distribution of the radical anions of paracyclophane derivatives[43–45] (e.g. **M**), phenylcyclooctatetraene[46] **N**, spirodienones[47] (e.g. **O**), hexa-*tert*-butyldiphenylacetylene[48] **P**, and *cis*-10,11-dimethyldiphensuccindan-9,12-dione[49] **Q** showed the charge to be localized, for example, in **L**, **O**, and **Q** and delocalized in, for example, **M** and **P** on the ESR time scale. However, the term "MV compound," which was employed for the first time in inorganic chemistry in 1958, was not used for the organic analogues until the 1980s.[50] Thus, this first period of organic MV chemistry until the 1980s was mostly dominated by ESR investigations and theoretical calculations of spin delocalization; MV chemistry in general was still a typical domain of inorganic chemical research.

This situation changed dramatically in the 1990s when the spectroscopic analysis of the so-called intervalence charge-transfer (IV-CT) bands in the context of Marcus–Hush theory was applied to organic MV compounds.[51,52] The IV-CT band was observed in most inorganic MV compounds and attributed to an optically induced charge transfer from one redox center to the other. Hush's analysis of this absorption band to gain information about electronic couplings has become, and still is, quite popular. From a practical point of view, organic MV compounds are well-suited for an analysis of these characteristic IV-CT bands because they usually appear in the near-infrared (NIR) region and, unlike in inorganic MV complexes, are often not overlapped by other transitions. In many inorganic MV systems IV-CT bands are weak and/or often obscured by ligand–metal charge-transfer (LMCT) or metal–ligand charge-transfer (MLCT) bands, which render an IV-CT band analysis more difficult.

One of the main impulses for the growing interest in organic MV compounds was driven by the ambition to design

molecular or polymer electronic devices that are based on small molecular π systems or conjugated polymers. In addition, the immense potential of (organic) MV compounds to mimic key steps in the even more complex ET reactions in nature (e.g. photosynthesis)[24,53–60] was recognized, and the requirement for a detailed understanding of ET processes prompted chemists to synthesize various organic MV systems whose ET behavior was studied extensively (especially by spectroscopic methods). This process was supported additionally by continuous refinement of ET theories. In particular, the influence of the type and length of the spacer (bridge) unit, the effect of temperature, solvent effects, or counterions on the ET processes were the focus of the investigations.

In this Review we intend to provide an overview of this rapidly emerging and developing topic of modern physical organic chemistry. Although inorganic MV compounds have been reviewed many times before[21,27,61,62] organic MV compounds have not been addressed as such in reviews.[326] We do not intend to give a comprehensive overview about organic MV compounds, but will instead concentrate on some families of very prominent types which allow structure property relationships to be developed in a more systematic way. Even though many theoretical ET models were discussed in detail previously in some reviews,[17,23,26,28,29,61,63–67] we will outline the most common and most important ET theories to provide the reader with a basic knowledge for a better understanding of this topic (Section 2). In Section 3 we give an overview about those types of organic MV compounds that are currently at the focus of interest and in the last section we address some possible practical applications of MV compounds.

2. Basic Aspects of ET Theories

In this section we briefly outline the basic ideas and concepts for a quantitative treatment of ET reactions in MV systems to provide the uninformed reader with the theoretical background necessary to understand the outcome of the numerous studies which will be highlighted in Section 3.

2.1. Marcus Theory—A Diabatic Treatment

In the 1950s Marcus developed the first fundamental and generally accepted quantitative description of ET reactions in solution.[68,69] Originally, this theory was based on investigations of "self-exchange reactions" and "cross-reactions"[70] of metal ions in solution, but the general concept also proved to be applicable to intramolecular ET process in inorganic and organic MV systems.

In the framework of Marcus theory[24,66,71,72] the free-energy surfaces (FES) of a MV system with two redox centers can be reduced to two diabatic (formally non-interacting) one-dimensional parabolic (harmonic) profiles along a dimensionless reaction coordinate x.[73] One potential represents the reactant (A) and the other the product state (B) after the ET process has taken place. In Figure 1 the two possible ET pathways are shown: First, thermally induced ET along the reaction coordinate x from the free-energy minimum of state A to the free-energy minimum of state B with the free activation energy ΔG^* and, second, optically induced ET (i.e. a process initiated by absorption of a photon which directly leads to charge transfer as opposed to "photo-induced," in which an initial state is prepared by photoexcitation which then relaxes into a charge-separated excited state) which leads through vertical excitation (following the Franck–Condon principle) from the minimum of the reactant state A to the product surface of state B. The energy needed for this optically induced ET is called Marcus reorganization energy λ. In the harmonic approximation, twice the reorganization energy divided by the square of the length dimension equals the force constant of the harmonic oscillator. Two parameters contribute to λ: the solvent reorganization energy λ_o, which considers the reorientation of the solvent molecules after ET has taken place, and the inner reorganization energy λ_v, which represents the changes of bond lengths and bond angles at the redox centers while changing their oxidation states (see also Figure 1). Although the changes in the molecular geometry of inorganic MV compounds are often identified with metal–ligand bonds, the situation is much more complicated in organic MV systems, where the charge is delocalized over more atom centers (mostly π systems) rather than localized at a specific atom.

Concerning the redox centers, two different types of MV compounds can be discerned: degenerate MV compounds,

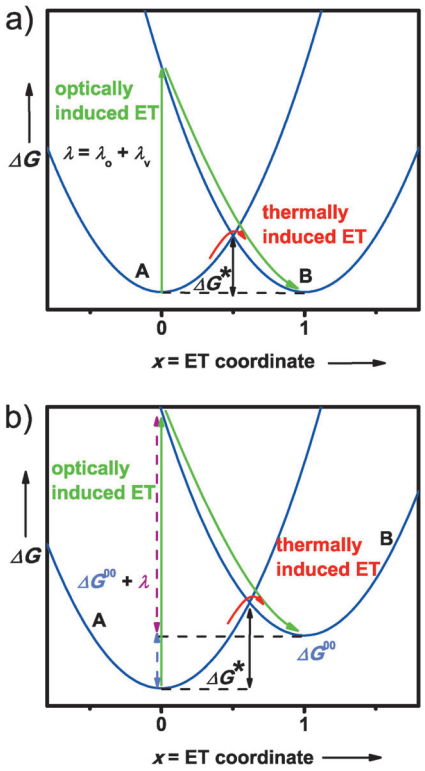

Figure 1. Diabatic free energy surfaces (blue lines) of a MV compound with a) degenerate MV states and b) nondegenerate MV states, and the two possible pathways for ET: Optically induced ET (green) and thermally induced ET (red).

where both redox centers are identical, and thus, reactant and product states are degenerate (Figure 1a), and so-called nondegenerate MV systems, where the two redox centers differ and the two MV states are nondegenerate (Figure 1b). In the latter, there is a free-energy difference ΔG^{00} between the states A and B and, as can be seen from Figure 1b, the energy needed for an optically induced ET corresponds to the sum of the Marcus reorganization energy λ and ΔG^{00}.

On a molecular level, thermally and optically induced charge-transfer (CT) reactions can also be depicted by a straightforward model (Scheme 2): Before the CT event the

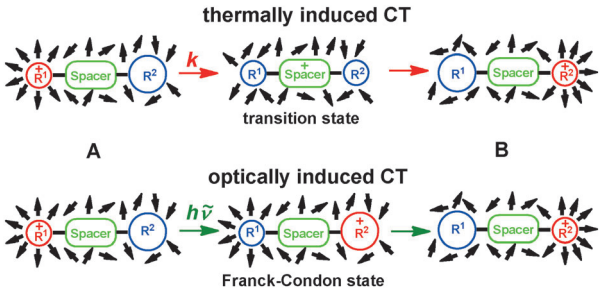

Scheme 2. Reaction pathways of thermally and optically induced CT reactions of a MV compound with two identical redox centers R^1 and R^2. The black arrows represent the solvent dipoles. The size of the redox centers represents changes in the geometry in different redox states.

charge is localized on the redox center R^1 and the solvent dipoles are systematically oriented around this redox center to stabilize the charge (in state A). As a consequence of the weaker interaction, the second, neutral redox center R^2 is surrounded by solvent molecules in a more disordered way. Both redox centers have different geometries (bond lengths and angles), as symbolized by the different sizes of the circles. After the CT event, the charge is localized on redox center R^2 (in product state B) and the total geometric and electronic situation is a mirror image of the reactant state. The main difference between thermally and optically induced CT refers to the states between the reactant and product states. In the thermally induced CT, the charge-transfer event in the MV system is induced by thermal fluctuations and collisions of solvent molecules. Both the geometries of the two redox centers (associated with the inner reorganization energy λ_v) change and the solvent molecules reorient (associated with λ_o) at the same time along the free-energy surfaces while passing a transition state with a free energy of activation ΔG^*. The total free energy of the system is kept constant by thermal equilibration with the solvent bath. In contrast, the optically induced CT leads to (partial) electron transfer before the solvent as well as the geometry of the redox centers can respond to the new situation (according to the Franck–Condon principle). Hence, the free energy of $\lambda_o + \lambda_v$ ($+ \Delta G^{00}$ in the nondegenerate case) is necessary for the optical excitation, after which the molecule and the surrounding solvent relax (see Figure 1).

While the inner reorganization energy is an intrinsic parameter of each MV system and hence cannot be calculated in a straightforward manner, Marcus showed that the outer-sphere reorganization energy λ_o can be calculated by using a dielectric continuum model. In the context of this model, the donor and acceptor redox centers are assumed to have spherical geometries with the radii r_1 and r_2 and a center to center distance of r_{12}. The solvent reorganization energy can then be calculated by Eq. (1), where n is the index of refraction and D is the permittivity of the solvent.[68,74]

$$\lambda_o = \frac{e^2}{4\pi\varepsilon_0}\left[\frac{1}{2r_1}+\frac{1}{2r_2}-\frac{1}{r_{12}}\right]\left[\frac{1}{n^2}-\frac{1}{D}\right] \tag{1}$$

In Marcus theory the rate constant k of ET (CT)[1] is given by an Arrhenius-type Equation [Eq. (2)], where k_B is the Boltzmann constant, T is the temperature, and ΔG^* is the free energy of activation needed for the thermally induced ET transfer. The factor A again depends on the nuclear motion frequency through the transition state ($\nu_n \approx 10^{13}\ s^{-1}$) and on the electron transmission coefficient κ_{el}, which is unity in the classical treatment.

$$k = A\exp\left(\frac{-\Delta G^*}{k_B T}\right) \quad \text{with} \quad A = \nu_n \kappa_{el} \tag{2}$$

Within a classical treatment, the diabatic free energy surfaces A and B are parabolas with identical λ values, hence it follows by a simple algebraic analysis that ΔG^* can be calculated by Equation (3).

$$\Delta G^* = \frac{(\lambda + \Delta G^{00})^2}{4\lambda} \tag{3}$$

The combination of Equations (2) and (3) yields the well-known Marcus Equation of thermally induced ET [Eq. (4)].

$$k = A\exp\left(-\frac{(\lambda + \Delta G^{00})^2}{4\lambda k_B T}\right) \tag{4}$$

It should be remembered that the classical Marcus theory represents a purely diabatic theory with the assumption that the electronic coupling V, which is a measure of the electronic communication between reactant and product states, is small compared to the thermal energy $k_B T$. Since an electronic coupling is a general precondition in MV compounds, Marcus theory, similar to any other diabatic theory, is only applicable to MV compounds with only a small electronic interaction (coupling). Nevertheless, classical Marcus theory is often used to treat kinetic ET problems in MV compounds.

The most famous prediction which directly stems from the classical Marcus theory is the presence of a so-called Marcus-inverted region,[75,76] which means that the rate of an ET reaction becomes slower for very exergonic reactions. While this prediction is often found for back electron transfer after a photoinduced (in contrast to optically induced, see above) forward electron transfer, it usually plays no role in MV systems (for an exception, see Section 3.5) and is, thus, not treated further here.

2.2. Marcus–Hush Theory/Mulliken–Hush Theory—An Adiabatic Treatment

The Marcus–Hush theory[23,77,78] extends classical Marcus theory and allows the analysis of MV systems in which the electronic communication between the donor and acceptor moieties (which is a necessary requirement for intramolecular ET or CT) is large compared to the thermal energy $k_B T$. In these cases, an adiabatic theory which takes this effect into account is required. The magnitude of the interaction is quantified by the electronic coupling V. Furthermore, Hush formulated pioneering equations that allow the calculation of this electronic coupling by analysis of the absorption spectra of MV compounds.[66,67] The basis of this procedure is the observation of an intervalence charge-transfer (IV-CT) band in the absorption spectrum of MV compounds. This IV-CT band arises from an optically induced CT from the donor to the acceptor moiety. The IV-CT band usually (but not always) appears as the lowest energy transition in the near-infrared region (NIR) or visible region of the absorption spectrum (Figure 2).

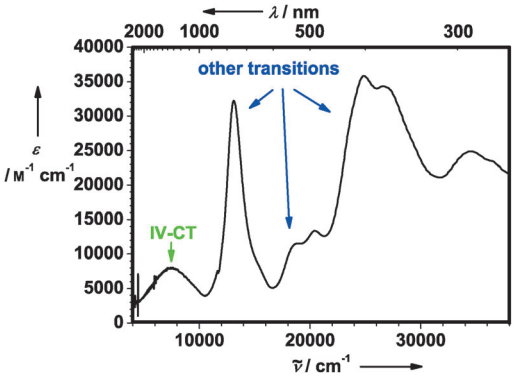

Figure 2. Absorption spectrum of organic MV compound $\mathbf{4}^+$.[79] The IV-CT band is usually the lowest energy transition in the absorption spectrum.

In Figure 3 the adiabatic free energy surfaces (black solid lines) of a MV compound with degenerate (Figure 3a) and nondegenerate (Figure 3b) MV states are shown. These adiabatic potentials can be calculated by solving the secular Equation (5) in which two diabatic harmonic potentials V_{11} and V_{22} are coupled through the electronic coupling V_{12} (in the following often simply given as V). The eigenvalues ε may be obtained from these equations and represent the one-dimensional adiabatic profiles of the ground and the excited state. Although quadratic (harmonic) diabatic free-energy surfaces (FESs) are often used in practise, this need not necessarily be the case.[73,80]

$$\begin{bmatrix} V_{11}-\varepsilon & V_{12} \\ V_{12} & V_{22}-\varepsilon \end{bmatrix} = 0 \quad \text{with} \quad V_{11} = \lambda x^2 \quad V_{22} = \lambda(1-x^2) + \Delta G^{00} \tag{5}$$

From Figure 3 it can easily be seen that the two diabatic free energy surfaces (blue dashed lines) couple to two

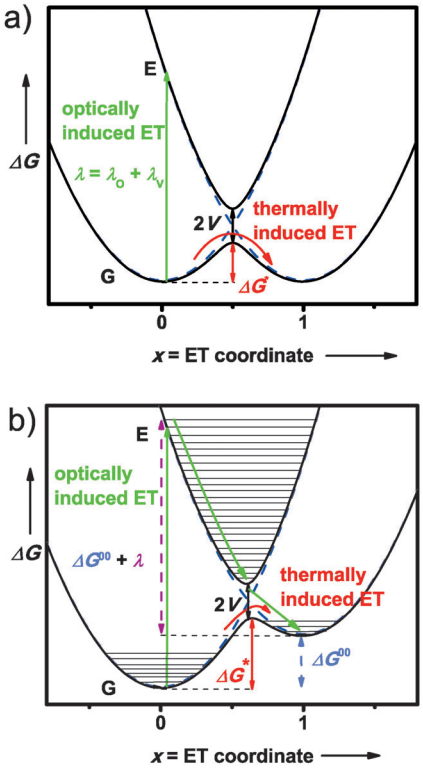

Figure 3. Adiabatic free energy surfaces (black solid lines) of a MV compound with a) degenerate MV states and b) nondegenerate MV states for $0 < V < \lambda/2$ (Robin–Day class II). The free energy difference between the electronic ground (G) and excited (E) states at the crossing point of the diabatic free energy surfaces (blue dashed lines) corresponds to 2 V.

adiabatic free-energy surfaces, where in this case ($V < \lambda/2$) the adiabatic ground state has a double minimum. The minima of the adiabatic surfaces are stabilized by resonance delocalization V^2/λ versus the diabatic surfaces. The barrier for the thermally induced CT (ΔG^*) is clearly decreased compared to the barrier in the diabatic approximation. In the harmonic approximation, Equation (3) transforms to Equation (6) for the barrier in the case of degenerate MV states. Thus, as in the diabatic Marcus theory, the ET barrier in Marcus–Hush theory is mainly due to the total reorganization energy, but diminished by the electronic coupling and corrected by resonance delocalization of the adiabatic ground state V^2/λ. The latter quantity is often neglected in practice, and is a good approximation if $V \ll \lambda$.

$$\Delta G^* = \frac{\lambda}{4} - V + \frac{V^2}{\lambda} \tag{6}$$

The optically induced CT proceeds from the Boltzmann-weighted vibrational states of one minimum of the electronic ground state G, according to the Franck–Condon principle, into the vibrational manifold of the excited electronic state E. Relaxation from the excited state yields the product state with the charge being transferred. In this context, we have to keep in mind that a Boltzmann-weighted population of vibrational states is a necessary condition for the validity of the Marcus–

Hush approach. This condition is only fulfilled at the so-called high-temperature limit (HTL) where $h\tilde{\nu} \ll k_B T$ or, expressed more descriptive, if the energy separation of the vibrational modes $h\tilde{\nu}$ is sufficiently small to ensure a Boltzmann-weighted population of vibrational states at a given temperature. A further important fact which can be seen in Figure 4a and 4b relates to the electronic coupling V: the separation between the adiabatic ground and adiabatic excited state at the nuclear configuration $x = 0.5$ at the crossing point of the diabatic FES corresponds to 2 V.

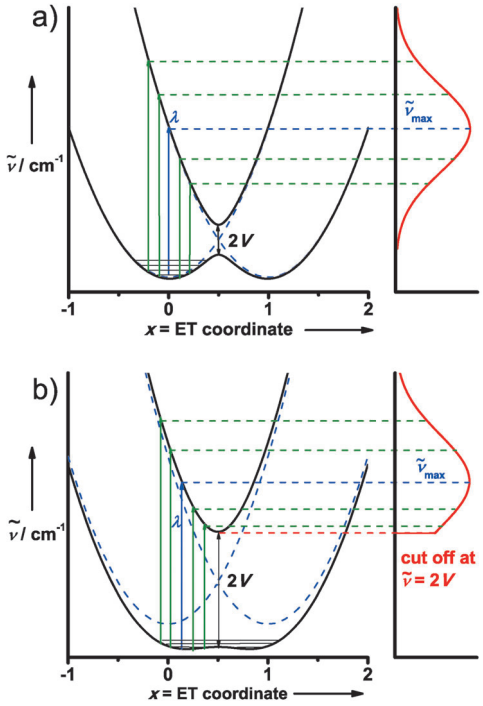

Figure 4. Formation of a nearly Gaussian shaped IV-CT band in MV compounds with a relatively small electronic coupling V (a) and asymmetric IV-CT band in MV compounds with a relatively strong coupling V (b). Both figures reflect the situation for MV systems with degenerate MV states with $0 < V < \lambda/2$.

The free-energy surfaces in Figure 4a and b correspond to a so-called class II MV compound (see Section 2.4) with a small electronic coupling of $0 < V < \lambda/2$. The profiles of the free-energy surfaces strongly depend on the ratio of Marcus reorganization energy λ to electronic coupling V. Before we discuss these issues in detail, we turn to the factors that determine the energy and band shape of the IV-CT band. The formation of an IV-CT band of a MV compound with degenerate MV states is shown on the right-hand side of Figure 4a. Excitation with light leads from the (Boltzmann-weighted) vibrational states of the ground state to the excited state, and each transition eventually contributes to the IV-CT band. As a consequence of the Boltzmann-weighted population of vibrational states of the electronic ground state, the probabilities of transitions are reflected by a Gaussian band shape of the IV-CT band. Thus, the Gaussian-shaped IV-CT band is composed of many inhomogeneously broadened vibrational transitions of different intensities (see also Section 2.7). The maximum of the IV-CT band has the energy $\tilde{\nu}_{max} = \lambda$ ($\lambda + \Delta G^{00}$ for nondegenerate MV states), which is the transition with the highest probability starting from the vibrational ground state (blue line in Figure 4a and b). The IV-CT band for MV compounds with a relatively small electronic coupling V is nearly perfectly Gaussian shaped with a band width $\tilde{\nu}_{1/2}$(HTL) at the high-temperature limit (HTL) given by Equation (7) which depends on $\tilde{\nu}_{max}$.

$$\tilde{\nu}_{1/2}(\mathrm{HTL}) = \sqrt{16 \ln 2 k_B T \tilde{\nu}_{max}} \tag{7}$$

This band width is often used to identify an IV-CT band, but in reality both larger and smaller values are found, and different reasons may account for this effect. The IV-CT band gets more and more asymmetric as the electronic coupling V increases. This fact is explained in Figure 4b, where the formation of the IV-CT band of an MV compound with a strong coupling V is sketched. The asymmetric character is a result of a cut-off of the transitions at the energy 2 V, which is the smallest energy possible for an electronic transition.[79,80] In reality, the IV-CT band is not cut off at this energy as indicated in Figure 4b, but decreases strongly and continuously. An alternative/supplementary explanation for asymmetric IV-CT bands is the coupling with symmetric vibrational modes (see Section 2.5).

The explanation of the IV-CT band thus far rests on the assumption of harmonic diabatic potentials. While this assumption is often a good approximation, the use of, for example, quartic augmented functions leads in some cases to a better agreement with experiments because it leads to broader and slightly asymmetric bands.[80,81]

The most important achievement of Marcus–Hush theory is not only a reasonable semiquantitative description of the IV-CT band shape but also the possibility to extract the electronic coupling through IV-CT band analysis. For this purpose we present here equations that result from a mathematically more rigorous derivation, the Mulliken–Hush theory [Eq. (8)–(10)],[66,67,82–85] which may be considered to be a generalization of the Marcus–Hush theory as no concrete assumptions about the shape of the diabatic potentials (e.g. harmonic) or the number of involved states (two) are made.

$$V_{12} = \frac{\mu_{ab}\tilde{\nu}_{max}}{\Delta\mu_{12}} \qquad \text{with} \qquad \tilde{\nu}_{max} = \Delta G^{00} + \lambda \tag{8}$$

$$\mu_{ab}^2 = \frac{3hc\varepsilon_0 \ln 10}{2000\pi^2 N} \frac{9n}{(n^2+2)^2} \int \frac{\varepsilon}{\tilde{\nu}} d\tilde{\nu} \tag{9}$$

$$\Delta\mu_{12} = \sqrt{\Delta\mu_{ab}^2 + 4\mu_{ab}^2} \tag{10}$$

By using Equation (8), the electronic coupling V_{12} (arabic numeral subscripts refer to diabatic states) can be directly calculated from the transition moment between the adiabatic states μ_{ab}(latin letter subscripts refer to adiabatic states), the energetic maximum of the IV-CT band $\tilde{\nu}_{max}$, and from the difference in the diabatic dipole moments between the ground and excited states $\Delta\mu_{12}$. The transition moment μ_{ab}

can in turn readily be calculated from integration of the (reduced) IV-CT band through Equation (9), where a solvent refractive index (n) correction is taken into account.[86,87] In contrast, the determination of the difference in the dipole moment $\Delta\mu_{12}$ between the diabatic states is a tedious task because it is not directly accessible. Most authors approximate it by the difference between the adiabatic dipole moments, which in turn is calculated from geometrical estimates (e.g. $\mu = e\,r$), such as the distance r between metals in inorganic MV compounds. However, this is erroneous, as the adiabatic distance is always smaller than the diabatic one and practically never reaches the distance between redox centers. This approximation is even worse in organic MV systems, where often no clear redox "center" exists. However, in the context of Mulliken–Hush theory the difference in the diabatic dipole moment can be calculated with Equation (10) from the transition moment μ_{ab} between the adiabatic states and the difference between the adiabatic dipole moment $\Delta\mu_{ab}$ in the ground and excited states. The latter value is not accessible from a Marcus–Hush band analysis and, thus, either has to be calculated by quantum chemical analysis or, in rare cases, be determined by Stark spectroscopy.[4,88–90] Both methods are afflicted with mayor inaccuracies and, hence, the determination of $\Delta\mu_{ab}$ is in practice the challenge or weak point of the Marcus–Hush or Mulliken–Hush theory.

2.3. Methods for the Separation of λ_o and λ_v

Mulliken–Hush theory does not allow for a separate estimation of the Marcus reorganization parameters λ_o and λ_v. Therefore, solvatochromic methods are often used to separate λ_o and λ_v in D–A compounds.[2,5,91,92] These studies rest on the assumption that only λ_o is solvent-dependent and that λ_v is a solvent-independent quantity. While the Marcus Equation [Eq. (1)] is often used to estimate the influence of solvent on λ_o in electron-transfer phenomena, the Onsager model is usually applied for donor–acceptor compounds.[28,75,93,94] Both models treat the solvent as a dielectric continuum which is well characterized by its refractive index n and its permittivity D. The temperature dependence of both D and n also introduces a temperature dependence in the electron-transfer phenomena of MV compounds.[28] In practice, the IV-CT bands of a MV compound are measured in solvents of different polarity and the energies of these bands at the transition maxima (which correspond to the total Marcus reorganization energy λ for degenerate MV compounds in the classical harmonic potential approximation) is plotted against a solvent polarity (either Marcus or Onsager) function. The inner reorganization energy λ_v can be determined by extrapolating a linear regression of the data points to the gas phase (Figure 5). However, especially for charged compounds, ion-pairing effects increase with decreasing solvent polarity and, therefore, the values for the inner-sphere reorganization energies determined by solvatochromic methods might be too large. Nelsen and Ismagilov performed concentration-dependent measurements to discern the ion-pairing effect from solvent effects.[95] The effect of ion-pairing and solvent

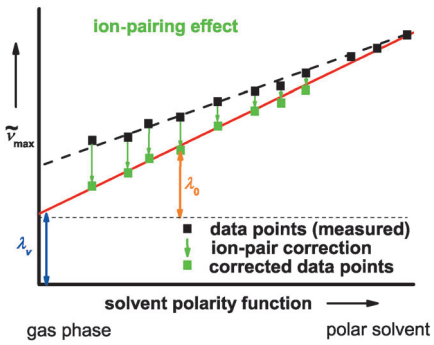

Figure 5. Schematic plot of IV-CT band energies versus solvent polarity function to discern internal λ_v and solvent λ_o contributions, as well as ion-pairing effects on the total reorganization energy $\lambda = \tilde{\nu}_{max}$.

polarity on the reorganization energies are sketched in Figure 5. In practice, ion-pairing can often be neglected in highly polar solvents and be treated as an extra contribution to the internal reorganization energy in low-polarity solvents.[91]

Quantum-chemical methods often refer only to the gas phase. While this is usually considered to be a drawback, it gives the chance to calculate the internal reorganization energy of cationic MV compounds by what is often called the "neutral in cation geometry" (NICG) method. That is, one calculates λ_v by Equation (11), where $\mathbf{n}^+$ is the energy of the radical cation in the optimized neutral geometry etc.[51,96]

$$\lambda_v = (\mathbf{n}^+ + \mathbf{c}^0) - (\mathbf{n}^0 + \mathbf{c}^+) \tag{11}$$

This method yields λ_v for compounds that are clearly class II, that is, for localized MV systems. While the NICG method based on semiempirical AM1 computations proved to be very useful for radical-cation MV compounds with nitrogen redox centers, it fails for radical anions because Koopmans' theorem does not hold in this case because, unlike the cationic situation, errors arising from electron correlation and electron relaxation do not cancel out.[97,98] However, the lowest energy transitions for delocalized radical anions (class III) could be calculated successfully by the "neural in anion geometry" (NAG) method by using hybrid density-functional methods.[99,100]

A further method for the separate determination of both reorganization parameters is a band-shape analysis in the context of the Bixon–Jortner theory (see Section 2.7.2). By applying this method we were able to extract the values of λ_v and λ_o separately for several neutral organic MV compounds in a large variety of solvents of different polarity.[4,92]

2.4. Classification of MV Compounds—The Robin–Day Classes

As mentioned above, the profiles of adiabatic FES strongly depend on the electronic coupling V or, more precisely, on the ratio of V and the Marcus reorganization energy λ. In the late 1960s Robin and Day classified MV compounds and D–A systems in general.[31] Consequently, all D–A systems can be divided into three classes: D–A

compounds where no electronic coupling between the donor and acceptor moieties exists belong to class I. The two redox centers do not influence each other and can be seen as totally isolated moieties. Therefore, no intramolecular ET or CT can take place in such compounds, neither optically nor thermally induced, and they cannot be considered as MV compounds at all. In Figure 6 the diabatic (blue dashed lines) and adiabatic (black solid lines) FES for MV compounds of Robin–Day classes I–III are shown. As can be seen in Figure 6a and b only diabatic FESs exist for class I compounds because of a lack of any electronic communication ($V=0$). Robin–Day class II corresponds to all D–A compounds where the electronic coupling V is smaller than half the Marcus reorganization energy λ: $0<V<\lambda/2$ (Figure 6c and d). In this case, the diabatic FESs are split into two adiabatic FESs, with the adiabatic ground state consisting of a double minimum. The latter aspect is only true for D–A compounds with degenerate MV states; in D–A compounds with non-degenerate MV states, the existence of a double minimum additionally depends on the ratio of ΔG^{00} and λ. This fact is demonstrated in Figure 6d and 6e. The double minimum vanishes if the ΔG^{00} value is on the order of λ. In a strict sense, only those systems that belong to class II should be termed MV compounds because only in these cases can a state exist in which charge is mainly localized at one redox center. The charge can then be either thermally or optically induced to transfer to the other redox center. Only an optical excitation is possible in the nondegenerate case of Figure 6e, which results in a charge shift in the excited (Franck–Condon) state. D–A compounds where $V>\lambda/2$ are class III compounds. In these compounds, the adiabatic ground state has a single minimum and the charge is totally delocalized over both redox centers (Figure 6f and g). In the nondegenerate case, the minima of the ground and excited states are somewhat shifted on the ET coordinate. No CT process, not even optically induced, is possible in degenerate class III MV compounds because the difference in the dipole moments between the ground and excited states is zero. Dispite this fact, absorption bands of class III systems are often termed "IV-CT" bands because they appear at similar energy and result from similar state interactions. While there is a discrete difference between classes II and III in the degenerate case, that is, double versus single minimum, this situation is obscure in the nondegenerate case (cf. Figure 6e and g). The boundary between classes II and III has been the focus of many studies on both inorganic and organic MV systems.[4,17,79,101–103]

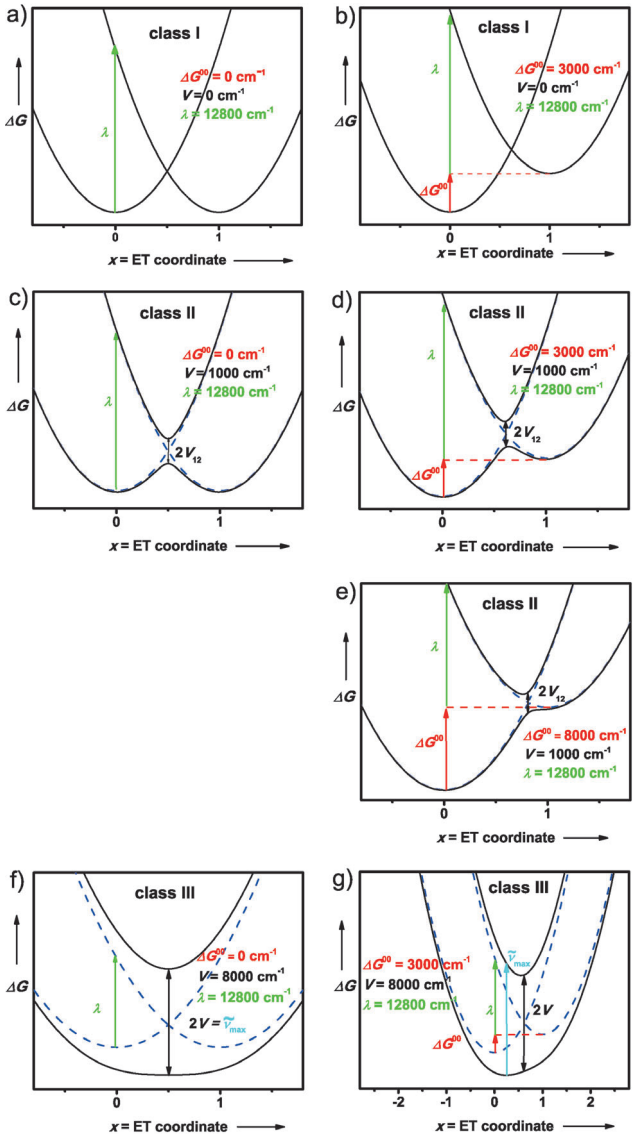

Figure 6. Calculated [by Eq. (5)] diabatic (blue dashed lines) and adiabatic (solid black lines) FES of class I–III systems with degenerate (left hand side, a, c, f) and nondegenerate (right hand side; 6b, 6d, 6e, 6g) MV states. Plots (d) and (e) demonstrate that the existence of a double minimum adiabatic ground state for class II systems is not obligatory, but depends on the ratio of λ and ΔG^{00}.

2.5. Mulliken–Hush Theory and the Two-Mode Model

The Marcus–Hush theory describes the ET process in one dimension, and refers to an averaged asymmetric vibration of the total system. Already in the late 1970s and in the 1980s Hush, Schatz, Piepho, Onderchen, and Zink developed models that extend this limitation to two dimensions with a symmetric and an asymmetric averaged mode.[63,104–113] As mentioned in Section 2.2, the main weakness of the one-mode model of Marcus–Hush/Mulliken–Hush theory is the necessity to determine or estimate the adiabatic dipole moment difference between the ground and the excited state $\Delta\mu_{ab}$ to evaluate the electronic coupling V. This problem can be circumvented at least for strongly coupling systems with relatively asymmetric IV-CT bands (e.g. compounds at the boundary of Robin–Day classes II and III) if a two-mode model is applied. For this purpose, it is necessary to introduce a second, symmetric coordinate y which refers to an averaged totally symmetric mode.[108,110,114–116] This coordinate y is orthogonal to the asymmetric ET coordinate x. The diabatic potentials can then be expanded as power series which depend on both coordinates and in which the diagonal elements are truncated after the quadratic term (neglecting mixed terms which depend on both coordinates) and the off-diagonal elements after the linear term. Equation (12) shows

the vibronic matrix for a degenerate class II MV compound in the two-mode description, where λ_x and λ_y are the Marcus reorganization energies (quadratic coupling constants) and l_x and l_y are the linear coupling constants of the symmetric and asymmetric mode, respectively.

$$\begin{vmatrix} V + l_x x + \lambda_x x^2 + l_y y + \lambda_y y^2 - \varepsilon & V + l_y y \\ V + l_y y & V - l_x x + \lambda_x x^2 + l_y y + \lambda_y y^2 - \varepsilon \end{vmatrix} = 0 \quad (12)$$

The displacement of the surfaces of the ground and the excited states along the x and y mode is given by $\delta Q_y = l_y/\lambda_y$ and $\delta Q_x = l_x/2\lambda_x$, respectively. For simplification the linear ($l_x = l_y = l$) and quadratic coupling constants ($\lambda_x = \lambda_y = \lambda$) are chosen to be equal to fix the minima of both diabatic FESs at $x = \pm 0.5$. Diagonalization of the matrix gives two adiabatic two-dimensional free-energy surfaces. Assuming a Boltzman-weighted population of vibrational states, the experimental IV-CT band of a MV compound can then be fitted by variation of the parameters V, l, and λ.[63,117] The decisive advantage of the two-mode model is the direct extraction of the electronic coupling V from spectroscopic data. However, as mentioned above, this method is only practical for MV systems with strong electronic coupling V and, consequently, relatively asymmetric IV-CT bands. For weakly coupled systems, the IV-CT band becomes symmetric and its shape does not depend on V. Furthermore, it could be demonstrated that the ET parameters determined by the two-mode model are more accurate than those extracted from a one-mode analysis because of the inclusion of a further degree of freedom.[114–116]

2.6. The Generalized Mulliken–Hush (GMH) Theory and the Three-State Model

Besides IV-CT bands, MV systems often show additional absorption bands that are associated with charge-transfer processes. Thus, it seems desirable to include these transitions in a multistate treatment. In fact, Cave and Newton developed a formalism to treat MV systems with any number of diabatic states in the context of Mulliken–Hush theory. This extension is often termed Generalized Mulliken–Hush (GMH) theory.[82,83,118–120] This formalism rests on a unitary transformation of energy and dipole matrices, as given in Equations (13) and (14) for a three-state system with two degenerate MV states and a third one in which the charge is localized at the bridge. We call this third state the "bridge state" in the following. The adiabatic dipole matrix $\boldsymbol{\mu}_{\text{adiab}}$ contains the differences between the dipole moments (diagonal elements) and the transition moments (off-diagonal elements) between all adiabatic states. These quantities are in principle measurable. The adiabatic energy matrix $\mathbf{H}_{\text{adiab}}$ contains all the transition energies to the excited states (that is, two absorption bands with energy $\tilde{\nu}_a$ and $\tilde{\nu}_b$). The unitary transformation with matrix $\mathbf{C}$ diagonalizes $\boldsymbol{\mu}_{\text{adiab}}$, which yields the differences in the diabatic dipole moments between all states in $\boldsymbol{\mu}_{\text{diab}}$. The same transformation applied to $\mathbf{H}_{\text{adiab}}$ yields the desired electronic couplings V between all states in $\mathbf{H}_{\text{diab}}$.

$$\boldsymbol{\mu}_{\text{adiab}} = \begin{pmatrix} \mu_{gg} & \mu_{ga} & \mu_{gb} \\ \mu_{ga} & \mu_{aa} & \mu_{ab} \\ \mu_{gb} & \mu_{ab} & \mu_{bb} \end{pmatrix} \xrightarrow{\boldsymbol{\mu}_{\text{diab}} = \mathbf{C}^{\dagger}\boldsymbol{\mu}_{\text{adiab}}\mathbf{C}} \boldsymbol{\mu}_{\text{diab}} = \begin{pmatrix} \mu_{11} & 0 & 0 \\ 0 & \mu_{22} & 0 \\ 0 & 0 & \mu_{33} \end{pmatrix} \quad (13)$$

$$\mathbf{H}_{\text{diab}} = \begin{pmatrix} H_{11} & V_{12} & V_{13} \\ H_{12} & H_{22} & V_{23} \\ V_{13} & V_{23} & H_{33} \end{pmatrix} \xrightarrow{\mathbf{H}_{\text{diab}} = \mathbf{C}^{\dagger}\mathbf{H}_{\text{adiab}}\mathbf{C}} \mathbf{H}_{\text{adiab}} = \begin{pmatrix} 0 & 0 & 0 \\ 0 & \tilde{\nu}_a & 0 \\ 0 & 0 & \tilde{\nu}_b \end{pmatrix} \quad (14)$$

For a two-state model with diabatic states, this GMH theory is equivalent to the Mulliken–Hush theory introduced above or, more precisely, the Mulliken–Hush two-state model is a special case of the GMH theory. While all matrix elements can be evaluated by quantumchemical calculations for a multistate system,[83,121] this is almost impossible by experiment, even for a three-state system. Thus, mixed experimental/quantum-chemical input is used in practice.[122,123]

The necessity to treat some systems as a three-state system is apparent if their absorption spectra show more than one band that can be traced back to an optically induced charge transfer. In some cases, these bands can be assigned to a CT process from one redox center to the bridge moiety and these bridge bands usually appear at higher energy than the IV-CT band in the absorption spectra. In this case, the electronic couplings between the ground and the first excited state V_{12}, between the ground and the second excited state (bridge state) V_{13}, as well as the reorganization energies for each transition can be extracted from the analysis of the absorption spectrum by applying the above-mentioned GMH three-state model provided that some dipole moments are calculated by quantum-chemical methods.[67,106,107,122–127] The one-dimensional projection of a FES of a MV system with two degenerate MV states and one bridge state is shown in Figure 7.

More detailed analyses show that the FES for three-state systems should be expanded in at least two dimensions, that is, an asymmetric and a symmetric averaged mode is necessary for a proper description of a system with two degenerate MV states and one bridge state. In Figure 8, the diabatic potentials for a system as given in Figure 7 are sketched as a contour plot. These potentials can be coupled in $\mathbf{H}_{\text{diab}}$ to yield the adiabatic FES from which the spectra can then be calculated, for example, either by the classical method as detailed above or by, for example, time-dependent formalisms.[128] The parameters that govern the adiabatic FES (reorganization energies of the potentials, relative energy of the bridge potential to the other potentials, electronic couplings) can then be determined by a best fit of the calculated to the experimental spectra.

In Figure 9 the adiabatic FESs of a MV compound with two degenerate MV states and one bridge state are shown. These adiabatic potentials refer to the diabatic ones in Figure 7. The projection of the adiabatic FES onto the x coordinate (cf. Figure 7) is marked as yellow lines. It is clear that the minima of this projection do not necessarily

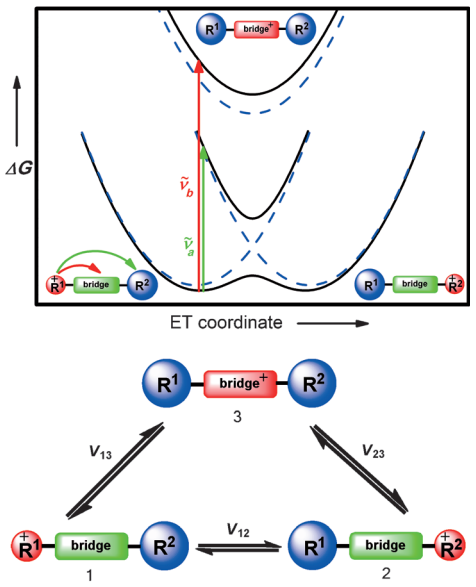

Figure 7. CT pathways in a MV compound with two degenerate MV states and one bridge state. The charge is either located on one of the two identical redox centers or on the bridge unit. The two observable optically induced CT processes are those from one redox center to the bridge (red arrow) and from one redox center to the other (green arrow; adiabatic potential black solid and diabatic potentials dashed blue lines).

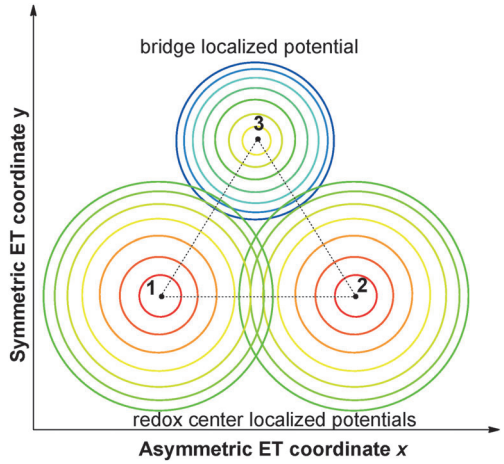

Figure 8. Diabatic FES as a contour plot in the *x*-*y* plane for a MV compound with two degenerate MV states and one bridge state, as in Figure 7. Red to yellow represent low energy, green to blue high energy.

coincide with the global minima of the two-dimensional adiabatic FES (see, for example, the second excited state where the global minimum is shifted towards higher *y* values).

Although multistate and multimode analyses are useful for a more complete description of MV systems, these approaches are not straightforward and are limited to MV systems where the MV states can be clearly identified by spectroscopic methods. Nevertheless, the three-state model is an effective model to analyze bridge states and the corresponding transitions. Furthermore, it is evident that the ET parameters extracted by this model are more accurate than

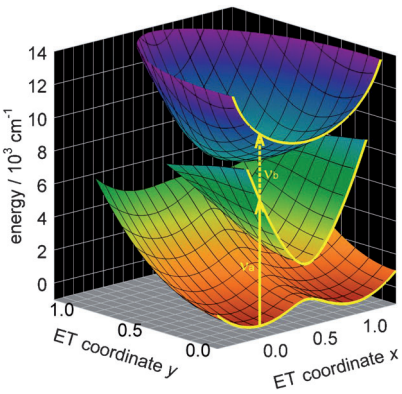

Figure 9. Adiabatic FESs of a MV system with two degenerate MV states and one bridge state. The yellow curves are the one-dimensional projection onto the *x* coordinate. Reproduced from Ref. [129] with permission.

those extracted by a two-state model. Recently, we were able to show that the barriers of thermally induced electron-transfer processes in some MV compounds calculated by a three-state model compare more accurately with experimental values than the barriers calculated from data extracted from a two-state Mulliken–Hush analysis.[129] This is not surprising in view of the fact that optical CT processes between donor and acceptor moieties are directly influenced by transitions to higher excited states, such as bridge states, by mechanisms such as vibronic coupling, Herzberg–Teller coupling, or intensity borrowing.[130–132]

2.7. Quantum-Chemical Approaches

2.7.1. Vibronic Coupling Model

Although the above-mentioned adiabatic theories aim at constructing FESs from diabatic potentials, they are still classical methods inasmuch as they treat all vibrations (molecular and solvent) as being harmonic and independent of the electronic wave function. The ET behavior of MV compounds has also been investigated by quantum-chemical methods, which go beyond the classical approximations. In this context, one approach is the so-called vibronic coupling theory, where movement of nuclei during the ET is explicitly taken into account. This theory rests on the assumption that the electronic coupling in MV systems is strongly influenced by the movement of nuclei and, thus, is vibronically coupled to this movement. The most commonly used model to consider these effects is the one developed by Piepho, Krausz, and Schatz, which takes two vibronic normal modes (symmetric and asymmetric) into account.[63,104,108,109] By using this vibronic coupling model, Coropceanu et al. were able to calculate the IV-CT bands of organic MV compounds by numerical calculation of the eigenfunctions of a Hamiltonian which contains both kinetic and potential energy terms. The results were in excellent agreement with experimental data.[117,133,134] Talaga and Zink[111] as well as Engel and co-workers[128] used a similar Hamiltonian but calculated the absorption spectra by a time-dependent formalism. The ET

parameters derived in the framework of the vibronic coupling model conform excellently with those parameters extracted by the classical GMH theory, particularly for weakly coupled systems.[128] However, vibronic coupling theory is not limited to two normal modes; in fact there are approaches which take more modes into account and even include all possible vibrations in a molecule.[60,110,113]

2.7.2. Bixon–Jortner Model

Although the former theories usually use adiabatic FESs for the calculation of the electronic spectra, there is a truly diabatic theory to describe transitions between different surfaces which was developed by Bixon and Jortner in 1968.[135–138] In this model, a high-energy vibrational mode $\tilde{\nu}_v$ is introduced which represents a weighted average of all the vibrational modes of the MV compound. While this averaged vibrational mode is treated quantum-chemically, the influence of the solvent—which are low-energy vibrations—is treated classically as a harmonic potential, much in the same way as in Marcus theory. The high-energy character of the vibrational mode is indispensable for the application of the Bixon–Jortner model and should be larger than 1000 cm^{-1}. This is because in this case the energetic separation of the vibrational states is large enough to ensure that only the lowest vibrational state of the electronic ground state is populated and, hence, all optical transitions originate from this lowest vibrational state. Bixon–Jortner theory is essentially a Golden Rule expression [Eq. (15)][135,139] in which the Franck–Condon factor is replaced by a simple algebraic term which depends on the Huang–Rhys factor S, that is, the ratio of λ_v and $\tilde{\nu}_v$. Thus, the IV-CT band is given as a series of vertical transitions from the vibrational ground state of the reactant state into the vibrational manifold of the product state, whose intensities and energetic separations follow the Franck–Condon progression and which are Gaussian-broadened by the interaction with the solvent.

$$\varepsilon/\tilde{\nu} = \frac{2000N\pi^2}{3\varepsilon_0 \ln 10}\frac{(n^2+2)^2}{9n}\mu_{ab}^2\sum_{j=0}^{\infty}\frac{e^{-S}S^j}{j!}\sqrt{\frac{1}{4\pi hc\lambda_o kT}}$$
$$\exp\left[-\frac{hc(j\tilde{\nu}_v+\lambda_o-\tilde{\nu}+\Delta G^{00})^2}{4\lambda_o kT}\right] \text{ with Huang-Rhys factor } S=\frac{\lambda_v}{\tilde{\nu}_v} \quad (15)$$

Although the Bixon–Jortner model is a diabatic theory, it was used successfully by Nelsen et al.[140] and by us[4,92] to simulate IV-CT bands of organic MV compounds which are truly adiabatic in nature. One main advantage of this model is the chance to extract discrete values for both the inner reorganization energy and the solvent reorganization energy from absorption spectra. Furthermore, the Bixon–Jortner theory is also applicable to emission spectra. In practice, the use of this model is limited by the value of the Huang–Rhys factor S. This factor has to be small enough to ensure preferably asymmetric IV-CT bands, since otherwise the band fits are not defined and the values of the fitted parameters are interdependent. A further restriction is that Bixon–Jortner theory is only applicable to weakly electronically coupled MV compounds as it is a diabatic approach. In this way, the quantumchemical Bixon–Jortner theory and the classical Marcus–Hush theory complement each other in regard to their applicability to weakly and strongly coupled MV systems, respectively.

2.7.3. Semiempirical, Ab Initio and Density Functional Approaches

Although the above-mentioned approaches are useful for analyzing the optical spectra of MV systems, they do not give insight into the electronic nature of MV compounds, that is, into the electron-density distribution and related properties, such as dipole moments etc. The size of organic MV compounds meant that quantum-chemical approaches to compute these properties were restricted in the past to semiempirical methods such as the AM1 methods. The AM1-UHF method proved useful for strongly localized bishydrazine MV compounds,[85,141,142] but fails for strongly coupled bis(triarylamine) systems because of the tendency of the UHF method to localize charge artificially.[79] To overcome this problem, AM1-CI computations including the COSMO model for simulating solvent effects were successfully performed on triarylamine MV compounds.[112] Ab initio UHF calculations suffer from the same problem as the AM1-UHF calculations, but ab initio calculations on organic MV compounds beyond the SCF limit are scarce and restricted to very small systems.[143–145] On the other hand, density functional methods tend to delocalize charge even in localized class II systems because of self-interaction error.[117,133,146] Recently, Kaupp and co-workers were able to overcome this problem by adjusting the exact HF exchange admixture in hybrid density functional methods to reproduce correctly the classII/classIII borderline behavior in bis(triarylamine) radical cations.[147,272]

2.8. Influence of Geometrical Factors on the Electronic Coupling and the ET Rate Constant

In this section we intend to give an idea of the way particular geometrical parameters influence the ET behavior of MV compounds. A precise understanding of these effects is a helpful precondition to handle the multitude of organic MV compounds with similar structures but sometimes very different physical properties that we describe in Section 3.

In cases where the electronic coupling V is small and the ET is in the diabatic regime, the rate of ET is governed by the square of the coupling, as reflected in the classical Golden rule expression at the high temperature limit, [Eq. (16)].[24,148]

$$k_{ET} = 4\pi^2 hc^2 V^2 FC$$
$$\text{with} \qquad FC = \sqrt{\frac{1}{4\pi hc\lambda_o kT}}\exp\left[-\frac{hc(\lambda_o+\lambda_v+\Delta G^{00})^2}{4\lambda_o kT}\right] \quad (16)$$

In cases where ET is adiabatic, the electronic coupling V no longer influences the rate through the prefactor but through its influence on the ET barrier [see Eq. (6)]. The

electronic coupling V in turn depends on the magnitude of the interaction between the orbitals which control the electronic interaction between the redox centers and the bridge unit(s). In particular, the frontier orbitals of the redox centers and the bridge unit(s) have an important impact on the ET behavior. Thus, modification of molecular orbital overlap through, for example, the distance of the redox centers and bridges or their relative orientation will ultimately influence the ET rate.[149]

In this context, two different pathways for ET need to be distinguished: The incoherent hopping mechanism, where the charge is transferred step by step via bridge units between the donating redox center and the accepting redox center. In this case, the charge has a finite lifetime at the bridge(s). The alternative is the coherent superexchange mechanism,[149,150] where the charge is at no time located on the bridge unit(s) but is transferred by tunneling processes, mediated by virtual states, from the donor redox center to the other acceptor redox center. The frontier orbitals for a cationic MV compound and an anionic MV compound as well as the two different ET pathways are outlined in Figure 10. In this context, it is useful to distinguish between hole transfer (HT) and electron transfer (ET) although only electrons are physically transferred. The difference in superexchange and hopping mechanisms is the participation of bridge states, which is real in hopping and virtual in superexchange, and which depends on the energy gap between the donating state and the bridge states. If the bridge states lie high in energy, superexchange will dominate, but if they are low in energy or even resonant with the donor state, hopping may dominate. In the latter case, each individual step (e.g. donor→bridge) may be conceived as a superexchange process.

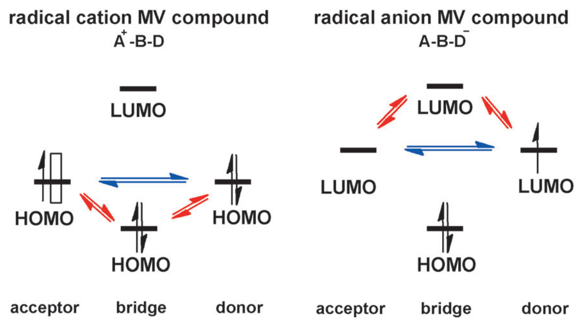

Figure 10. Frontier orbitals of cationic (left-hand side) und anionic (right-hand side) MV compounds and the two pathways of ET (HT): superexchange mechanism (blue) and hopping mechanism (red). For the cationic system, it is useful to view the transfer of a hole (□) from the acceptor to the donor rather than the transfer of an electron.

Thus, it is apparent that the relative energy of the frontier orbitals of the bridge unit essentially determines the main pathway of ET: high-energy bridge HOMOs in cationic MV compounds promote the hole-hopping mechanism and low-energy bridge LUMOs in anionic MV compounds promote the electron-hopping mechanism. Actually, both the hopping and superexchange mechanisms often contribute concomitantly to the ET. Independent from the ET mechanism, it is evident from the distance dependence of orbital overlap that the electronic coupling and, consequently, the ET rate decrease as the distance between the redox centers increases and, hence, the length of the spacer (bridge) unit increases. However, both ET mechanisms show different distance dependencies.[151] In the case of the hopping mechanism, a reciprocal (wirelike) dependence of the ET rate on the distance between the donor and acceptor redox centers or, alternatively, the number N of intervening bridge moieties between the redox centers is expected [Eq. (17)].

$$k_h \propto \frac{1}{N} \tag{17}$$

The superexchange mechanism behaves differently: following the formalism of McConnell, the decrease in the ET rate is described by an exponential function [Eq. (18)] with an "attenuation factor" β. N is the number of repeating bridge units with unit length a and with energy ΔE_{DB} relative to the donor center and which are coupled to each other by V_{BB}.[149]

$$k_s = k_0 \exp[-\beta N a] \quad \text{with} \quad \beta = -\left(\frac{2}{a}\right)\ln\left(\frac{V_{BB}}{\Delta E_{DB}}\right) \tag{18}$$

This exponential dependence on the length is based on the exponential dependence of the coupling [Eq. (19)], as was verified for, for example, organic MV systems with triarylamine redox centers and conjugated bridges of different lengths (see Figure 11).[79,123,141,152]

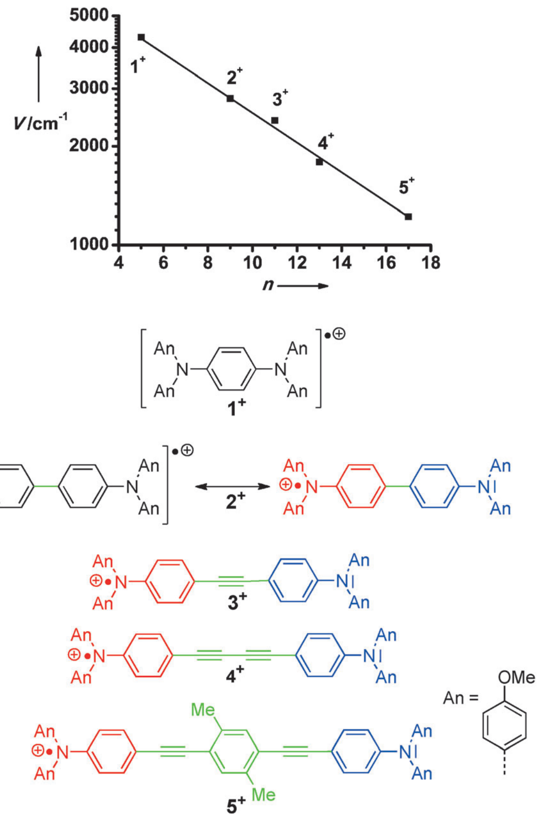

Figure 11. Dependence of the electronic coupling V on the number of bonds n between the nitrogen redox centers. Values are taken from Ref. [123].

$$V_{DA} = V_0 \exp[-(\beta/2)Na] \quad (19)$$

It is noteworthy that the superexchange mechanism dominates in practically all organic MV compounds, since the observation of an IV-CT band requires a sizable electronic coupling between the donor and acceptor redox centers, which makes the ET adiabatic.

It could be shown in many studies that another important factor that determines the electronic coupling is the type of bonds between the redox centers.[79,141,153,154] For example, unsaturated bonds increase the electronic communication between the redox centers relative to saturated ones. This can easily be seen from MV compounds $\mathbf{5}^+$ and $\mathbf{6}^+$, in which the central benzene ring is replaced by a cyclophane bridge (Scheme 3).

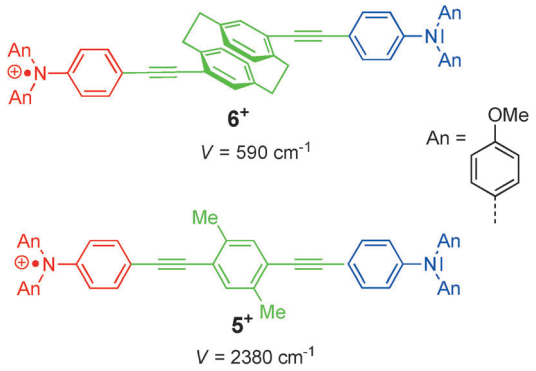

Scheme 3. Two bis(triaryamine) radical cations $\mathbf{5}^+$ and $\mathbf{6}^+$. The electronic coupling in $\mathbf{6}^+$ is clearly diminished due to the saturated paracyclophane spacer.

Thus, MV compounds with saturated bridges show higher values for β.[123] In addition, β depends on further specific properties of the spacer unit, such as the length of the bridge unit a, the coupling between the bridge units (if the spacer consists of more than one bridge unit) V_{BB}, and, as sketched in Figure 10, on the relative energy difference between the spacer units and the redox centers ΔE_{DB} [Eq. (18)].

In a similar way, the electronic coupling V between two directly linked redox centers also depends on the degree of conjugation along the ET pathway. This also applies for the hopping mechanism, which can be viewed as consecutive coupled superexchange ET processes. It could be shown that, especially in the case of biphenyl spacer units, the twist angle between the phenyl rings and the existence of many conformers play a decisive role in modulating the electronic coupling V. This was, for example, demonstrated by the differences of the electrochemical redox potentials in the tetraaryl benzidine series in Scheme 4.[149,155–157] The influence of the twist angles on the coupling between the spacer units and redox subunits can be modeled by trigonometric functions.[30,141]

Another important effect on the electronic coupling is the topological kind of linkage itself. A *meta*-linked phenyl spacer unit (non-Kekulé-type structure) is by far a less-effective coupling linker than a phenyl spacer which is *para* substituted (Kekulé-type structure).[3] For example, MV compound $\mathbf{10}^-$

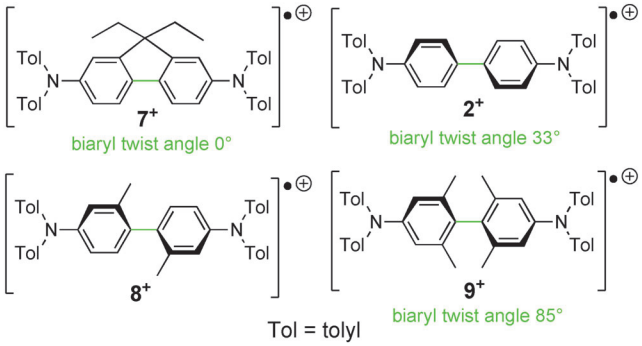

Scheme 4. Bis(triarylamine) radical cations with various twist angles of their biphenyl bridge unit.

(Scheme 5) shows a strong IV-CT band and the ET rate constant could be measured by temperature-dependent EPR spectroscopy, while no such observations could be made for $\mathbf{11}^-$ (Scheme 5) because of its weak electronic coupling.

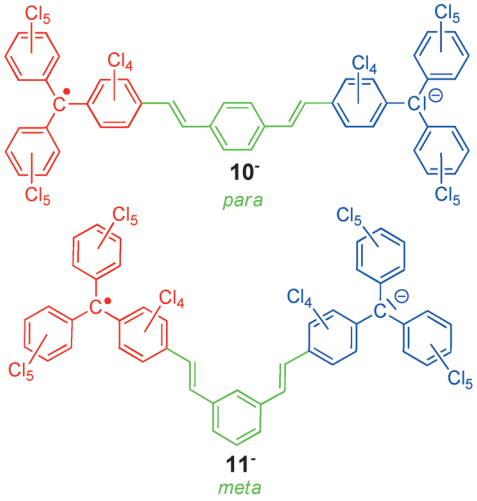

Scheme 5. MV radical anions with *meta*- and *para*-linked phenylene spacer units.

A further example which demonstrates the different effects of superficially very similar spacer units on the ET behavior is a bis(triarylamine) radical cation which is changed from a Robin–Day class II to III system simply by replacing the acetylene spacer unit by an ethylene unit (the distance of the redox centers is nearly the same in both compounds; Scheme 6).[158]

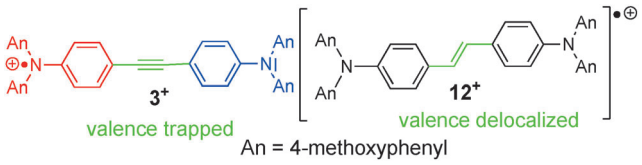

Scheme 6. Two bis(triarylamine) radical cations, where the type of spacer (ethylene/acetylene) determines the classification as Robin–Day classes II or III.

All the above-mentioned effects have an influence on the electronic coupling and, therefore, as shown in Equation (2), together with Equations (6) and (16) on the ET rate constant k_{ET}. In the following, we trace the parameters which have a direct impact on the rate constant by exerting influence on the ET barrier ΔG^* but have no effect on the electronic coupling V. One main factor is the Marcus reorganization energy λ. As can be seen from Figure 12 and Equation (6), the ET barrier

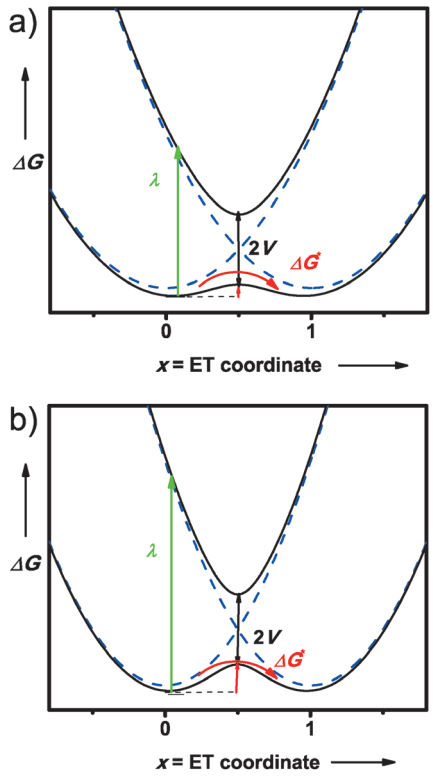

Figure 12. FESs of two class II MV systems (a) and (b) with degenerate MV states and equal electronic coupling V. The higher reorganization energy in system (b) directly yields a higher ET barrier ΔG^* and, consequently, a lower ET rate constant.

increases with increasing λ. This means that both the solvent polarity as well as the structure of the redox centers control the ET rate constant, as these factors determine the solvent and inner-sphere reorganization energy, respectively. Generally, polar solvents exert a high reorganization energy and, consequently, the ET is slower than in nonpolar solvents. The size of the MV compound also determines the solvent reorganization energy through the distance r_{12} between the redox centers, as an approximation of the effective charge-transfer distance [see Eq. (1)]. Thus, charge transfer in larger MV compounds suffers from a higher solvent reorganization than smaller systems. In the same way, relatively large structural changes in the redox centers during the ET process result in a relatively slow ET process because of a large internal reorganization energy λ_v. Nelsen et al. demonstrated the latter aspect by the investigation of structurally similar bis(hydrazyl) and bis(hydrazine) radical cations[51] (see also Section 3.1.1). While these types of redox centers generally have a relatively high internal reorganization energy, triarylamines and perchlorinated triphenylmethyl radicals possess a relatively small inner reorganization energy. For triarylamines, this is due to the charge being delocalized within the aryl systems, for hydrazines it is due to a rehybridization upon charging as well as interactions of the lone pairs of electrons in the neutral hydrazines.

3. Organic Mixed-Valence Compounds

After having introduced the concept of mixed valency and the most important theoretical models that are currently being used to describe the charge-transfer phenomena in MV compounds in the foregoing sections, we now turn to organic mixed-valence systems as chemical species that may be defined by chemical substructures. That is, we classify organic MV compounds on the basis of the functional groups that acts as the redox centers. While a simple classification in inorganic MV systems can rest on the type of the metal centers, this classification is not applicable to organic MV systems, as the charge never solely resides on a single atomic center but is delocalized over more than one atom. Thus, a classification into different organic redox functional groups is merely a topological guide rather than reflecting the actual charge distribution. Furthermore, we will not only present an overview on organic MV compounds, we will also give a critical review about the results of the physicochemical investigations associated with the different kinds of organic MV species. In particular, we will discuss the influence of different structural units (redox centers, bridge moieties) on the ET characteristics.

3.1. Organic MV Compounds with Nitrogen-Containing Redox Centers

3.1.1. Bis(hydrazyl) and Bis(hydrazine) Radical Cations

Bis(hydrazyl) and bis(hydrazine) radical-cation systems represent two important classes of organic MV compounds that have been designed and investigated for about two decades by Nelsen et al. Although they were not the first systems that were investigated in terms of their mixed valency, they are probably the most intensely studied organic MV compounds. The CT behavior of dozens of compounds has been studied in detail by various different physical and theoretical methods. Both classes share the advantage of reversibility and stability of their redox centers.

The bis(hydrazine) systems themselves can be subdivided into two classes, which differ in the type of spacer unit that connects the hydrazines as well as in the way the hydrazine redox centers are connected to the spacer: 1) bis(hydrazines) with saturated bridge units and 2) bis(hydrazines) with aromatic bridges. However, before we deal with bis(hydrazine) systems in detail, we first turn to the structurally related organic MV compounds, the bis(hydrazyl) radical cations.

3.1.2. Bis(hydrazyl) Radical Cations

Bis(hydrazyl) radical-cation MV compounds can be viewed as consisting of a diazenium cation redox center, which acts as the electron acceptor, and a reduced diazenium cation redox center, which is therefore uncharged and which acts as the electron donor. These radical cations may be termed "distonic", since the radical center (donor) and charge (acceptor) are located on different units.[159] Both, the unpaired "extra electron" of the donor center as well as the positive charge of the acceptor center are delocalized over both nitrogen atoms. These organic MV compounds can be synthesized starting from the corresponding bis(azo) compounds of the type **13** by a so-called bis(*tert*-butylation) reaction.[51,160,161] This reaction yields isomeric mixtures of the bis(diazenium) dications $\mathbf{14}^{2+}$ which can be transformed in situ into the corresponding bis(hydrazyl) radical cations by one-electron reduction initiated electrochemically or by chemical reduction (Scheme 7). In some cases the two isomers (*syn* and *anti*) are separable, but their charge transfer behavior is practically identical.[51,161,162]

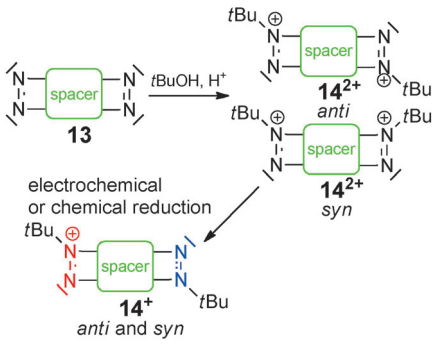

Scheme 7. Synthesis of bis(hydrazyl) radical cations starting from bis(azo) compounds **13**.

One characteristic feature of this class of organic MV compounds is the "double linkage" of each redox center to the bridge unit. Scheme 8 shows a small number of bis(hydrazyl) radical cations ($\mathbf{15}^{+}$–$\mathbf{18}^{+}$) that differ solely in the type of bridge unit.

One important motive for the investigation of these bis(hydrazyl) systems was to find purely organic analogues of the well-known inorganic transition-metal MV complexes

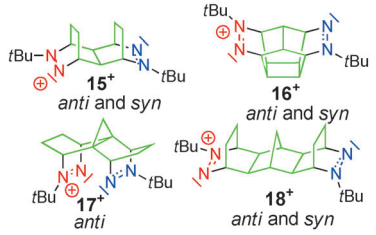

Scheme 8. Bis(hydrazyl) radical cations $\mathbf{15}^{+}$–$\mathbf{18}^{+}$.

such as the Creutz–Taube ion (**F**, Section 1) and to elucidate the applicability of Marcus–Hush theory to organic MV systems. A further goal was to compare the outcome of optical investigations with those of temperature-dependent electron spin resonance (ESR) spectroscopy. For analysis by ESR spectroscopy, the charge-transfer rate in MV compounds should be relatively slow and should fall into the 10^{8}–$10^{9}\ s^{-1}$ region. Thus, MV systems with a high reorganization energy that slows down the charge-transfer rates are particularly interesting.

As mentioned above, bis(hydrazyl) cations can be generated electrochemically in situ or by chemical reduction with tetramethylammonium thiophenolate ($Me_4N^{+}PhS^{-}$) as the reducing agent.[51] The redox potentials E(Red1) and E(Red2) of the reversible reductions of the bis(hydrazyl) dications as well as the splitting of the redox potential ΔE of these reduction processes, as determined by cyclic voltammetry, are given in Table 1.[51,162] The separation of the redox

Table 1: Redox potentials of bis(hydrazyl) compounds *anti*-$\mathbf{15}^{+}$–*anti*-$\mathbf{18}^{+}$ in acetonitrile. All potentials are referenced versus a saturated calomel electrode.[51,140]

Compound	E(Red1) [V]	E(Red2) [V]	ΔE [V]
anti-$\mathbf{15}^{2+}$	−0.41	−0.75	0.34
anti-$\mathbf{16}^{2+}$	−0.40	−0.77	0.39
anti-$\mathbf{17}^{2+}$	−0.04	−0.76	0.72
anti-$\mathbf{18}^{2+}$	−0.68	−0.80	0.12

potentials ΔE is often used as a qualitative indicator of the strength of the electronic coupling V between the two redox centers. In general two non-interacting identical redox centers show a statistical half-wave separation of $\Delta E = 35.6$ mV at 25 °C.[163,164] This separation increases as the electronic coupling of the degenerate MV states increases and is maximal for a totally delocalized (class III) MV system. In other words, as the electronic coupling increases, the second redox process is increasingly influenced by the first. However, it is hard to gather quantitative information about the electronic coupling from ΔE because it is influenced by ion-pairing (with counterions from the electrolyte) and because ΔE intrinsically reflects properties of M versus M^{+} and M^{+} versus M^{2+}, while the electronic coupling in a MV species solely refers to the mixed-valence species M^{+}.[79,165,166] Nevertheless, cyclovoltammetric measurements are widely used in MV chemistry to obtain information about the electronic coupling of the system. From the redox potentials given in Table 1, Nelsen et al. deduced a higher electronic coupling V for compounds $\mathbf{15}^{+}$ and $\mathbf{16}^{+}$, where the redox centers are separated by four σ bonds, than for compound $\mathbf{18}^{+}$, where six σ bonds are between the two redox centers (Table 2). This is in accordance with the well-known fact that V decreases as the distance between the redox centers increases.[123,141,167–170] The presumably very large electronic coupling in $\mathbf{17}^{+}$ could not be confirmed experimentally.

However, bis(hydrazyl) compounds $\mathbf{15}^{+}$–$\mathbf{17}^{+}$, are less suitable for ESR measurements because the ET process in these compounds is much too fast even for measurements at low temperature. The main reason for these high ET rates

Table 2: IV-CT absorption maxima λ_{max} and electronic coupling V determined by Hush analysis for bis(hydrazyl) radical cations.

	λ_{max} [nm] ([cm^{-1}])	V [cm^{-1}]
syn-**15**$^{+}$[a]	1062 (9420)	1295
anti-**15**$^{+}$[a]	1081 (9250)	1085[b]
anti-**16**$^{+}$[a]	1199 (8340)	1190
syn-**18**$^{+}$[c]	763 (13100)	(580)[d]
anti-**18**$^{+}$[c]	763 (13100)	(560)[d]

[a] See Ref. [162]. [b] Nelsen et al. assume that the electronic coupling was determined to be too small and that *syn*- and *anti*-**15**$^{+}$ have the same V value. See Ref. [162], Table 3, footnote [d]. [c] See Ref. [91]. [d] Solvent-corrected V values (see Ref. [91]).

and, hence, small ET barriers ΔG^{*} is the remarkably small inner reorganization energy λ_v of bis(hydrazyl) compounds. Nelsen et al. showed that there are only very small structural differences between oxidized and reduced bis(hydrazyl) redox centers: in both forms the nitrogen centers are sp^2 hybridized and have a planar structure.[51,96] Consequently, the geometrical changes and, thus, the reorganization energy during the ET event are very small (Scheme 9).

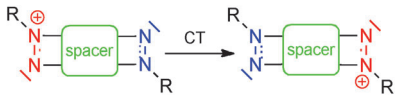

Scheme 9. ET in bis(hydrazyl) radical cations: Each nitrogen atom, both at the donor and the acceptor, is sp^2 hybridized and has a planar structure.

Therefore, it is impossible to determine rate constants for bis(hydrazyl) radical cations **15**$^{+}$–**17**$^{+}$ by ESR spectroscopy. On the other side, the small inner reorganization energy offers excellent conditions for optical investigations of the IV-CT bands because they are placed in the NIR region (λ_{max} = 1050–1240 nm in solvents of different polarity) and, therefore do not overlap with other transitions.[51] A Marcus–Hush band analysis yields ET rates k_{ET} of about 10^{10} s^{-1}, which were in agreement with the rates estimated qualitatively by ESR spectroscopy.[51]

The hydrazyl groups in compound **18**$^{+}$ are separated by six σ bonds, which decrease the electronic coupling V (Table 2) compared to **15**$^{+}$ and **16**$^{+}$ and increase the ET barrier according to Equation (6). At the same time, the solvent reorganization energy rises as a result of the increased effective charge-transfer distance [see Eq. (1)]. Both effects work together and slow down the ET sufficiently so that it is on the ESR time scale. The values for the electronic coupling V of bis(hydrazine) radical cations are summarized in Table 2.

Furthermore, the bis(hydrazyl) MV systems were studied in detail by resonance Raman spectroscopy, which allows identification of the active modes that participate in the resonant excitation, which, in the case of MV compounds, is associated with the charge-transfer event.[171] An excitation in the NIR region at 1064 nm directly into the IV-CT transition of MV compound **15**$^{+}$ shows that the averaged vibrational mode $\tilde{\nu}_v = 1100$ cm^{-1} is mainly composed of six modes, where the N=N stretching modes are most important. The high value of $\tilde{\nu}_v$ as well as the small inner reorganization energy λ_v together cause a small Huang–Rhys factor S [see Eq. (15)] and consequently allow analysis of the IV-CT band by Bixon–Jortner theory. Applying the Golden Rule expression to *syn*-**18**$^{+}$ through band-shape analysis yields reorganization parameters λ_o and λ_v, as well as the electronic coupling V.[162] However, the values obtained by Bixon–Jortner theory strongly depend on the value of the averaged vibrational mode $\tilde{\nu}_v$, which was treated as a constant input for the fits.

3.1.3. Bis(hydrazine) Radical Cations

As mentioned above, the bis(hydrazine) radical cation systems can be subdivided into two classes: bis(hydrazines) with aromatic bridge units and bis(hydrazines) with saturated bridge units. This classification is justified by the fact that the two types of bis(hydrazines) are linked differently to the spacer unit. Although both classes consist of the same redox centers in identical redox states, bis(hydrazines) with aromatic spacers are singly linked through one hydrazine nitrogen atom, while those with saturated spacer units are connected by both nitrogen atoms of each hydrazine redox center to the spacer unit. Thus, the latter ones are structurally more related to the bis(hydrazyl) MV systems.

3.1.3.1. Bis(hydrazine) Radical Cations with Saturated Bridge Units

Bis(hydrazine) radical-cation MV systems consist of two hydrazine redox centers where the donor center is a neutral hydrazine, and an oxidized, positively charged hydrazine moiety acts as the acceptor center. Three electrons and, therefore, also the positive charge are delocalized over both sp^2-hybridized nitrogen atoms of the acceptor. While the nitrogen atoms of the donor center have pyramidal structure (sp^3), the nitrogen centers of the acceptor are planar. In contrast to the bis(hydrazyl) MV systems in which charge and spin reside on different hydrazyl units (distonic radicals), the charge and spin share the same hydrazine units in the bis(hydrazine) radical cations. Although bis(hydrazine) MV systems with saturated spacers are structurally very similar to bis(hydrazyl) radical cations, they show very different ET behavior.

In an extension of the synthesis of bis(hydrazyl) MV compounds, bis(hydrazine) systems (Scheme 10) were synthesized starting from the corresponding bis(azo) compounds **13**. To obtain the bis(hydrazine) systems **19**, **20**, **22a**, and **22b** the bis(azo) compounds were converted into the bis(diazenium) dications **14** by a bis(*tert*-butylation) reaction.[51,160,161] Reaction with two equivalents of the corresponding organolithium compounds or Grignard reagents yielded the bis(hydrazine) (Scheme 11).[91,161] Compound **22c** can also be obtained from the corresponding bis(azo) species, whereupon the four phenyl substitutents can be introduced stepwise by reaction with four equivalents of phenyllithium in total.[91] However, the synthesis of **21** is more complex.[172] The corresponding monocationic MV compounds are generated

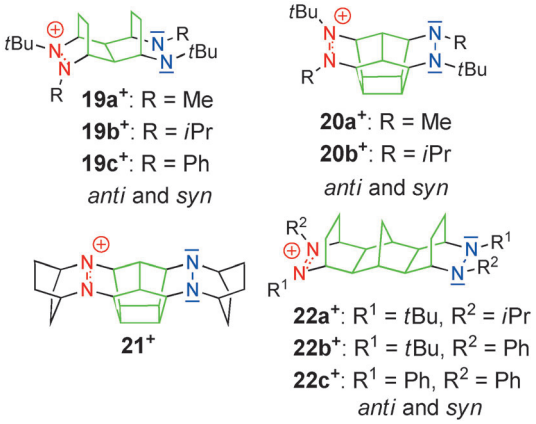

Scheme 10. Bis(hydrazine) radical cations $\mathbf{19}^+$–$\mathbf{22}^+$.

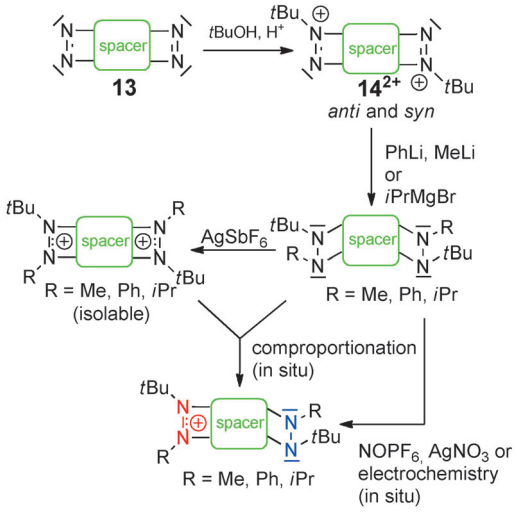

Scheme 11. Synthesis and formation of bis(hydrazine) radical cations with saturated spacers. Generation by comproportionation reaction is preferred for optical analyses. For the synthesis of bis(hydrazine) compounds $\mathbf{21}^+$ and $\mathbf{22c}^+$, see the text.

either by chemical oxidation or by electrochemistry. For optical analyses it proved advantageous to synthesize the MV species by a comproportionation reaction of equimolar amounts of neutral bis(hydrazines) **19**–**22** and bis(hydrazine) dications $\mathbf{19}^{2+}$–$\mathbf{22}^{2+}$.[91] The dications $\mathbf{19}^{2+}$–$\mathbf{22}^{2+}$ can be obtained in a straightforward manner by chemical oxidation of the neutral bis(hydrazines) with $AgSbF_6$ and they can be isolated as salts.[91,140] The generation of bis(hydrazine) MV compounds with saturated spacers is outlined in Scheme 11.

Cyclovoltammetric measurements[51,140] showed two reversible oxidation processes for the bis(hydrazines). The results of these measurements for some bis(hydrazines) compounds are listed in Table 3. As can be seen from these data, all the bis(hydrazines) can be oxidized to the corresponding radical monocations at low potentials, which confirms the relatively strong donor properties of hydrazine redox centers.

The values for the redox potential splitting ΔE between first and second oxidation process in Table 3 are significantly smaller than for the corresponding bis(hydrazyl) radical

Table 3: Redox potentials of bis(hydrazines) in acetonitrile versus a saturated calomel electrode.[51,140]

	E(Ox1) [V]	E(Ox2) [V]	ΔE [V]
anti-**19a**	+0.04	+0.18	0.14
anti-**19b**	−0.21	+0.04	0.25
anti-**20b**	−0.06	+0.19	0.25

cations (see Table 1), which, seen alone, implicates a smaller electronic coupling V in bis(hydrazine) MV compounds. However, as is shown below, this is not the case and again demonstrates the unreliability of ΔE values as a quantitative measure for the electronic coupling V. In some cases, the small difference in the redox potentials ΔE between the first and second oxidation processes of bis(hydrazines) causes problems in generating the MV monocation species selectively by chemical oxidation or electrochemistry. This is one of the reasons why the comproportionation method is preferred to generate MV systems.

Bis(hydrazines) proved to be much more suitable for dynamic ESR spectroscopic investigations because the ET rates of the bis(hydrazines) are smaller by about two orders of magnitude compared with the corresponding bis(hydrazyl) radical cations.[51,80] The main factor responsible for the significantly slower electron transfer in bis(hydrazine) systems is their relatively large inner reorganization energy λ_v. The main reason for this high inner reorganization energy is the fact that the donor and acceptor centers are hybridized significantly differently in a bis(hydrazine) radical cation and, therefore, have different geometries (Scheme 12).

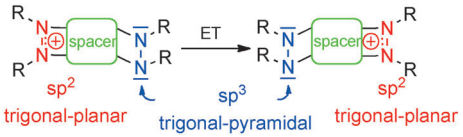

Scheme 12. ET in bis(hydrazine) radical cations: A relatively large structural change is associated with the ET process, which produces a large inner reorganization energy λ_v.

A further consequence of the large inner reorganization energy of bis(hydrazines) is that IV-CT bands are shifted to higher energy (blue-shifted) compared to the corresponding bands of the bis(hydrazyl) systems. For example, the absorption maximum $\tilde{\nu}_{max}$ of the IV-CT band of compound $\mathbf{20a}^+$ has an energy of 18250 cm^{-1} (548 nm) in acetonitrile, while the maximum of the corresponding bis(hydrazyl) MV compound $\mathbf{16}^+$ appears at much lower energy (8340 cm^{-1}, 1199 nm).[51] The electronic couplings derived from the IV-CT bands of bis(hydrazine) and bis(hydrazyl) MV compounds are quite similar for identical bridges (cf. compound $\mathbf{18}^+$ and $\mathbf{22a}^+$–$\mathbf{22c}^+$ in Table 4). This fact demonstrates the reliability of Hush theory for the analysis of IV-CT bands in different spectral regions.

The ET rate constants determined by Mulliken–Hush analysis (k_{opt}) and the ET rate constants determined by ESR measurements (k_{ESR}) are in an excellent agreement (Table 5) provided that electronic couplings V_L corrected for the

Table 4: ET parameters of some bis(hydrazine) radical cations determined by Mulliken–Hush analyses of the optical spectra in acetonitrile.[91] For comparison, the data of bis(hydrazyl) radical cation **18**$^+$[91] are also listed.

	$\tilde{\nu}_{max}$ [cm^{-1}]	λ_o [cm^{-1}]	λ_v [cm^{-1}]	μ_{ab} [D]	V_{12} [cm^{-1}][a]
21$^+$	16300	2000	14300	1.95	1490
syn-**19b**$^+$	18000	4900	13100	1.73	1460
anti-**22a**$^+$	21100	7900	13100	0.95	640
syn-**22a**$^+$	21100	7900	13100	0.94	630
anti-**22b**$^+$	17400	7600	9800	1.14	620
syn-**22b**$^+$	17900	8400	9300	1.11	630
22c$^+$	11200	4200	7000	1.12	370
18$^+$	13100	7600	5600	1.26	560

[a] Calculated using Equation (8) (Section 2).

Table 5: Comparison of ET rate constants determined by ESR measurements (k_{ESR}) and optical analyses (k_{opt}) of the IV-CT bands.[80]

	k_{ESR} [$\times 10^8$ s^{-1}]	V_L [cm^{-1}][a]	k_{opt}/k_{ESR}
21$^+$	1.3	1180	1.1
20b$^+$	1.3	880	1.6
anti-**19b**$^+$	1.1	1060	0.9
syn-**19b**$^+$	1.0	1060	0.9

[a] V_L = refractive-index-corrected electronic coupling.

refractive index [i.e. using the refractive index corrected equation for the determination of the transition moment, see Eq. (9)] are used for the semiclassical adiabatic calculation of rate constants from the optical data.[80]

3.1.3.2. *Bis(hydrazine) Radical Cations with Aromatic Bridge Units*

The most apparent difference between (bis)hydrazine MV compounds with aromatic spacers and their analogues with saturated bridge units is the type of linkage between the cationic (acceptor) and the neutral (donor) hydrazine redox centers through the bridging units. In fact, the aromatic spacers are connected only to one nitrogen atom of the hydrazine redox centers. It is remarkable that all these systems **23**$^+$–**31**$^+$ (Scheme 13) are composed of nearly identical bicyclic hydrazine redox centers and, therefore, this class of organic MV compounds is a good model system for the investigation of the influence of the bridge unit on the ET behavior.

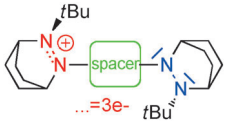

Bis(hydrazines) with unsaturated spacers can be synthesized in a straightforward way: the key step of the syntheses is the reaction of diazenium iodides **32** with the corresponding dilithio compounds of the bridge units which yields the neutral bis(hydrazine) system. The radical cations can then be generated in situ by chemical oxidation with silver nitrate or by a comproportionation reaction of a 1:1 mixture of the neutral and dicationic bis(hydrazine) compounds (Scheme 14).

The electronic coupling in bis(hydrazine) radical cations with aromatic spacers is significantly higher than that in their saturated analogues or the bis(hydrazyl) MV compounds with the same number of bonds between the redox centers. This is

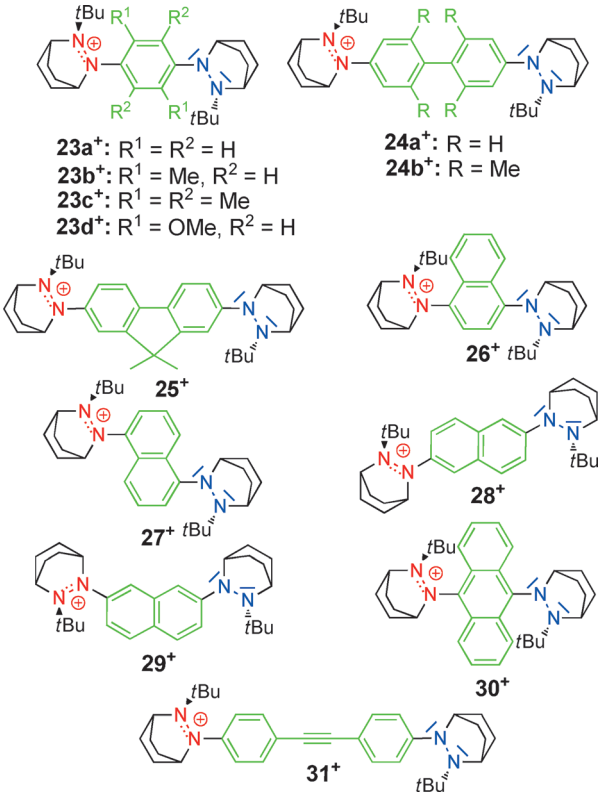

Scheme 13. Bis(hydrazine) radical cations **23**$^+$–**31**$^+$ with aromatic spacer units.

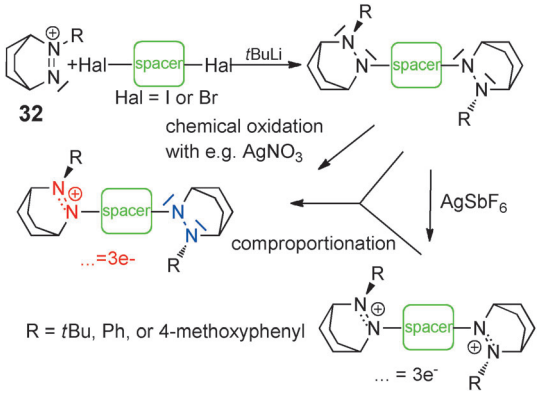

Scheme 14. Synthesis and formation of the radical cations of bis(hydrazines) with aromatic bridge units.

not surprising given the fact that unsaturated spacers show much smaller β values and therefore are better mediators for ET processes [see Eqs. (18) and (19) in Section 2). In general, the electronic coupling V is so strong in MV compounds with a simple phenylene spacer unit that they usually belong to Robin–Day class III, where the charge is delocalized over both redox centers and the phenylene spacer. A very prominent example is the radical cation of tetramethyl-*p*-phenylenediamine (TMPD, **33**$^+$; Scheme 15).[115] However, the corresponding bis(hydrazine) radical cation **23a**$^+$ is clearly a class II system, where the charge is localized at one hydrazine redox center. There are two main reasons for

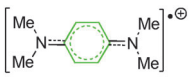

TMPD$^+$
33^+

Scheme 15. Tetramethylphenylenediamine radical cation (TMPD$^+$), an example of a typical class III compound.

this behavior: 1) the conjugation of the redox centers is reduced by a twist of the lone pairs of electrons on the nitrogen atoms and the π system of the spacer and, 2) hydrazine redox centers have significantly higher inner reorganization energies than, for example, the amine redox centers in TMPD.

Bis(hydrazine) MV compounds with aromatic bridge units are suitable systems for the investigation of the effect of the bridge on the ET behavior. As can be seen from Table 6, the electronic coupling V of the mixed-valence bis(hydrazine) radical cations decreases as the substitution of the phenyl spacer in **23a**$^+$–**23c**$^+$ increases. This trend is due to an increasing twist of the nitrogen lone pair of electrons and the π system of the spacer unit, which lowers the electronic communication between the redox centers significantly. This allows the determination of the ET rate constants for **23b**$^+$ and **23c**$^+$ by temperature-dependent ESR measurements. The ET process in **23a**$^+$ is too fast even at low temperatures (Table 6).[81] This is even more evident in bis(hydrazines) **24a**$^+$ and **24b**$^+$ with biphenyl bridging units. The electronic coupling between the redox centers decreases as the spacer length increases (Table 6). However, the twist of the two phenylene rings of the spacer unit also has an important effect. A significant electronic coupling was extracted by Hush analysis of an IV-CT band of **24a**$^+$ with a nonsubstituted biphenyl spacer, while no IV-CT is visible at all in the tetramethyl-substituted MV compound **24b**$^+$.[91] Thus, all the evidence indicates that **24b**$^+$ is either a class I compound or at least has a very small electronic coupling V. This behavior can only be explained by an almost orthogonal twist of the two phenylene subunits of the spacer induced by the sterical hindrance of the methyl substituents. This interpretation is confirmed by the fact that the electronic coupling in compound **25**$^+$, where the biphenyl moiety is forced to be planar by a methylene group (fluorene spacer), is even stronger and the barrier for thermal electron transfer ΔG^* is smaller than in **24a**$^+$ (Table 6).

Another factor which has a direct impact on the electronic coupling between the two hydrazine redox centers is the length of the π system in the bridging unit. The electronic coupling decreases when changing the spacer from a phenylene in **23a**$^+$ to a naphthalene in **26**$^+$ because of a larger twist between the nitrogen lone pairs of electrons and the π system of the bridging unit (Tables 6 and 7). This effect is overcompensated when changing to an anthracene bridge unit in **30**$^+$. The ET rate of **30**$^+$ is more than 100-fold larger than that of **23c**$^+$. At first sight this behavior is surprising because **30**$^+$ shows comparable twist angles (66.7° and 53.2°)[173] to **23c**$^+$ (66.2° and 50.2°)[81] and, therefore, should suffer from very similar sterical hindrance by the spacer subunit. However, the main effect of introducing a larger π system in the bridge unit is to raise the HOMO energy of the bridge. The bridge might then participate actively as a third redox center[112,122] in a hopping mechanism of the ET process (see also Section 2) or might lead to a better mixing of the donor and acceptor orbitals because of a better energetic match. Unfortunately, Hush analysis of **30**$^+$ is cumbersome and the interpretation of spectroscopic data is not straightforward.

The naphthalene-bridged bis(hydrazine) radical cations **26**$^+$–**29**$^+$ demonstrate, in particular, that the electronic coupling V not only depends on the distance between the redox centers and on sterical effects between structural moieties but is also sensitive to electronic effects. Despite the nearly the same distance between the redox centers in **26**$^+$ and **27**$^+$ as well as in **28**$^+$ and **29**$^+$, the electronic coupling and, therefore, the ET rate constants as well as the spectroscopically derived ET parameters are rather different (Table 7). This behavior can mainly be traced back to the type of substitution pattern (Kekulé in **26**$^+$ and **28**$^+$ and non-Kekulé in **27**$^+$ and **29**$^+$).[176]

Table 6: IV-CT band data and Hush analysis derived reorganization energies as well as rate constants determined by temperature-dependent ESR measurements of bis(hydrazine) MV compounds with aromatic spacer units in acetonitrile.

	$\tilde{\nu}_{max}$ [cm^{-1}]	λ_o [cm^{-1}]	λ_v [cm^{-1}]	V [cm^{-1}]	ΔG^* [cm^{-1}]	k_{ET} [s^{-1}]
23a$^+$	13200[a]	7650[b]	5600[b]	2510[b,c]	1235[b,c]	too fast
23b$^+$	14200[c]	6220[b]	8170[b]	1710[b]	1910[b]	5.2×10^8[b]
23c$^+$	14100[a,c]	5420[b]	8840[b]	1150[b,c]	2060[b]	8.1×10^8[b]
23d$^+$	12800[d]	–	—	–	–	–
24a$^+$	15200[a,c]	–	–	1080[c]	2600[c]	1.3×10^8[c,e]
25$^+$	13550[c]	–	–	1430[c]	2170[c]	2.4×10^8[c,f]

[a] See Ref. [91]. [b] See Ref. [81]. [c] See Ref. [174]. [d] See Ref. [175]. [e] T = 328.1 K. [f] T = 273.1 K.

Table 7: IV-CT band data and Hush analysis derived parameters, as well as calculated rate constants of bis(hydrazines) **26**$^+$–**29**$^+$.[176]

	Solvent	$\tilde{\nu}_{max}$ [cm^{-1}]	V [cm^{-1}]	ΔG^* [cm^{-1}]	k_{ET} [s^{-1}][a]
26$^+$	acetonitrile	12640	1510	1820	32.3×10^8
27$^+$	1,2-dichloroethane	13060	620	2510	0.9×10^8
28$^+$	acetone	13300	1300	2170	5.2×10^8
29$^+$	acetonitrile	18560	230	3400	0.004×10^8

[a] Calculated for 25 °C.

MV compounds **23d**$^+$ and **31**$^+$, which are both class II systems, were used for a qualitative evaluation of the polarity of ionic liquids.[175] The systematic dependency of the IV-CT band energy on solvent polarity means that MV class II compounds can be used to characterize the polarity of solvents. However, a Hush analysis of the IV-CT bands of these compounds has not yet been published.

Quite recently Nelsen and Schultz synthesized a series of MV radical cations with aryl-substituted redox centers (**34**$^+$–**42**$^+$; Scheme 16). The replacement of the *tert*-butyl substituent by an aromatic one results in a much larger electronic coupling between the redox centers as a consequence of a reduced twist between the nitrogen lone pairs of electrons and the π system of the bridging units.[177]

The increase in the electronic communication between the redox centers is in fact so strong that all the compounds **34**$^+$–**37**$^+$ lie at the boundary of Robin–Day classes II and III.[177]

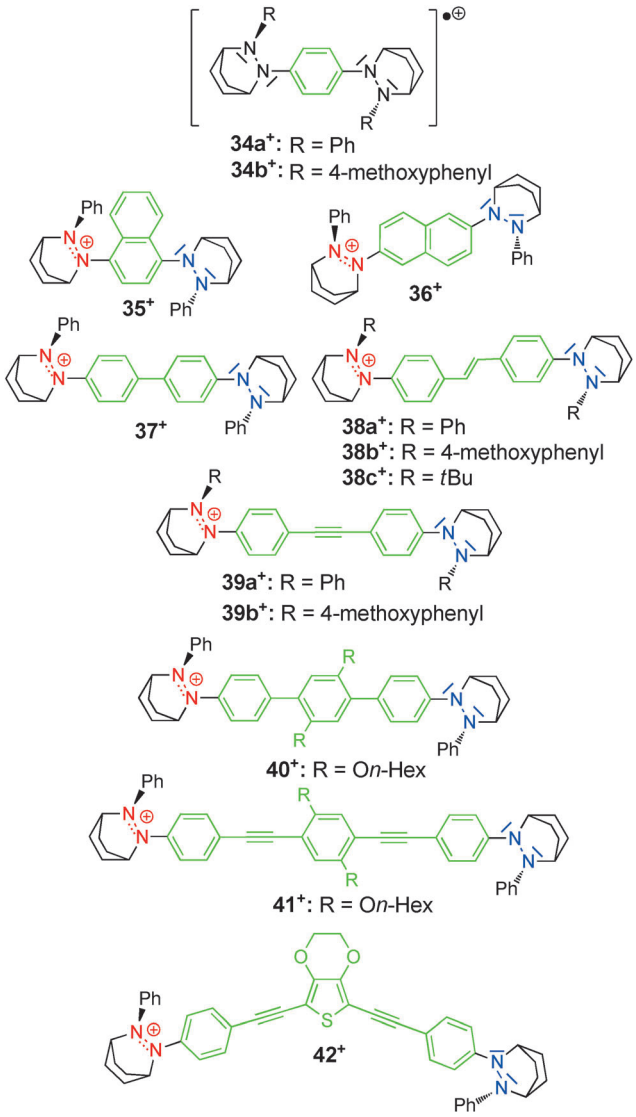

Scheme 16. Bis(hydrazine) radical cations **34**$^+$–**42**$^+$ with aromatic spacer units.

An analysis of the IV-CT bands in solvents of different polarity results in the assignment of compounds **34a**$^+$ and **34b**$^+$ as being totally delocalized class III systems. Even **37**$^+$ lies at the boundary in dichloromethane, while the *t*Bu-substituted analogue **24a**$^+$ is definitely a class II compound. Only in very polar acetonitrile, with accordingly a very large solvent reorganization energy λ_o, is the charge localized and **37**$^+$ is a class II compound. A classification of **35**$^+$ and **36**$^+$ by IV-CT band analysis was too ambiguous to be definite.

The aromatic hydrazine substituents in **38**$^+$–**42**$^+$ result in the electronic coupling being strong enough to investigate the ET dynamics by ESR measurements, even with these large bridging units.[178] The tolan and stilbene bridge units, and in some cases the phenyl substituents at the hydrazine redox centers, were deuterated so as to obtain ESR spectra with as little hyperfine interactions as possible. This enabled measurements of the ET rate constants of **38**$^+$–**40**$^+$ (see Table 8), but the ET rate of **41**$^+$ with its large bridge (17 bonds) was too slow to be evaluated quantitatively.

Table 8: Rate constants k_{ET} measured by temperature-dependent ESR spectroscopy of the corresponding deuterated compounds and optical data from IV-CT band analysis.[178]

	$\tilde{\nu}_{max}$ [cm^{-1}]	V [cm^{-1}]	λ [cm^{-1}]	Rel. k_{ET}[e]
31$^+$[a]	15600			
39a$^+$[b]	12460	850	12330	$1 = 6.68 \times 10^7$ s^{-1}
38c$^+$[a]	13600			
37$^+$[b]	11660	1280	11550	10.8
40$^+$[c]	11630	840	11030	0.64
39b$^+$[b]	12840	940	12570	0.39
38a$^+$[a]	9700			
38b$^+$	10700[a]			6.2[b]
42$^+$[d]				1.8

[a] In acetonitrile. [b] In butyronitrile. [c] In 1,2-dichloroethane. [d] In dichloromethane; no optical analysis was possible. [e] Relative to **39a**$^+$.

As can be seen from the data in Table 8, the ET rate for stilbene-bridged compound **38b**$^+$ is significantly higher than that of the corresponding tolan-bridged system **39b**$^+$. The IV-CT band analyses also suggest that the electronic communication mediated by stilbene bridges is stronger than by tolan bridges (the N-N distance between the redox centers is nearly the same). Nelsen and Schultz interpret this effect by a drastic change of the solvent reorganization energy λ_o, that is, the two hydrogen atoms of the ethylene spacer unit reduce the solvation of the spacer, which directly yields a smaller solvent reorganization energy. This interpretation is corroborated by the lower energies of the IV-CT bands in the stilbene-bridged MV compounds.[178]

In summary, bis(hydrazine) MV compounds provided the basis for detailed investigations by optical, ESR spectroscopic, and computational methods. These studies clearly show that the concept of Mulliken–Hush theory as a (semi)classical adiabatic theory allows at least a semiquantitative, if not quantitative, analysis of the ET behavior of organic MV systems.

3.1.4. Dinitroaromatic Radical Anions

ET processes in dinitroaromatic radical anions were investigated in the early 1960s by ESR spectroscopy. The main intensions of these studies were to find out whether the

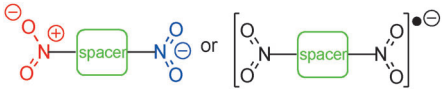

dinitroaromatic radical anions were localized or delocalized systems and to assess those factors that govern their ET behavior. Since these studies did not apply optical methods and the concept of mixed valency was unknown in those days, we concentrate on more current investigations on this class of organic MV compounds in which the concepts of mixed valency together with temperature-dependent ESR studies were applied.

As indicated above, all the dinitroaromatic MV compounds investigated so far lie near the class II/III boundary.

This may be due to the fact that strongly localized nitroaromatic anions (those with a large spacer) are too unstable to be investigated by the usual methods. The main focus of current investigations is to determine the factors which cause delocalization of the charge (and spin) in a dinitro radical anion over both nitro groups and the spacer unit or which result in a localization of the charge (and spin) on one nitro redox moiety. For this, Mulliken–Hush analyses of the IV-CT bands of these compounds were used in particular. An important precondition for Mulliken–Hush analyses is the accurate measurement of the absorption spectra, which is not straightforward for dinitro radical anions because of their moderate stability in solution.

Dinitroaromatic radical anions were generated either electrochemically or from their neutral precursors by chemical reduction with sodium/mercury amalgam. A large excess of a cryptand is added to avoid ion-pairing effects between the radical anions and the, for example, sodium cations by shielding the small sodium cation.[179,180]

As described in Section 2.4, the ratio of total reorganization energy λ to electronic coupling V determines whether a compound is assigned to Robin–Day class II (localized, $\lambda > 2V$) or class III (delocalized, $\lambda < 2V$). While λ can be influenced by the solvent polarity, the electronic coupling V between the MV states is mainly determined by the aromatic bridge and the substitution pattern. In Kekulé-substituted compounds such as **43**$^-$ (Scheme 17), the electronic coupling

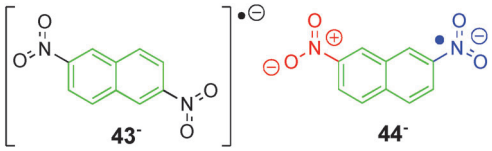

Scheme 17. Dinitroaromatic radical anions **43**$^-$ and **44**$^-$ with different substitution patterns.

V is so strong that the charge is even delocalized in polar solvents such as DMF. In non-Kekulé-substituted compounds, the electronic coupling is much weaker, which often causes the systems to have a localized charge (and spin) density at one nitro group. This fact can exemplarily be shown by comparison of the optical spectra of radical ions of 2,6-dinitronaphthalene (**43**$^-$) and of 2,7-dinitronaphthalene (**44**$^-$; Scheme 17).[181] While the former is clearly a class III system in dimethylformamide (DMF) with a very intense ($\varepsilon > 55\,000\,\text{M}^{-1}\text{cm}^{-1}$) IV-CT band arising from a very strong electronic coupling $V = 8500\,\text{cm}^{-1}$ caused by the Kekulé substitution pattern, the non-Kekulé-substituted isomer **44**$^-$ is clearly a class II MV compound with a broad and much less intense ($\varepsilon = 215\,\text{M}^{-1}\text{cm}^{-1}$) IV-CT band in the same solvent. Furthermore, the IV-CT band of **43**$^-$ is quite narrow and shows vibronic fine structure which is a typical indicator of class III compounds.

Analysis of the optical spectra of a series of dinitro radical anions **45**$^-$–**52**$^-$ (Scheme 18) with slightly different spacer lengths and different substitution patterns indicate class III behavior in DMF.[182]

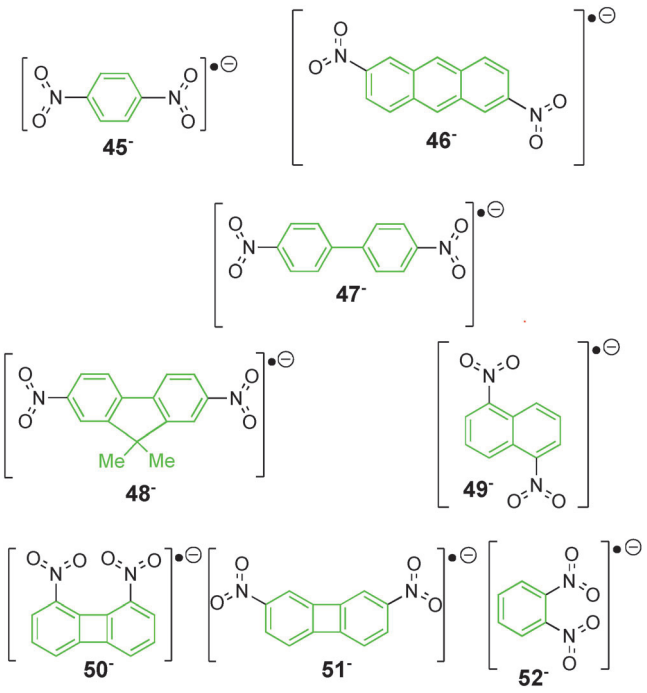

Scheme 18. Dinitroaromatic radical anions **45**$^-$–**52**$^-$ with class III character in DMF.

The band maxima $\tilde{\nu}_{max}$, which are twice the electronic coupling ($\tilde{\nu}_{max} = 2V$) in a Marcus–Hush two-state model for class III species, are listed in Table 9. As can be seen from this

Table 9: IV-CT band data and electronic coupling of class III compounds **43**$^-$ and **45**$^-$–**52**$^-$ in DMF.[182,183]

	$\tilde{\nu}_{max}$ [cm^{-1}]	ε [M^{-1}cm^{-1}]	V [cm^{-1}][a]	Bonds[b]
43$^-$	8500	55 200	4250	7
45$^-$	10 820	20 300	5410	5
46$^-$	7380	39 900	3690	9
47$^-$	6900	9920	3450	9
48$^-$	6790	16 470	3400	9
49$^-$	6800	6380	3400	5
50$^-$	6800	–[c]	3400	5
51$^-$	7070	–[c]	3540	7
52$^-$	9440	–[c]	4720	3

[a] Assuming $V = \tilde{\nu}_{max}/2$ for class III compounds. [b] Number of bonds of the shortest pathway from one nitrogen atom to the other one. [c] Not determined.

Table, the electronic coupling for bridges with identical substitution patterns generally decreases as the distance between the redox centers increases (**45**$^-$ > **43**$^-$ > **46**$^-$). In those cases where the substitution pattern is not identical, the geometrical distance between the redox centers is no longer the only determining factor for electronic coupling. In addition to steric effects, electronic effects also determine the coupling through the spacer (Kekulé versus non-Kekulé pathways[182]).

The electronic coupling in the twisted[184] dinitro aromatic compound **47**$^-$ is nearly the same as in the fluorenediyl compound **48**$^-$, where there is no twist around the central

biaryl C–C bond. This behavior is in contrast to the corresponding hydrazine radical cations **24a**$^+$, **24b**$^+$, and **25**$^+$ and can be traced back to the fact that the energy gap between the SOMO of the donor (nitro) moiety and the LUMO of the spacer unit is small in radical anion systems. This orbital interaction mainly determines the electronic communication, which apparently overcompensates the influence of the twist.[182] Nelsen et al. argued that the Marcus–Hush model is inappropriate for studying class III compounds and these authors used new approaches such as the "dianion in anion geometry (DAG)" method and the "neighboring orbital model" to analyze the IV-CT bands in class III dinitro radical anions.[183] Both methods produce significantly higher values for the electronic coupling V than the Marcus–Hush model. From our viewpoint, there is a basic difference in these models, as the Marcus–Hush model refers to diabatic electronic states that can be defined in different ways (e.g. that the transition moment between diabatic states vanishes), while the "neighboring orbital model" rests on orbitals within a one-electron approximation. Thus, these two-models do not necessarily yield the same coupling, and the couplings derived by each approach are only useful in comparisons within the same model.

There are two possibilities for dinitroaromatic radical anions that lie close to the class II/III boundary to cross from delocalized to localized systems: 1) to lower V by, for example, increasing the spacer length, using non-Kekulé substitution patterns, or inducing twists between the redox centers or within the bridge and 2) to increase λ by increasing the solvent polarity. In fact the pseudo-*para*-dinitro-[2.2]paracyclophane radical anion **53**$^-$ (Scheme 19) is so

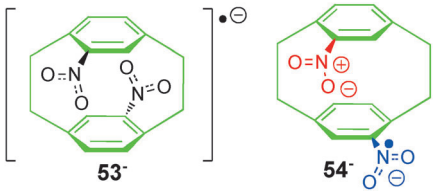

Scheme 19. Isomeric dinitroparacyclophane radical anions **53**$^-$ and **54**$^-$.

close to the boundary that changing the solvent from DMF to acetonitrile causes a crossing from class III to II. However, the pseudo-*ortho* isomer **54**$^-$ (Scheme 19) is a localized class II system in acetonitrile as well as in DMF, and is much far away from the boundary.[99] The strong electronic coupling particularly in **53**$^-$ was taken as proof for the existence of two different ET pathways in paracyclophanes: a through-bond and a through-space mechanism. Since the corresponding dinitrobenzenes with ethylene spacers show a very slow ET behavior,[40] it is the through-space mechanism which dominates the ET behavior in paracyclophane systems. It could be shown by MO computations on **53**$^-$ and **54**$^-$ that through-space electronic communication of the pseudo-*para* isomer is much more favored than in the *ortho* isomer as a result of better orbital interactions.[99]

Scheme 20 shows three dinitroaromatic radical anions **55**$^-$–**57**$^-$ which are also near the class II/III boundary. Despite the fact that all compounds show a Kekulé substitution pattern with 11 bonds between the nitro nitrogen atoms, their

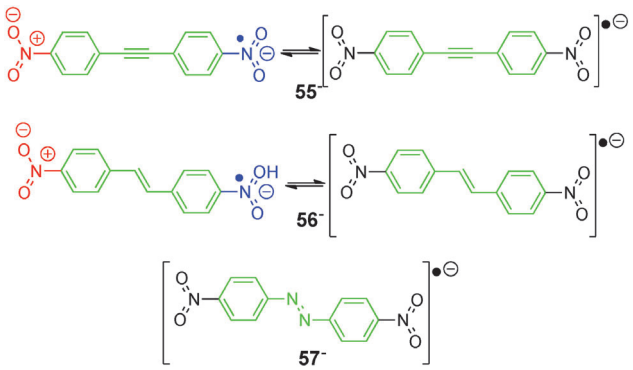

Scheme 20. Dinitroaromatic radical anions **55**$^-$, **56**$^-$, and **57**$^-$ with 11 bonds between the nitro redox centers.

ET behavior is quite different. While **55**$^-$ and **56**$^-$ with stilbene and tolan spacer units switch from class III behavior in moderately polar solvents such as tetrahydrofuran (THF) and hexamethyl phosphoramide (HMPA) to class II in very polar solvents such as acetonitrile or DMF, compound **57**$^-$ with an azo spacer unit is a delocalized system (class III) in all the solvents investigated. This behavior implicates a much stronger electronic coupling in **57**$^-$, which is confirmed by an analysis of the absorption spectra of **55**$^-$–**57**$^-$ in THF in which they all show class III characteristics (Table 10).[185] Nelsen

Table 10: IV-CT band data and electronic coupling of **55**$^-$–**57**$^-$ in THF, where all the compounds belong to class III.[185]

	$\tilde{\nu}_{max}$ [cm^{-1}]	ε [M^{-1} cm^{-1}]	V [cm^{-1}][a]
55$^-$	5860	11 700	2930
56$^-$	6530	15 300	3265
57$^-$	9460	22 200	4730

[a] Calculated by the Marcus–Hush two-state model ($V = \tilde{\nu}_{max}/2$).

et al. attributed this behavior to the lower reduction potential of the azo bridge unit in **57**$^-$, which again results in a lower energy gap and therefore in an increased electronic communication. Furthermore, the electronic coupling of the tolan-bridged compound **55**$^-$ is smaller than in the stilbene-bridged **56**$^-$, a fact which was also found in the analysis of the corresponding tolan- and stilbene-bridged bis(triarylamine) radical cations **3**$^+$ and **12**$^+$ by Barlow et al.[158] In more polar solvents, such as acetonitrile, both **55**$^-$ and **56**$^-$ are class II compounds with broad IV-CT bands which show the typical solvatochromic behavior of localized MV compounds. However, a simple two-state Marcus–Hush analysis of these bands results in electronic couplings which seem to be far too small for such compounds (Table 11). Nelsen et al. pointed out that the simple Marcus–Hush model is not suitable for the analysis of MV compounds very close the class II/III boundary because of non-Gaussian shaped IV-CT bands in these cases.

Table 11: Class II Marcus–Hush IV-CT band analysis of dinitroaromatic radical anions near the class II/III boundary in acetonitrile.[103,185]

	$\tilde{\nu}_{max}$ [cm^{-1}]	V [cm^{-1}]
47^{-}[a]	10260	930
48^{-}[a]	9700	1100
55^{-}[a,b]	11300	750
56^{-}[a,b]	9680	545
58^{-}[a]	12800	540
59^{-}[a]	10300	710
60^{-}[a]	9880	900
61^{-}[a]	9730	445

[a] Ref. [103]. [b] Ref. [185].

The gradual transition from delocalized to localized was also observed in dinitroaromatic radical anions **58**$^{-}$–**61**$^{-}$ (Scheme 21). The absorption spectra of these compounds

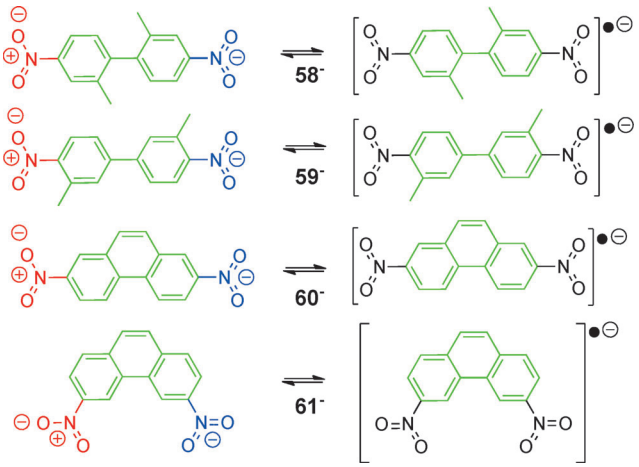

Scheme 21. Dinitrobiphenyl and dinitrophenanthrene radical anions very close the class II/III boundary.

clearly show that these compounds are mainly charge delocalized in nonpolar and mainly charge localized in polar solvents; but it is also apparent from the absorption spectra that the question is not whether these compounds are class II or III in a given solvent but to what mole fraction they are. This is because the absorption spectra recorded in nearly all solvents show typical evidence for both categories. A Marcus–Hush analysis of the IV-CT bands for class II compounds was only applicable in the strongly polar solvent acetonitrile, where the compounds show neither or nearly no class III character. The results of these IV-CT band analyses are given in Table 11.

As can be seen from Table 11, the values of the electronic coupling V determined by a Marcus–Hush two-state band analysis show the expected trends. The electronic coupling in the series of biphenylene-bridged radical anions decreases (**48**$^{-}$ > **47**$^{-}$ > **59**$^{-}$ > **58**$^{-}$) as the biaryl twist increases. The methyl substituents in **59**$^{-}$ do not influence the biaryl twist angle but influence the electron distribution compared to non-methylated **47**$^{-}$.[103] For the tolan-bridged (**55**$^{-}$) and stilbene-bridged (**56**$^{-}$) radical anions the electronic couplings in the localized systems in MeCN (Table 11) show the opposite trend as for the delocalized species in THF (Table 10) when both are analyzed by a two-state Marcus–Hush model.

As mentioned above, one weak point of the Marcus–Hush model when applied to MV compounds near the class II/III boundary is that asymmetric IV-CT bands (so-called cut-off effects) cannot be evaluated accurately.[79] Another effect which hampers the straightforward analysis of dinitro radical anions by a Marcus–Hush approach is that the measured spectra often show a superposition of the narrow CT band (with vibrational fine structure) of the delocalized species and the broad IV-CT band of the localized species. Nelsen et al. extracted the IV-CT bands of some localized dinitro radical anions by subtracting the corresponding class III spectra. These "pure" class II spectra clearly show the expected cut-off effect which is normally disguised by the concurrently measured class III spectrum.[103]

Quite recently Nelsen et al. published rate constants determined by temperature-dependent EPR spectroscopy of some dinitroaromatic radical anions near the class II/III boundary. However, the number of compounds for which this method is applicable is strongly limited by the ESR timescale.[186]

In summary, dinitroaromatic radical anions are the class of organic MV compounds of choice for the investigation of strongly coupled MV systems close to the class II/III boundary. The detailed studies available on this class of organic MV compounds allows a closer look at the effects MV compounds show near the boundary and demonstrate both the difficulties and problems the analysis of these compounds entail as well as the opportunities to achieve a better understanding of their ET behavior in general.

3.1.5. *Bis(triarylamine) Radical Cations*

Bis(triarylamine) radical cations are one of the most intensively studied classes of organic MV compounds. This lies in the fact that triarylamine redox centers display

excellent properties which facilitate a detailed optical investigation of their ET behavior. Furthermore, they are widely used as hole-transport components in photoconductors and light-emitting devices (see Section 4) and, hence, were one of the first types of organic MV compounds with possible practical applications.

Bis(triarylamine) radical cations consist of two triarylamine redox centers, one neutral when the formal oxidation number at nitrogen is −III and a radical cationic one with the formal oxidation number −II. These MV compounds can be

easily generated either by chemical oxidation or by anodic oxidation starting from the neutral bis(triarylamine). Triarylamines have to be substituted in all *para*-positions to guarantee the oxidation process is reversible, and prevent the dimerization processes that cause irreversibility of the oxidation processes for more localized class II systems.[187] Highly stabilized, delocalized class III systems may also be stable without *para*-protecting groups.[114,115,187] In addition to this protective effect, *para*-substituents not only effect the stability but also allow the oxidation potential of the triarylamine redox centers to be tuned over a wide range.[188,189] Furthermore, the optical absorption properties of bis(triarylamines) proved to be advantageous because the neutral species as well as the radical cation and dication show characteristic bands (at ca. 350 nm for M and 750 nm for M^+) which usually do not overlap too strongly with the broad IV-CT bands, which are shifted further in the NIR region. Therefore, bis(triarylamine) radical cations are very suitable systems for IV-CT band analyses by optical methods. The low energy of these IV-CT bands is due to a relatively small inner reorganization energy λ_v, which in turn is a consequence of the small structural changes between the neutral and cationic triarylamine redox centers.

A further advantage of bis(triarylamines) is their relatively straightforward synthesis, which is of importance for commercial applications. Triarylamine centers can easily be built up by palladium-catalyzed Buchwald–Hartwig amination reactions or by copper-catalyzed Ullmann condensation reactions[190] from the corresponding *para*-substituted haloarenes and aniline derivatives (Scheme 22). The high stability of triarylamine centers permits further functionalization and the attachment of various spacer moieties under various reaction conditions. The straightforward syntheses allow the systematic variation of the type and the length of the bridging unit and allow the distance dependence of their ET behavior to be investigated. A series of bis(triarylamine) radical cations $\mathbf{1}^+$–$\mathbf{5}^+$ and $\mathbf{62}^+$–$\mathbf{63}^+$ with systematically increasing distance between the redox centers was synthesized in our research group (Figure 11). All the radical cations were generated by chemical oxidation with $SbCl_5$ in dichloromethane[123] or by spectroelectrochemistry[79] and show a broad and intense band in the NIR region of the absorption spectra. The bis(triarylamines) with very small N–N distances $\mathbf{1}^+$–$\mathbf{3}^+$ and $\mathbf{62}^+$ are all very close to the class II/III boundary.

A systematic investigation of compounds $\mathbf{62}^+$ and $\mathbf{1}^+$–$\mathbf{3}^+$ (Scheme 23) by hybrid density functional methods combined with a continuum solvent model proved the significant influence of the solvent on the degree of charge delocalization in these organic MV compounds.[147] As for dinitroaromatic radical anions (see Section 3.1.4), the true electronic nature of bis(triarylamine) MV compounds near the class II/III boundary is not only a property of the compound itself but also depends on the solvent polarity, which in many cases proves decisive. Quantum-chemical calculations showed that compound $\mathbf{1}^+$ is definitely a class III system even in very polar solvents. In contrast, $\mathbf{2}^+$ and $\mathbf{3}^+$ switch from delocalized to localized character as the solvent polarity increases.

The shape of the IV-CT bands of $\mathbf{1}^+$–$\mathbf{4}^+$ and $\mathbf{62}^+$ (Scheme 23) confirm the changeover from class III to class II.

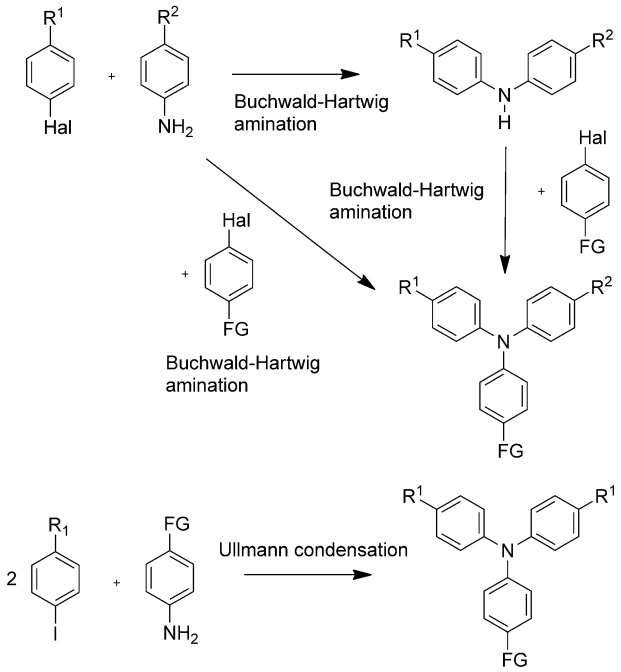

Scheme 22. Two routes for the synthesis of functionalized triarylamine centers with one functional group (FG) where spacer moieties can be attached. If the two *para*substituents R^1 and R^2 are different, both a step by step and a one-pot Buchwald–Hartwig amination may be followed. Alternatively, particularly when R^1 and R^2 are identical, a one-step copper-catalyzed Ullmann condensation reaction is preferred.

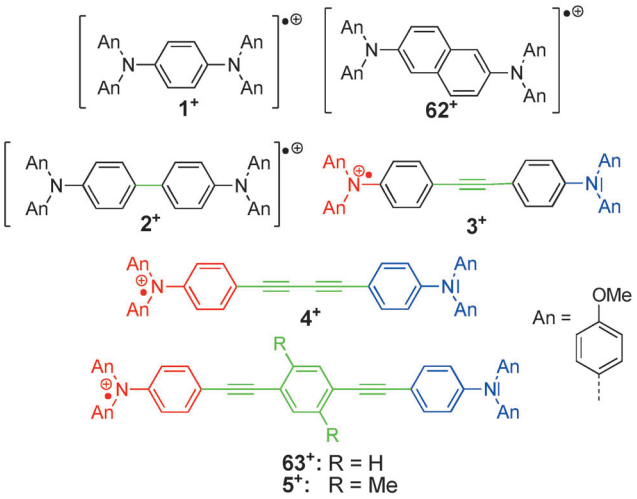

Scheme 23. Bis(triarylamine) radical cations $\mathbf{1}^+$–$\mathbf{5}^+$, $\mathbf{62}^+$, and $\mathbf{63}^+$. The increasing length of the spacer unit causes a changeover from class III to class II character.

The distance between the redox centers (N–N distance) in the series $\mathbf{4}^+$–$\mathbf{1}^+$ decreases, while the asymmetry on the low energy side of the IV-CT bands increases (given by the ratio of the bandwidth at half-height of the high-energy side and the low-energy side $\nu_{1/2}$(high)/$\nu_{1/2}$(low), see Table 12).[79] Along with this typical cut-off effect, the electronic coupling V decreases as the spacer length increases. We found a linear correlation between ln$V$ and the number of bonds between the nitrogen atoms for compounds $\mathbf{1}^+$–$\mathbf{5}^+$ (see Figure 11) with

Table 12: IV-CT band shape analysis, electronic coupling, and redox potentials of 1^+–5^+ and 62^+–63^+ in dichloromethane.

	$\tilde{\nu}_{max}$ [cm^{-1}][a]	ε [$M^{-1}cm^{-1}$][a]	$n-1$[b]	V [cm^{-1}]	$\nu_{1/2}$(high)/ $\nu_{1/2}$(low)	ΔE [mV][c]
1^+	9530	22680	4	4300[d]	1.76	495
62^+	7620	30110	6	–[e]	1.73	365
2^+	6360	28040	8	2800[f]	1.45	220
3^+	6190	21850	10	2400[g]	1.20	150
4^+	7550	8050	12	1790[h]	1.00	100
63^+	9490	4570	16	1000[j]	1.00	60
5^+	7500[i]	4660[i]	16	1220[k]	–	50

[a] Measured by spectroelectrochemistry.[79] [b] n = number of bonds between the two nitrogen centers. [c] $\Delta E = |E_{1/2}(Ox1) - E_{1/2}(Ox2)|$ in dichloromethane/0.1 M tetrabutylammonium hexafluorophosphate solution, scan rate = 250 mVs^{-1}.[79] [d] Determined by the Mulliken–Hush two-mode model.[116] [e] Not determined at the same level of accuracy as the other compounds. [f] Determined by the Mulliken–Hush two-mode model.[114] [g] Determined by vibronic coupling theory analogously to 1^+ and 2^+.[123] [h] Determined by the Mulliken–Hush two-mode model.[123] [i] Cation generated by chemical oxidation.[123] [j] Determined by a GMH three-state model.[112] [k] Determined by a GMH three-state model.[123]

a β value of 0.16 $Å^{-1}$. This value is very small even for unsaturated bridge units, and indicates that the hole transfer in these systems is mediated by a superexchange mechanism.[123] The results of the band-shape analyses of compounds 1^+–5^+ and 62^+–63^+ are listed in Table 12.

The systematic increase in V in the series 5^+–1^+ (Table 12) is also reflected by the oxidation potential splittings ΔE, as determined by cyclic voltammetry.[79,123] Even though, as argued above, the redox potential splittings are not a quantitative measurement of the electronic coupling, this example demonstrates impressively the use of ΔE as a semiquantitative indicator for V.

The small β value of this MV bis(triarylamine) series shows that there may be a significant electronic coupling V in bis(triarylamine) radical cations even with very long spacers. The main problem in analyzing the IV-CT bands of MV compounds with very long bridge units is the fact that these bands are usually overlapped by a second CT band caused by a hole transfer from the acceptor to the bridge unit. Barlow and co-workers synthesized bis(triarylamine) radical cations 12^+ and 64^+–66^+ with phenylene-vinylene spacer units of different lengths (Scheme 24) to study the ET behavior of bis(triarylamine) radical cations with ultralong spacer units.[152,191] However, a band-shape analysis of the CT or IV-CT bands was only possible for 12^+, $64a^+$ and $64b^+$ because the IV-CT bands are obscured by the above-mentioned "bridge" bands. No IV-CT band is visible at all for 66^+, which indicates that there is an extremely small electronic coupling and 66^+ is close to the class I/II boundary. This interpretation is supported by ESR measurements of the dications 12^{2+} and 64^{2+}–66^{2+}, which show only a minimal spin–spin coupling between the N–N centers in, for example, 66^{2+}, but a diamagnetic behavior of 12^{2+}. Thus, the electronic structure in the series 12^+, 64^+–66^+ ranges from delocalized class III to the boundary of class I/II compounds.

The results of the band-shape analysis of 12^+, $64a^+$, and $64b^+$ are summarized in Table 13. It is noteworthy that 12^+ is clearly a class III compound, while the corresponding tolan-bridged radical cation 3^+ is a class II system, at least in dichloromethane (from computational results 3^+ is assumed to be a class III compound in the gas phase or in nonpolar solvents).[147] In both radical cations, 11 bonds separate the nitrogen centers, which makes 12^+ the largest bistriarylamine radical cation that has a delocalized electronic structure. This class III character is also manifested in the X-ray crystallographic data of the $12^+[SbF_6]^-$ salt, by a considerably less solvatochromic shift of the CT band of 12^+ compared to 3^+, and by the asymmetry of the CT band in 12^+ (see also Table 13).[158] A significantly higher electronic coupling for stilbene-bridged 2,5-dimethoxy-4-methylphenyl radical cations (see Section 3.2.2) than for the tolan-bridged analogues were also found by Kochi and co-workers.[192] Recently, Barlow and co-workers performed temperature-dependent ESR measurements of tolan-bridged compounds 3^+ and 63^+ as well as of stilbene-bridged compounds 12^+, $64a^+$, and

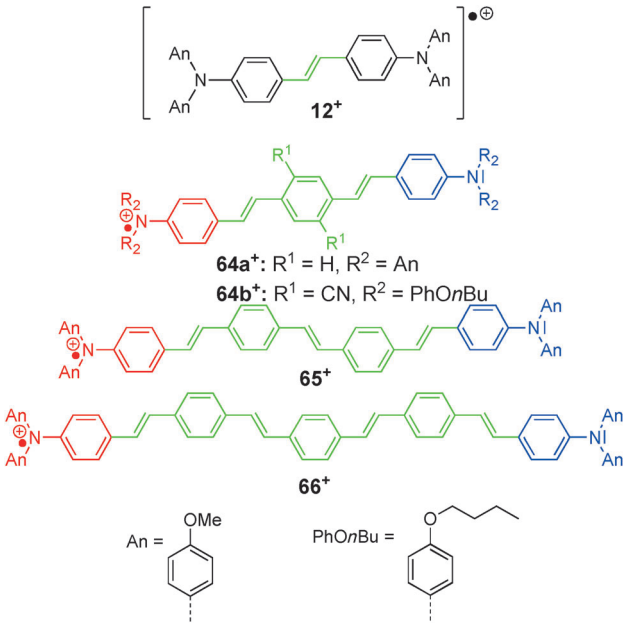

Scheme 24. Bis(triarylamine radical cations 12^+ and 64^+–66^+ with phenylene-vinylene spacer units.

Table 13: IV-CT band shape analyses, electronic coupling, and redox potentials of 12^+, $64a^+$, and $64b^+$ in dichloromethane.[152,158,191]

	$\tilde{\nu}_{max}$ [cm^{-1}][a]	ε [$M^{-1}cm^{-1}$]	$n-1$[b]	V [cm^{-1}]	$\nu_{1/2}$(high)/ $\nu_{1/2}$(low)	ΔE [mV][d]
12^+	6080	39300	10	2890[c] (3040)[e]	1.40	140
$64a^+$	6130	15510	16	1510[c]	1.00	[f]
$64b^+$	7450	–	16	1220[g]	–	–

[a] Radical cations were generated by chemical oxidation with tris(4-bromophenyl)aminium hexachloroantimonate. [b] n = number of bonds between the two nitrogen centers. [c] Determined by the GMH two-state model.[152] [d] $\Delta E = |E_{1/2}(Ox1) - E_{1/2}(Ox2)|$ in dichloromethane/0.1 M tetrabutylammonium hexafluorophosphate solution, scan rate = 50 mVs^{-1}. [e] Electronic coupling determined by $V = \tilde{\nu}_{max}/2$. [f] No redox potential splitting was observed. [g] Calculated with ΔG^* from ESR measurements and λ from optical analysis.[191]

64b$^+$.[191] Simulation of the ESR spectra showed that compounds **3**$^+$, **12**$^+$, and **64a**$^+$ exhibit very fast electron transfer at the upper limit of the ESR time scale, while the tolan-bridged MV compound **63**$^+$ shows temperature-dependent ESR spectra which directly yields smaller ET rates. These findings are in good agreement with the results of the optical analyses, thus confirming the stronger electronic coupling in **64a**$^+$ (V = 1510 cm^{-1})[152] compared to the tolan-bridged analogue **63**$^+$ (V = 1000 cm^{-1}).[112,152] Furthermore, MV compound **64b**$^+$ with a dicyano-substituted phenylene spacer shows also temperature-dependent ESR spectra and a smaller ET rate than **64a**$^+$ because of the lowering of the HOMO energy of the bridge in **64b**$^+$, which weakens the electronic coupling between the triarylamine redox centers. By comparison of optically and ESR-derived ET parameters, Barlow and coworkers estimated that the effective ET distance in these bis(triarylamine) MV compounds is much smaller (less than half in **63**$^+$ and **64b**$^+$) than the often used geometrical N–N distance.[191]

It is clear from the investigation of the stilbene-bridged bis(triarylamine) radical cations that a precondition for the optical investigation of MV compounds with very long spacer units is to avoid the overlap of IV-CT and "bridge" bands. We synthesized bis(triarylamine) radical cations **67a**$^+$ and **67b**$^+$ (Scheme 25) with n = 25 bonds and an AM1 calculated distance of 28.7 Å between the redox centers. Both compounds only differ by the substituents R on the bridge unit.[193]

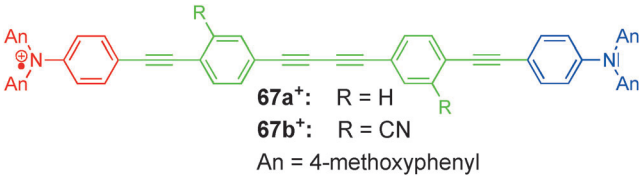

Scheme 25. Bis(triarylamine) radical cations **67a**$^+$ and **67b**$^+$.

The radical monocations **67a,b**$^+$ were generated by chemical oxidation with a solution of $SbCl_5$ in dichloromethane. Whereas no IV-CT band could be observed for **67a**$^+$, apparently because of strong overlap with the "bridge" band, a very weak IV-CT band could be detected for **67b**$^+$. This effect is due to the electron-withdrawing CN substituents, which decrease the HOMO energy of the bridge and, thus, increase the energy of the triarylamine-to-bridge hole excitation, which then blue-shifts compared to **67a**$^+$. This shift uncovers the IV-CT band and allowed a Mulliken–Hush band-shape analysis. The data for the IV-CT band of **67b**$^+$ and of both bridge bands are listed in Table 14. Compound **67b**$^+$ is, to date, the longest organic MV compound for which an optical analysis of the CT behavior was sucessfully performed.

Table 14: IV-CT and bridge band data, electronic coupling, and redox potential splittings of **67a**$^+$ and **67b**$^+$ in dichloromethane.[193]

	$\tilde{\nu}_{max}$(IV-CT) [cm^{-1}]	ε [M^{-1} cm^{-1}]	V [cm^{-1}]	$\tilde{\nu}_{max}$(bridge) [cm^{-1}]	ΔE [mV]
67a$^+$	–	–	–	11500	–
67b$^+$	11790	990	190	14100	55

Bis(triarylamine) MV compounds with paracyclophane spacers were used to elucidate the influence of cofacial π–π interactions on the ET behavior. The ability of a bridge unit to act as an ET mediator is mainly determined by whether it is a conjugated π system or a saturated spacer. As we showed above, unsaturated spacers result in β values being much smaller than 1, while compounds with saturated bridge units have β values near 1. With paracylophanes, a new aspect comes into play: there is a long-standing discussion of whether paracyclophane moieties act like a saturated spacer and, hence, show through-bond ET (along the σ bonds connecting the two benzene rings), or show through-space ET between the π faces, or allow direct π–π interactions of the cofacially oriented benzene rings and therefore act more like an unsaturated bridge unit. In this context we prepared a series of bis(triarylamine) radical cations with different distances between the triarylamine redox centers (**6**$^+$ and **68**$^+$–**69**$^+$; Scheme 26). Additionally, a [3.3]paracyclophane **70**$^+$

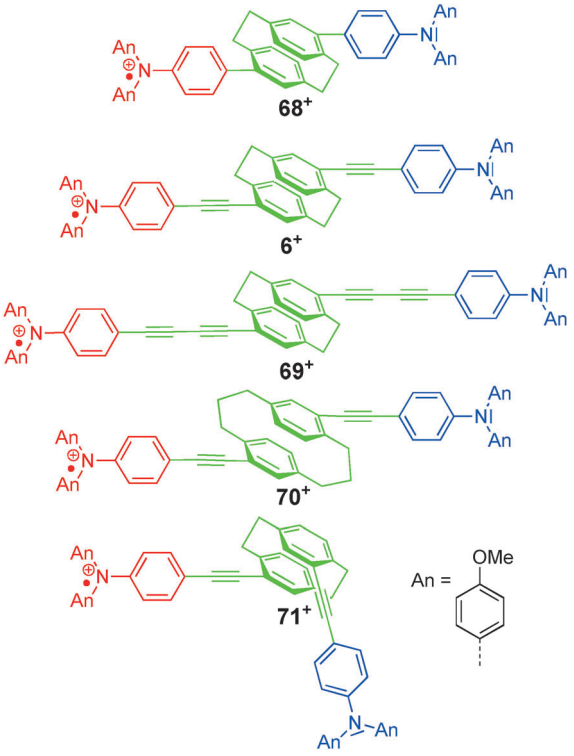

Scheme 26. Bis(triarylamine) MV compounds **6**$^+$ and **68**$^+$–**71**$^+$ with different paracyclophane spacer units.

was investigated to probe the influence of the distance and the type of connectivity of the central benzene rings in the cyclophane on ET. The pseudo-*ortho*-substituted regioisomer **71**$^+$ was also synthesized to study the influence of the relative orientation between the redox centers and the paracyclophane bridge unit on ET. The optical spectra of MV compounds **6**$^+$ and **68**$^+$–**71**$^+$ show an IV-CT band in the NIR region which is partially overlapped at the blue-edge by a more intense bridge band. Both the bridge band as well the

IV-CT band could be fitted by Gaussian functions and an optical band-shape analysis could be performed with the "traditional" Marcus–Hush two-state model as well as with the GMH three-state model.[123] The results of both optical analyses[123] as well as the results of temperature-dependent ESR spectroscopy[129] are collected in Table 15. As can be seen from these data, the electronic coupling decreases as the distance between the triarylamine redox centers in **68**$^+$, **6**$^+$, and **69**$^+$ increases. As expected, the thermal ET barrier ΔG^* increases and the rate constants also decreases as the distance increases.

Table 15: IV-CT band data, electronic couplings by optical analyses, and barriers and rate constants derived by temperature-dependent ESR in dichloromethane for **6**$^+$ and **68**$^+$–**71**$^+$.[123,129]

	$\tilde{\nu}_{max}$ [cm^{-1}]	V [cm^{-1}] two-state	V [cm^{-1}] three-state	ΔG^*_{ESR} [cm^{-1}]	k_{ESR} [×10^8 s^{-1}]
68$^+$	6230	710	970	780	1.4
6$^+$	6600	340	570	1150	0.69
69$^+$	7500	70	220	1500	0.2
70$^+$	8500	320	110[a]	1420	0.9
71$^+$	6280	380	430	–	–

[a] Uncertain value because of strong band overlap.[129]

Both models (two-state and three-state) show the same trends for the electronic coupling, and a linear correlation of ln V versus the numbers of bonds n between the redox centers within the series **5**$^+$ > **68**$^+$ > **6**$^+$ > **69**$^+$ was found. The β values of these correlations are 0.27 Å^{-1} (three-state) and 0.41 Å^{-1} (two-state) and are both somewhat higher than the β value (0.16 Å^{-1}) for the series **2**$^+$–**4**$^+$ and **63**$^+$ with unsaturated spacer units. These results show the paracyclophane moiety acts more as an unsaturated spacer than a saturated one. Hence, the through-space ET mechanism facilitated by π–π interactions of the benzene rings plays the dominating role in [2.2]paracyclophanes. The fact that the unsaturated compound **5**$^+$ fits well in the correlation of the paracyclophane compounds additionally supports this interpretation. It is noteworthy that temperature-dependent ESR measurements yielded ET rates for the bis(triarylamine) radical cations **63**$^+$ and **5**$^+$ of 1.3×10^7 and 1.6×10^7 s^{-1}, respectively, which are only one order of magnitude higher than for the paracyclophane-bridged MV compounds **6**$^+$ and **68**$^+$–**70**$^+$ (Table 15).[129]

The optical analyses of the pseudo-*ortho*-substituted paracyclophane **71**$^+$ yielded nearly the same values for V, although the through-space distance is clearly smaller than for the regioisomer **6**$^+$. Since the numbers of bonds between the redox centers is identical, the ET process is presumed to proceed by the through-bond pathway rather than through-space. Furthermore, the electronic interaction in the [3.3]paracyclophane **70**$^+$ is nearly the same as for the corresponding [2.2]paracyclophane **6**$^+$ despite the somewhat increased benzene–benzene distance (ca. 3.3 versus 3.1 Å). This observation excludes the ethylene and propylene handles participating in the ET process. It is surprising to see that the inner reorganization energy is significantly larger for **70**$^+$ than for **6**$^+$, even though both compounds only differ in the handles connecting the benzene rings of the spacer unit. This finding indicates that the spacers may have a pronounced influence on the internal reorganization energy, which is not predicted by standard ET theories.[129]

A comparison of the ET barriers ΔG^* determined by temperature-dependent ESR measurements and the values calculated by the two-state and the three-state models shows that the GMH three-state model produces significantly more accurate values.[129] Therefore, the GMH three-state model is the preferred treatment for the investigation of MV compounds where bridge states play an important role. Further studies focused on the type of spacer in bis(triarylamine) MV systems, with the N–N distance kept constant: **63**$^+$ and **72**$^+$–**75**$^+$ (Scheme 27).[112,122] The absorption spectra of these

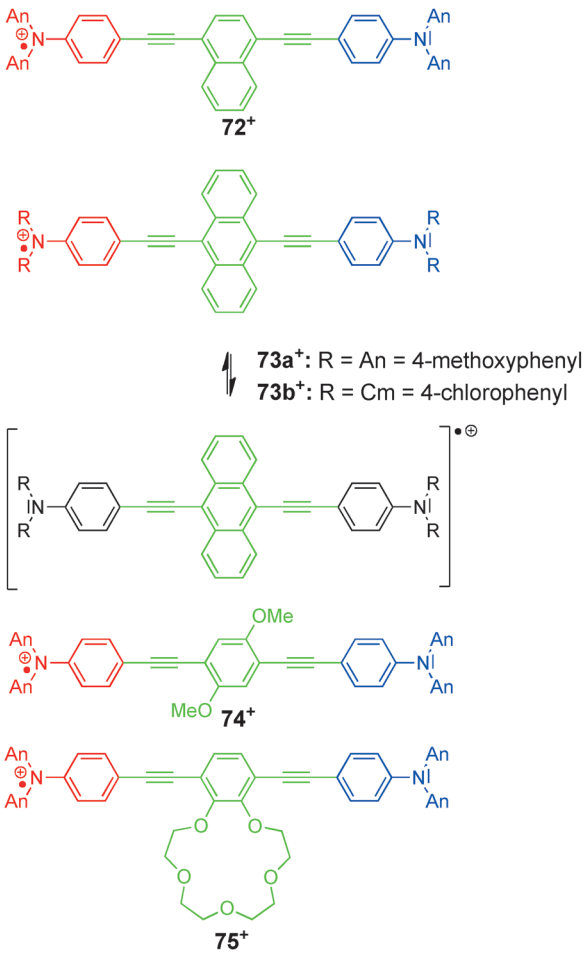

Scheme 27. Bis(triarylamine) radical cations **72**$^+$–**75**$^+$ with identical distance between the redox centers but different electronic properties of the spacer moiety.

compounds all show the two characteristic low-energy bands associated with the hole transfer from one oxidized triarylamine redox center to the other one (IV-CT band) and to the bridge unit (bridge band). A band-shape analysis in the context of the GMH three-state model yielded the two-dimensional FES (with a symmetric and an asymmetric mode). It is clear that in the series **63**$^+$, **72**$^+$, and **73a**$^+$ only the size of the bridging π system increases, which results in a decrease in the HOMO–LUMO gap of the bridge. This aspect

has a dramatic influence on the ET behavior of the MV compounds. In dichloromethane, compounds **63**$^+$ and **72**$^+$ are clearly class II systems with localized charges on one triarylamine redox center, while **73a**$^+$ is a class III system where the positive charge is delocalized over the anthracene and the neighboring acetylene groups. However, this delocalization is strongly influenced by the solvent polarity. In acetonitrile, **73a**$^+$ shows clear class II character, which can be explained by symmetry-breaking effects provoked by the increased solvent polarity.[112] In compound **73b**$^+$, where the MeO substituents are replaced by the more electron-withdrawing Cl substituents, the ground state shows charge delocalization in dichloromethane and the optical transition energy to the state where the charge is located at the triarylamine redox center is increased because of the destabilizing effect of the chloro substituents on the positive charge.[112] In bis(triarylamine) radical cation **74**$^+$ with the 2,5-dimethoxyphenylene spacer, only the HOMO energy of the bridge unit is increased compared to **63**$^+$. As discussed in Section 2.8, an increase of the HOMO energy should promote the ET pathway through the hopping mechanism. This was confirmed by the GMH three-state analysis, which yielded a triple minimum ground state FES (Figure 13). Both the relatively high energy of the HOMO and the high reorganization energy for the ET process (triarylamine-localized to bridge-localized) cause the third minimum and, hence, are necessary to promote an ET pathway by the hopping mechanism. It is remarkable that the ET behavior changes in this fundamental way simply on modification of the spacer type: a double minimum in charge-localized compound **63**$^+$, a triple minimum in **74**$^+$, and finally a single minimum potential for the symmetric delocalized **73a**$^+$ (see Figure 13).

The crown ether substituted bridge moiety in **75**$^+$ allowed the influence of metal ions, such as Ca^{2+}, on the ET to be probed when complexed by the crown ether ring. Coordination of Ca^{2+} was found to result in a mainly electronic influence on the ET. This follows from a Mulliken–Hush three-state analysis, which yields a distinctly smaller electronic coupling for **Ca-75**$^+$ than for the nonmetalated **75**$^+$, while the reorganization parameters do not change greatly.[122] These results go along with the generally observed trend that decreasing the HOMO of the bridge also decreases the electron coupling V in cationic MV systems.[112,194]

Replacing the central benzene bridge in **63**$^+$ by thiophene or azulene yields compounds **76**$^+$–**80**$^+$ (Scheme 28).[195] While compounds **76**$^+$ and **77**$^+$ are class II compounds, radical cation **78**$^+$ with the more electron-rich ethylenedioxythiophene bridge unit displays a similar behavior as compound **73a**$^+$, and is clearly a class III compound with a mainly bridge-

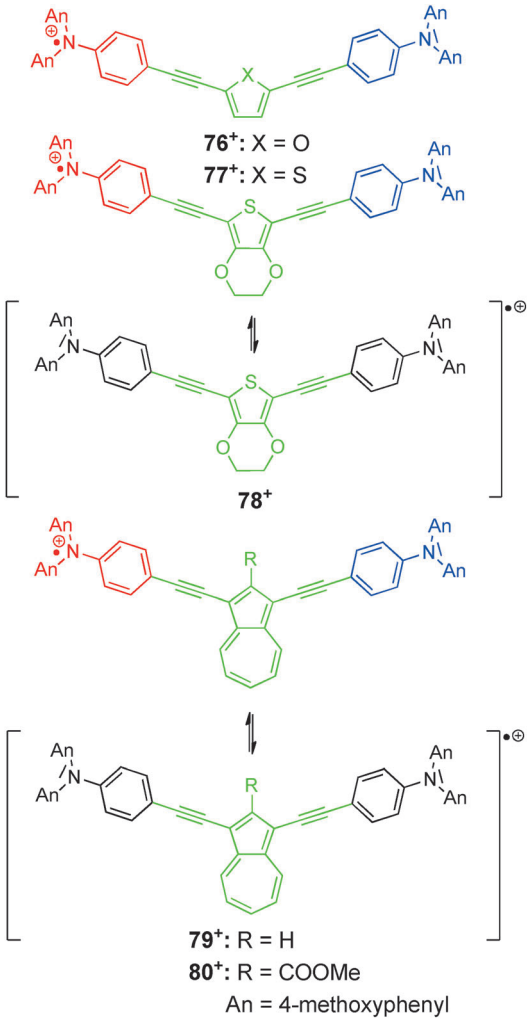

Scheme 28. Bis(triarylamine) MV systems **76**$^+$–**80**$^+$ with thiophene and azulene spacer units.

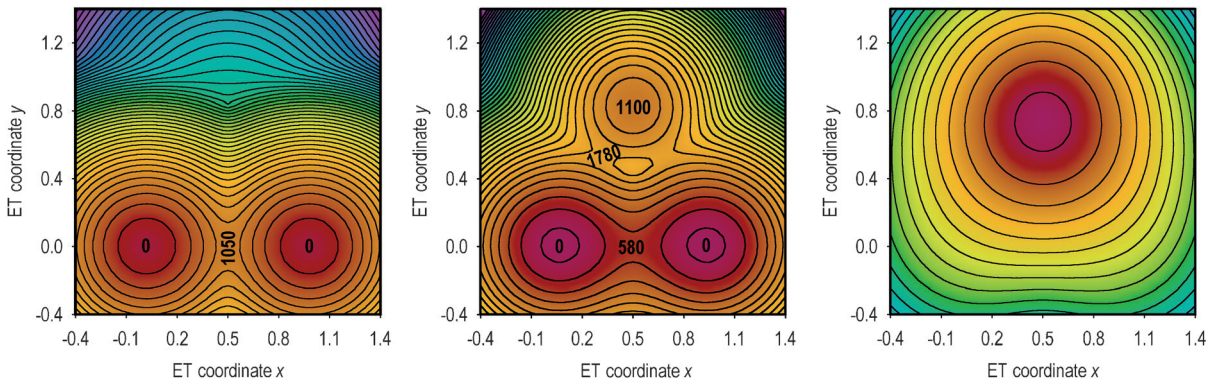

Figure 13. Contour plots of the ground state FES for **63**$^+$ (left), **74**$^+$ (middle), and **73a**$^+$ (right) in dichloromethane . Reproduced from Ref. [112] with permission.

localized positive charge. In this context, we have to allude that the bridge-localized charge in the ground state of both **73a**$^+$ and **78**$^+$ is a direct consequence of the class III character of the compounds because the isolated anthracene and ethylenedioxythiophene units possess higher oxidation potentials than the isolated triarylamine centers. Accordingly, the bridge-localized ground state is not a consequence of a possibly easier oxidation of the bridge, but follows from the delocalization of the charge in the class III system. In more polar solvents, such as acetonitrile, symmetry breaking occurs and **78**$^+$ shows class II character, as is observed for the anthracene-bridged analogue **73a**$^+$.[123]

The 1,3-azulene-bridged radical cations **79**$^+$ and **80**$^+$ can be compared with compound **72**$^+$ with the 1,4-substituted naphthalene spacer.[195] Although the azulene spacer should allow weaker electronic coupling because of an unfavorable *meta*-substitution pattern (see also Section 2.8), both azulene-bridged compounds **79**$^+$ and **80**$^+$ display a strong electronic coupling. Evidently, the unfavorable substitution pattern is overcompensated by the increased HOMO of the azulene spacers compared to naphthalene. Consequently, radical cation **79**$^+$ is clearly a class III system in dichloromethane. Unfortunately, it is not possible to investigate the ET behavior in more polar solvents such as acetonitrile because of instability. The ester substituent in the 2-position of **80**$^+$ increases the chemical stability of the radical cation and facilitates the optical investigation, even in acetonitrile. This electron-withdrawing substituent lowers the HOMO compared to **79**$^+$, with the consequence that dichloromethane is no longer apolar enough to ensure complete delocalization of the charge. Thus, the optical spectrum shows evidence of both class II and class III character. This behavior is similar to what Nelsen et al. observed for some dinitroaromatic compounds[103] (see also Section 3.1.4). Thus, the special electronic feature (very electron rich five-membered ring) of azulene induces a far stronger electronic coupling than the isoelectronic naphthalene bridge, despite the pseudo-*meta*-substitution pattern.

The electronic coupling in **81**$^+$–**83**$^+$ (Scheme 29) was determined by means of optical analysis (two-state-two-mode model, see Section 2.5), gas-phase UV photoelectron spectroscopy (UPS), and electronic-structure calculations (see Table 16).[116] All the methods yielded a reverse trend

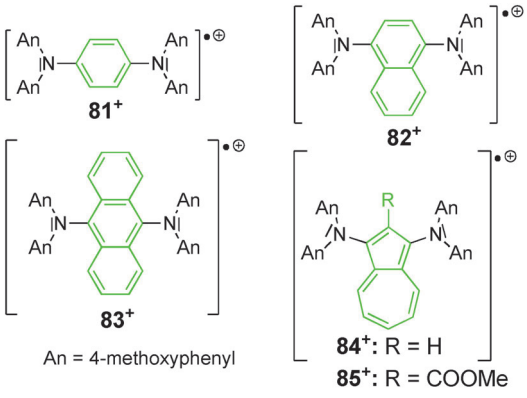

Scheme 29. Class III bis(triarylamine) radical cations **81**$^+$–**85**$^+$.

Table 16: IV-CT band data, electronic couplings, and redox potential differences of **81**$^+$–**83**$^+$ in dichloromethane.[116]

	$\tilde{\nu}_{max}$ [cm^{-1}]	ε [M^{-1} cm^{-1}]	V_{opt} [cm^{-1}][a]	V_{UPS} [cm^{-1}][b]	V_{III} [cm^{-1}][c]	ΔE [mV][d]
81$^+$	9480	22800	4300	3800	4740	495
82$^+$	8000	19100	3600	2960	4000	260
83$^+$	5140	18500	2200	2160	2570	90

[a] Determined by two-state two-mode model. [b] Determined by UPS and calculated from the first and second ionization potential of the neutral compound (IP_1 and IP_2) according to $V_{UPS} = \Delta IP/2 + L^*$. L^* is a correction term which takes relaxation effects into account and considers the determination of ΔIP at the geometry of the neutral compound (see also Ref. [116]). [c] Determined by $V_{III} = \tilde{\nu}_{max}/2$. [d] $\Delta E = |E_{1/2}\,(Ox1) - E_{1/2}\,(Ox2)|$ in dichloromethane/0.1 M tetrabutylammonium hexafluorophosphate solution, scan rate = 250 mV s^{-1}.

for the electronic coupling as for the related compounds **63**$^+$, **72**$^+$, and **73a**$^+$. The compounds **81**$^+$–**83**$^+$ are all class III systems or at least are at the boundary of classes II and III. The fact that the electronic coupling V decreases in the order **81**$^+$ > **82**$^+$ > **83**$^+$ is also supported by the redox potential splittings determined by cyclic voltammetry (Table 16).[157]

The reverse trend in the electronic coupling in **81**$^+$–**83**$^+$ can be explained by the increasing steric interactions between the bridging unit and the redox centers resulting in an increasing twist angle between the diarylamine and the bridge. This was confirmed by an X-ray crystal-structure analysis of **83** and calculations on the electronic structure.[116] Along with the decreasing electronic coupling, the reorganization parameters also decrease concomitantly, which makes **81**$^+$–**83**$^+$ all class III species. The corresponding azulene-bridged compounds **84**$^+$ and **85**$^+$ (Scheme 29) are also class III compounds and show nearly the same electronic coupling as the isoelectronic radical cation **82**$^+$.[196]

All the above discussed examples show that the type of spacer has a large influence on the ET behavior in organic MV compounds. Thus, the electronic properties of the spacer and the steric interplay between the spacer and redox centers have to be considered in particular. A further example of the efficiency of electron-rich bridging units (high-energy bridge HOMO) to act as electronic coupling moieties in radical cations is **86**$^+$ (Scheme 30) with a bithiophenyl spacer unit.[197] The authors classified this compound as a typical delocalized class III system on the basis of a qualitative comparison of the UV/Vis/NIR spectrum recorded in dichloromethane and quantum-chemically calculated transition energies. However, a quantitative investigation by, for example, a band-shape analysis was not performed.[197] Quite recently, Müllen and co-workers investigated the ET behavior of a series of bis(triarylamine) radical cations **87a**$^+$–**87c**$^+$ with ladder-type oligopentaphenylene bridging units (Scheme 30).[198] These spacer units allow a planar arrangement of the phenylene spacers and, hence, a maximum overlap of the corresponding π systems. Therefore, ideal conditions for a long-range ET are provided. However, only for **87a**$^+$ can an IV-CT band be observed in the UV/Vis/NIR spectrum. Apparently, the ET distance in **87b**$^+$ and **87c**$^+$ is too large for an electronic communication to be visible as an IV-CT band, even with these "ladder-type" bridging units. The remarkably intense

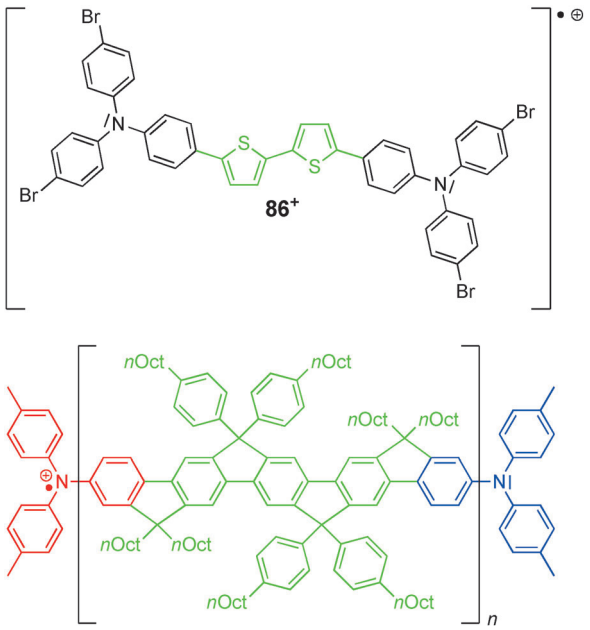

Scheme 30. Bis(triarylamine) MV systems **86**$^+$ and **87**$^+$ with spacer systems that warrant optimal conjugation of the redox centers.

IV-CT band of **87a**$^+$ was analyzed in the context of the Marcus–Hush two-state model (see Table 17).

Table 17: IV-CT band data, electronic coupling, and redox potential difference of **87a**$^+$ in dichloromethane.[198]

	$\tilde{\nu}_{max}$ [cm^{-1}]	ε [M^{-1} cm^{-1}]	$V_{opt.}$ [cm^{-1}]	ΔE [mV][a]
87a$^+$	5280	15200	550	100

[a] $\Delta E = |E_{1/2}\,(\mathrm{Ox1}) - E_{1/2}\,(\mathrm{Ox2})|$ in dichloromethane/0.1 M tetrabutylammonium hexafluorophosphate solution, determined by differential pulse voltammetry (DPV).

Radical cation **87a**$^+$ is a localized class II MV species with 21 bonds between the two redox centers. Compounds with similarly long-range ET distances such as **63**$^+$ (17 bonds) or **67b**$^+$ (25 bonds) show by far less intense IV-CT bands. Thus, the electronic coupling between the two redox centers in **87a**$^+$ as provided by "ladder-type" spacer units is quite strong, which is also supported by a relatively large redox potential splitting (Table 17).[157]

Although the platinum-bridged bis(triarylamine) MV compound **88**$^+$ (Scheme 31) synthesized by Marder and coworkers[199] is, strictly speaking, not an organic MV compound, it is very interesting inasmuch as the metal spacer permits electronic coupling in nearly the same range as a phenylene spacer unit would do. This is confirmed by a comparison of the IV-CT band analysis of **88**$^+$ ($V = 350$ cm^{-1}) and **63**$^+$ ($V = 440$ cm^{-1}).[199]

The special property of the diethynylethene spacer in **89**$^+$ (Scheme 31) is to switch between the *E* and *Z* isomers on

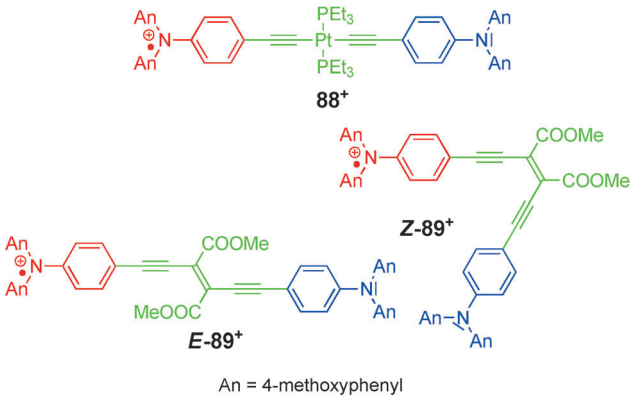

Scheme 31. Bis(triarylamines) **88**$^+$ with a platinum-bridged spacer, and **89**$^+$ with a photochromic diethynylethene bridge unit.

excitation with visible light.[200] This photochromism gives the possibility to switch between the different electronic communication pathways in (*E*)-**89**$^+$ and (*Z*)-**89**$^+$. The slightly decreased electronic coupling in the *Z* isomer was estimated by electrochemical measurements as well as by optical band-

Table 18: IV-CT band data and redox potential splittings of the *E*/*Z* isomers of **89**$^+$ in dichloromethane as well as calculated electronic couplings from a Marcus–Hush two-state analysis and by DFT calculations.[200]

	$\tilde{\nu}_{max}$ [cm^{-1}][a]	ε [M^{-1} cm^{-1}][a]	r(N-N) [Å][b]	ΔE [mV][c]	V_{Hush} [cm^{-1}][d]	V_{DFT} [cm^{-1}][e]
(*E*)-**89**$^+$	6954	6500	17.4	74	534	1524
(*Z*)-**89**$^+$	6803	2480	10.8	63	529	1286

[a] Results of a band deconvolution with Gaussian functions. [b] Geometrical distance between the N atoms. [c] $\Delta E = |E_{1/2}\,(\mathrm{Ox1}) - E_{1/2}\,(\mathrm{Ox2})|$ in dichloromethane/0.1 M tetrabutylammonium tetrafluoroborate solution, scan rate = 100 mV s^{-1}. [d] Determined using the geometrical through-bond distance between the nitrogen atoms.
[e] $V_{DFT} = (\varepsilon_{HOMO} - \varepsilon_{HOMO-1})/2$ using DFT computed orbital energies of the neutral compounds.

shape analysis (see Table 18), and is attributed to the larger steric hindrance of the methyl ester substituents in the *Z* isomer leading to a more pronounced distortion of the π system in (*Z*)-**89**$^+$ than in the *E* isomer.[157] The Gaussian-shaped symmetric IV-CT bands prove both isomers to be charge-localized class II compounds.

The electronic couplings in (*E*)-**89**$^+$ and (*Z*)-**89**$^+$ determined by the Mulliken–Hush formalism are only slightly different as a consequence of the almost identical through-bond N–N separation employed for the calculation. One might have estimated from the significantly more intensive IV-CT band of the *E* isomer that the electronic coupling is stronger in the *E* isomer. However, the adiabatic dipole moment difference (which goes along with the geometrical N-N distance) is also smaller in the *Z* isomer, which compensates for the smaller transition moment and yields similar values of *V* for both isomers [see Eq. (8)]. The same observations were made for cyclophanes **6**$^+$ and **71**$^+$.

Neutral bis(triarylamines) with biphenyl bridging moieties (tetraarylbenzidines) are widely used as hole-transporting materials in optoelectronic devices. Thus, there is great interest in the effects that the structure of both the spacer and the triarylamine redox centers have on the ET behavior of the corresponding charged species. Low et al. investigated a series of such tetraarylbenzidines to probe the influence of substituents attached to the spacer and the redox center on ET parameters, especially on the electronic coupling V.[114,156,201] The data in Table 19 show that the electronic coupling V strongly depends on the substitution pattern of the biphenyl spacer unit, which mainly influences the twist angle ϕ of the biphenyl moiety: $\mathbf{7}^+$ ($\phi = 0°$) > $\mathbf{2}^+$ ($\phi = 32.8°$) > $\mathbf{8}^+$ (ϕ = not determined) > $\mathbf{9}^+$ ($\phi = 85°$; Schemes 4 and 32).[156] No electronic coupling could be determined in $\mathbf{9}^+$ because no CT band is visible, which implies a very small electronic coupling. The same trend is visible for the phenyl-substituted bis(triarylamines) $\mathbf{90a}^+$ and $\mathbf{90c}^+$ (Scheme 32). A further steric effect on the electronic coupling concerns the twist of the nitrogen lone pair of electrons and the biphenyl π system, and can be seen when comparing the ΔE and V values of $\mathbf{2}^+$ and $\mathbf{91}^+$ (Table 19).

Table 19: Redox potentials and IV-CT band data of radical cations $\mathbf{2}^+$, $\mathbf{7}^+$–$\mathbf{9}^+$, and $\mathbf{90}^+$–$\mathbf{93}^+$ in dichloromethane.[114,156,201]

	E(Ox1) [mV][a]	E(Ox2) [mV][a]	ΔE [mV][b]	$\tilde{\nu}_{max}$ [cm^{-1}]	ε [$M^{-1} cm^{-1}$]	λ_v [cm^{-1}][c]	V_{Hush} [cm^{-1}][d]
$\mathbf{90a}^+$	390	640	250	7310	27300	1100	3655
$\mathbf{90b}^+$	340	560	220	–[e]	–[e]	1100	–[e]
$\mathbf{90c}^+$	440	590	150	–[f]	–[f]	–[f]	–[f]
$\mathbf{2}^+$	250	550	300	6820	32600	1000	3410
$\mathbf{91}^+$	350	470	120	5260	47200	1000	2630
$\mathbf{8}^+$	440	590	150	5350	57600	1600	2660
$\mathbf{9}^+$	460[g]			–[h]	–[h]	700	
$\mathbf{92a}^+$	290	510	220	7140	37800	1100	3570
$\mathbf{92b}^+$	250	510	260	7450	30680	–[f]	3725
$\mathbf{92c}^+$	250	510	260	7800	30680	1200	3680[i]
$\mathbf{93}^+$	280	650	370	7520	32200	1500	3760
$\mathbf{7}^+$	120	470	350	7520	36400	1100	3760

[a] Determined in dichloromethane/0.1 M tetrabutylammonium tetrafluoroborate solution; scan rate: 100 mV s^{-1}. [b] $\Delta E = E(Ox2) - (Ox1)$. [c] This quantity refers to the intermolecular hole transfer and was determined by BPW1-DFT calculations[156] by the NICG method (see also Section 2.3). [d] $V_{Hush} = \tilde{\nu}_{max}/2$ assuming class III behavior. [e] Optical analysis not possible because of insufficient stability of the radical cation. [f] Not determined. [g] No separation detected. Simulation of the CV was not possible.[156] [h] No CT band could be observed.[201] [i] Within the Mulliken–Hush two-state two-mode model the electronic coupling is determined as $V = 3300$ cm^{-1}.[114]

Knowledge about the reorganization energies especially of bis(triarylamines) is of great practical interest because λ and V (both for the intermolecular charge transfer, for example, for $\mathbf{92a}^+ + \mathbf{92a} \rightarrow \mathbf{92a} + \mathbf{92a}^+$) correlate directly with the so-called hole-transport mobility, which is a fundamental characteristic of hole-transport materials for which these compounds are widely used (in this context **92a** is commonly referred to as TPD in the literature).[202] Low et al. calculated the inner reorganization energies for the intermolecular hole transfer by the NICG method (see Section 2.3) by using DFT optimized geometries (Table 19).[156] The lowest reorganization energy is calculated for $\mathbf{9}^+$, where no planarization of the biphenyl spacer upon oxidation can occur and, therefore, the geometrical changes are small. The first oxidation potentials of these compounds are also of great practical interest to optimize the hole-injection processes in, for example, OLEDs. It can be seen from Table 19 that the oxidation potentials are mainly influenced by inductive effects of the substituents on the peripheral phenyl rings. In general, electron-donating methyl substituents lower the oxidation potential significantly ($\mathbf{2}^+$, $\mathbf{92a}^+$–$\mathbf{92c}^+$, and $\mathbf{7}^+$ versus $\mathbf{93}^+$; see Scheme 32). In this context an *ortho*- or *para*-substitution pattern ($\mathbf{92b}^+$, $\mathbf{92c}^+$) is more effective than *meta* substitution ($\mathbf{92a}^+$). Besides these electronic influences, steric effects also control the redox potential. It is clear that radical cations with a significant twist angle between the nitrogen lone pair of electrons and the biphenyl π system ($\mathbf{91}^+$) or with a high intra-biphenyl twist angle ($\mathbf{8}^+$ and $\mathbf{9}^+$) show higher first oxidation potentials (Table 19).

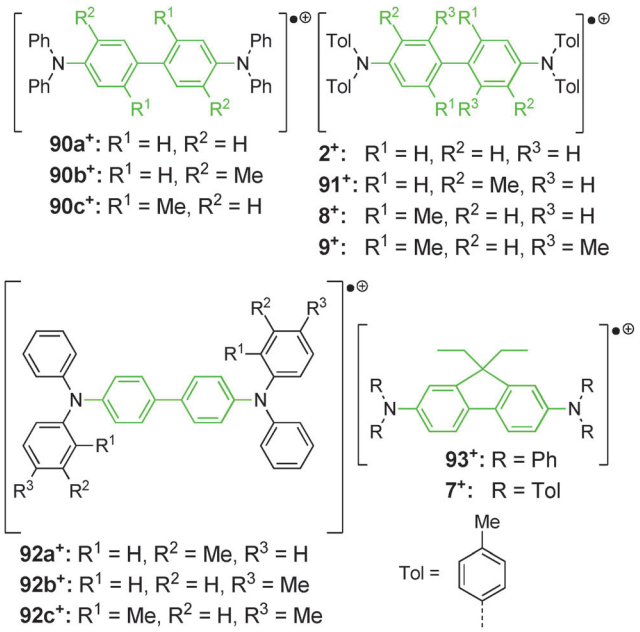

Scheme 32. Bis(triarylamine) radical cations with biphenyl bridge units.

para-Phenylenediamine radical cations with different substitution patterns of type $\mathbf{94}^+$, $\mathbf{95}^+$, and $\mathbf{96}^+$ (Scheme 33) were investigated to probe the influence of the donor/acceptor character of the substituents R on the redox potentials of these class III compounds.[203,204] The potentials of the first and second oxidation processes in $\mathbf{94}^+$ and $\mathbf{95}^+$ correlate directly with the Hammett parameters of the substituents. The *para*-phenylenediamines $\mathbf{94}^+$–$\mathbf{96}^+$ are all class III compounds and, thus, the electronic coupling is not very sensitive to the electronic properties of the redox centers, as was also observed for the related compounds with biphenyl spacers, for example, $\mathbf{90}^+$–$\mathbf{93}^+$.

The class III character of *para*-phenylendiamine radical cations is not surprising given the short distance between the redox centers, with only five bonds separating the nitrogen atoms. However, this distance is only one factor which

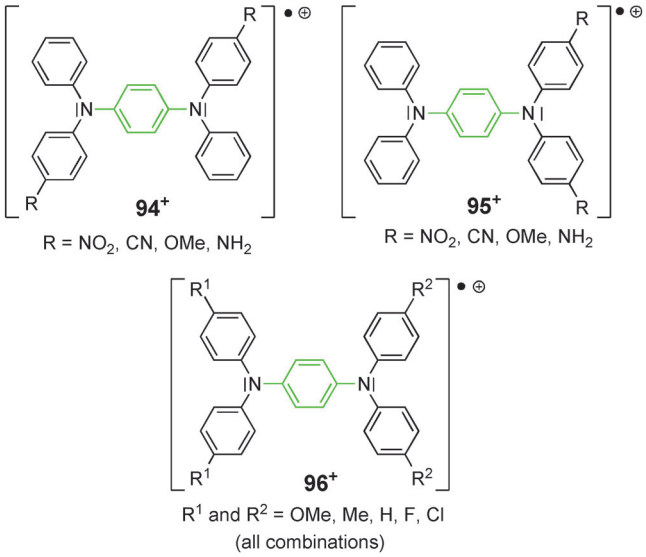

Scheme 33. *para*-Phenylenediamine radical cations with different donor and acceptor substituents R.

controls the electronic coupling. A similarly large influence is exerted by the substitution pattern of the bridge, a factor that we discussed above in the context of the different ET behavior of Kekulé and non-Kekulé substituted dinitroaromatic radical anions. Diamines such as *meta*-phenylenediamines **97**$^+$ (Scheme 34) are interesting substructures because they form polycationic high-spin states.[205,206] The influence of substituents R^1 and R^2 in the *para* positions is twofold: first, they generate electrochemical stability by preventing dimerization or polymerization reactions and, second, the substituents R^1 in particular control the redox potentials in the same manner as observed for the *para*-substituted phenylenediamines **94**$^+$ and **95**$^+$. Unfortunately, radical cations of type **97**$^+$ have not been investigated by optical methods, hence, all information about the electronic coupling in these compounds are deduced from cyclovoltammetric measurements or ESR measurements. These studies suggest a much smaller electronic communication in the *meta*-substituted bis(triarylamine) radical cations, as derived from a significantly decreased redox potential splitting $\Delta E \approx 150$–190 mV[205] compared to $\Delta E \approx 420$ mV for *para*-phenylenediamines.[203]

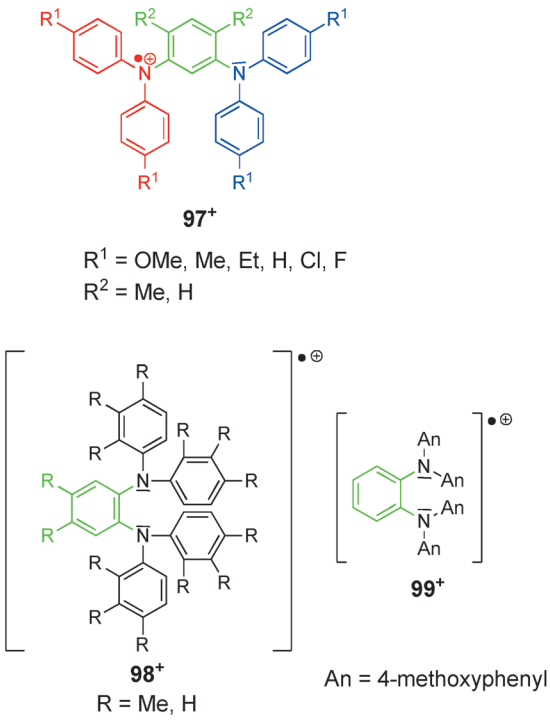

Scheme 34. *meta*- and *ortho*-bridged phenylenediamine radical cations **97**$^+$–**99**$^+$.

ESR studies of the dications **97**$^{2+}$ show the ground state to have triplet spin multiplicity, which is also evidence for the decreased coupling provided by the *meta* linkage of the bridge. In contrast, *ortho*-substituted phenylenediamines **98**$^+$ (Scheme 34) exhibit very large redox potential splittings $\Delta E = 500$–530 mV, which are even larger than the corresponding *para*-substituted derivatives.[207] Plater and Jackson suggested that the proximity of the redox centers in *ortho*-phenylenediamines is the main reason for the very high redox potential splitting because a second oxidation is unfavorable as a result of Coulomb repulsion. Nöll and Avola studied the absorption spectra of *ortho*-phenylenediamine **99**$^+$ (Scheme 34).[208] They found a moderately intense and asymmetric CT band at about 4250 cm^{-1} ($\varepsilon \approx 2080\,\text{M}^{-1}\text{cm}^{-1}$) in dichloromethane, with negligible solvatochromic behavior typical of a class III system. The redox potential splitting in dichloromethane is $\Delta E = 405$ mV, which is significantly smaller than the values found for other *ortho*-substituted derivatives **98**$^+$ and also slightly smaller than for the *para*-substituted analogue **1**$^+$. Nöll and Avola argued that the steric hindrance by the dianisylamine moieties results in an unfavorable conformation which precludes an effective conjugation of the nitrogen lone pairs of electrons with the π system of the bridge. On this basis they suggest that both through-bond and through-space interaction contribute to the electronic communication in **99**$^+$.[208]

Most of the bis(triarylamine) radical cations discussed above have degenerate MV states (the exceptions are **95**$^+$ and some compounds of type **96**$^+$ but which are all delocalized class III compounds). However, nondegeneracy was introduced step by step in the bis(triarylamine) MV series **100**$^+$–**102**$^+$ (Scheme 35) by replacing the methoxy substituents R in **3**$^+$ by less electron donating methyl groups and finally by electron-accepting cyano substituents.[194]

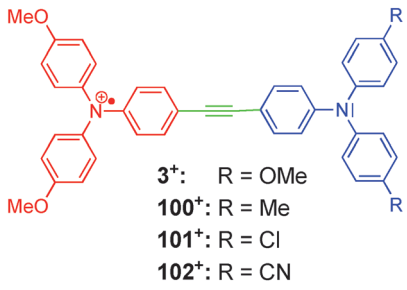

Scheme 35. Bis(triarylamine) MV compounds with nondegenerate redox centers **100**$^+$–**102**$^+$.

MV compounds $\mathbf{100}^+$–$\mathbf{102}^+$ were investigated optically in the context of GMH theory as well as electrochemically.[194] The results of these studies are summarized in Table 20. The redox potential splitting ΔE increases continuously as the acceptor strength of R increases. Concomitantly, the energy maximum of the IV-CT bands shifts to higher energies as the acceptor strength of R increases, because $\tilde{\nu}_{max}$ corresponds to the sum of the total Marcus reorganization energy λ and the free energy difference of the diabatic states ΔG^{00} which qualitatively correlates with ΔE (see Figure 6d,e). The electronic coupling V is nearly identical for all compounds provided that they have identical effective ET distances r. This assumption is reasonable, as the ET pathway is the same in all compounds and because semiempirical UHF-AM1 calculations on model compounds show only a weak influence of the substituents R on the adiabatic dipole moment difference.[194] The validity of identical electronic couplings is also supported by the linear correlation between the ΔG^{00} and ΔE values for $\mathbf{3}^+$ and $\mathbf{100}^+$–$\mathbf{102}^+$. A closer look at the trends of ΔG^{00} and ΔG^* in this series shows that there is a change between all three possible types of FES situations a class II compound can adopt, and which we discussed in detail in Section 2.4 (see Figure 6c–e). In this context, we stress that the ground state for $\mathbf{102}^+$ no longer has a double minimum. In general, the optical analyses of compounds $\mathbf{3}^+$ and $\mathbf{100}^+$–$\mathbf{102}^+$ show impressively the validity and applicability of the Mulliken–Hush model for nondegenerate MV compounds.

Table 20: Redox potential splittings, IV-CT band data, and free energy data derived by optical band-shape analysis of $\mathbf{3}^+$ and the nondegenerate MV compounds $\mathbf{100}^+$–$\mathbf{102}^+$ in dichloromethane.[194]

	ΔE [mV][a]	$\tilde{\nu}_{max}$ [cm^{-1}]	ε [$M^{-1}cm^{-1}$]	V [cm^{-1}]	ΔG^{00} [cm^{-1}]	ΔG^* [cm^{-1}]
$\mathbf{3}^+$	150	6190	21900	1120	0	550
$\mathbf{100}^+$	220	6490	15000	950	400	910
$\mathbf{101}^+$	370	8260	14100	1060	2000	1870
$\mathbf{102}^+$	540	10560	8900	940	4200	0[b]

[a] $\Delta E = E(Ox2) - E(Ox1)$, determined by cyclic voltammetry in dichloromethane/0.2 M tetrabutylammonium hexafluorophosphate solution. [b] No double minimum in the electronic ground state, similar to that described in Figure 6e (Section 2.4).

Another example of an organic MV compound with nondegenerate MV states is $\mathbf{103}^+$, where the asymmetry is due to the asymmetric 2,6-disubstituted azulene spacer unit. The strong IV-CT band in the NIR region ($\tilde{\nu}_{max} = 7420\ cm^{-1}$, $\varepsilon = 16500\ M^{-1}cm^{-1}$ in dichloromethane/0.2 M tetrabutylammonium hexafluorophosphate (TBAH) solution) was analyzed by GMH theory, and yielded an electronic coupling of 1140 cm^{-1}.[209] This coupling is comparable with that found for the tolan-bridged bis(triarylamine) radical cation $\mathbf{3}^+$ under equivalent conditions ($V = 1200\ cm^{-1}$).[79] Since the number of bonds between the nitrogen redox centers in $\mathbf{103}^+$ (Scheme 36) and $\mathbf{3}^+$ (Scheme 35) is equal ($n = 11$), these results show that the azulene spacer in $\mathbf{103}^+$ also acts as a powerful electronic coupler that is comparable to the tolan-bridging moiety.

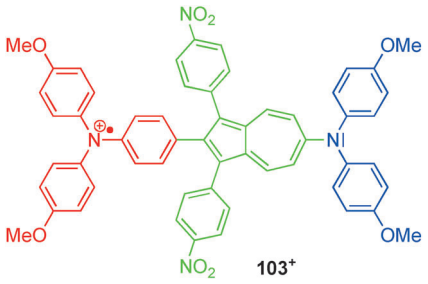

Scheme 36. Bis(triarylamine) radical cation $\mathbf{103}^+$ with an azulene bridge unit.

The large electronic coupling in $\mathbf{103}^+$ was also supported by cyclovoltammetric measurements, which yield a ΔE value of 265 mV in dichloromethane (0.2 TBAH solution).[157,209] Since the reorganization energy λ is unknown, the thermal ET barrier ΔG^* could not be determined by GMH analysis; however, a value of 1200 cm^{-1} for ΔG^* was estimated for $\mathbf{103}^+$ by assuming a reorganization energy equal to $\mathbf{3}^+$.[209]

We close this section with the intriguing organic MV compound $\mathbf{104}^+$ (Scheme 37), which contains two triarylamine redox centers with an extraordinary spiro-fused silicon bridge unit.[210,211]

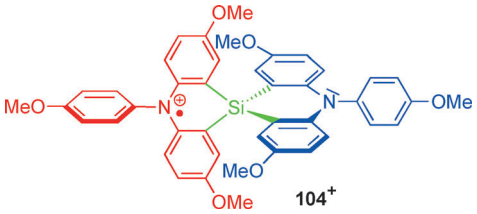

Scheme 37. Bis(triarylamine) radical cation $\mathbf{104}^+$ with a spiro-fused silicon spacer unit.

Despite the perpendicular arrangement of the donor and acceptor triarylamine units in $\mathbf{104}^+$, temperature-dependent ESR measurements revealed an intramolecular spin transfer and, hence, an ET with a rate of $4.2 \times 10^9\ s^{-1}$ at 293 K in *n*-butyronitrile.[211] Cyclovoltammetric measurements in acetonitrile gave a redox potential splitting of $\Delta E = 160$ mV between the first and the second oxidation processes, which indicates a significant electronic coupling between the MV states.[210] However, monitoring of the chemical oxidation of **104** by spectroscopy showed no IV-CT band for the monocation down to a wavelength of 2000 nm.[211] The reasons for the lack of an optical transition associated with a CT process might be that the optical band is just too weak to be observable or that the IV-CT band is shifted further into the NIR region, beyond 2000 nm. The latter reason is strengthened by the fact that the Marcus reorganization energy, which corresponds to $\tilde{\nu}_{max}$ in the weakly coupling class II limit, is exceptionally small due to the rigid skeleton of this spiro-fused MV compound.

3.1.6. MV Compounds with Diarylamine Redox Centers and Thiophene Spacers

Bis(diarylamine) radical cations with thiophene-based spacer units are very closely related to bis(triarylamine) MV systems. A series of such radical cations (**105**$^+$–**108**$^+$; Scheme 38) were synthesized by Barlow and co-workers and their ET behavior was studied by means of optical as well as ESR spectroscopy.[212]

The compounds **105**$^+$–**108**$^+$ are all strongly delocalized class III systems whose electronic couplings are at least 50% higher than those of the corresponding bis(triarylamine) radical cations. Radical cation **108a**$^+$, for example, shows the strongest electronic coupling reported to date (see Table 21).[212] These extremely high electronic communications between the redox centers can be attributed to the high-lying HOMO of the bridge units, which provokes a delocalization of the charge onto the bridge rather than onto the peripheral phenyl moieties. ESR measurements also support these compounds as being class III MV compounds and can not be considered as bridge-oxidized species as the nitrogen atoms clearly bear the largest spin density in these radical cations.[212]

The excellent electronic coupling qualities of the thiophene moiety make oligo- and polythiophenes promising candidates for electronic devices. Therefore, a fundamental understanding of the CT characteristics of doped (cationic) polythiophenes is crucial. In this context, Lacroix et al. used "the mixed-valence approach" and studied the ET behavior of such oligomers and polymers by comparison of the CT behavior of oligothiophenes of type **109**$_n^+$ (Scheme 39) with the corresponding bis(dianisylamine) radical cations with different oligothiophenes as bridging units **110**$_n^+$ (Scheme 39).[213]

AM1-UHF calculations of the geometry and charge distribution of radical cations **110**$_n^+$ clearly demonstrate that the charge is symmetrically delocalized for small bridging units (**110**$_1^+$ and **110**$_2^+$), and these compounds can be assigned to Robin–Day class III. As the bridge length increases, the charge is no longer symmetrically distributed and from $n > 4$, the charge is clearly localized on the redox centers and these systems are class II MV compounds. A similar behavior is found for the thiophene oligomers **109**$_n^+$, where the small oligomers ($n < 13$) show symmetrical charge distribution at the center of the molecule, while the charge is clearly localized close to one end of the oligomer chain for longer oligomers ($n > 14$).[213] However, for further interpretation of these results it must be taken into account that the UHF method tends to overestimate charge localization, and it is bipolarons (doubly charged, spin coupled) or bipolaron pairs (doubly charged, spin decoupled) which are the charge carriers in polythiophene materials and not single charges (polarons).[214]

Table 21: IV-CT band data and electronic couplings of **105**$^+$–**108**$^+$ in dichloromethane.[212]

	$\tilde{\nu}_{max}$ [cm^{-1}]	ε [M^{-1} cm^{-1}]	V [cm^{-1}][a]
105$^+$	8750	9480	4375
106$^+$	10100	10020	5050
107$^+$	10500	10300	5250
108a^{+}[b]	12500	11600	6270

[a] $V = \tilde{\nu}_{max}/2$ assuming class III behavior. [b] Compound **108b**$^+$ shows almost identical data.

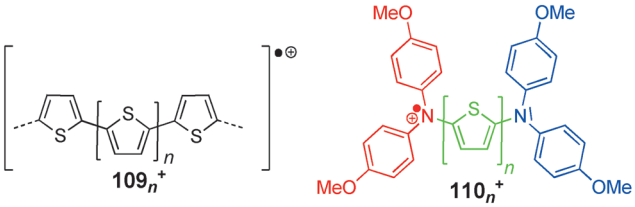

Scheme 39. Positively charged polythiophene **109**$_n^+$ and bis(diarylamine) radical cations **110**$_n^+$ with different oligothiophene moieties acting as spacer units.

3.1.7. MV Compounds with Phenothiazine and Dihydrodimethylphenazine Redox Centers

Triarylamine and diarylamine redox centers are the most common and most intensively studied organic MV compounds containing aromatic nitrogen redox centers. Although the geometrical changes upon oxidation of these redox centers are small, yielding small inner reorgan-

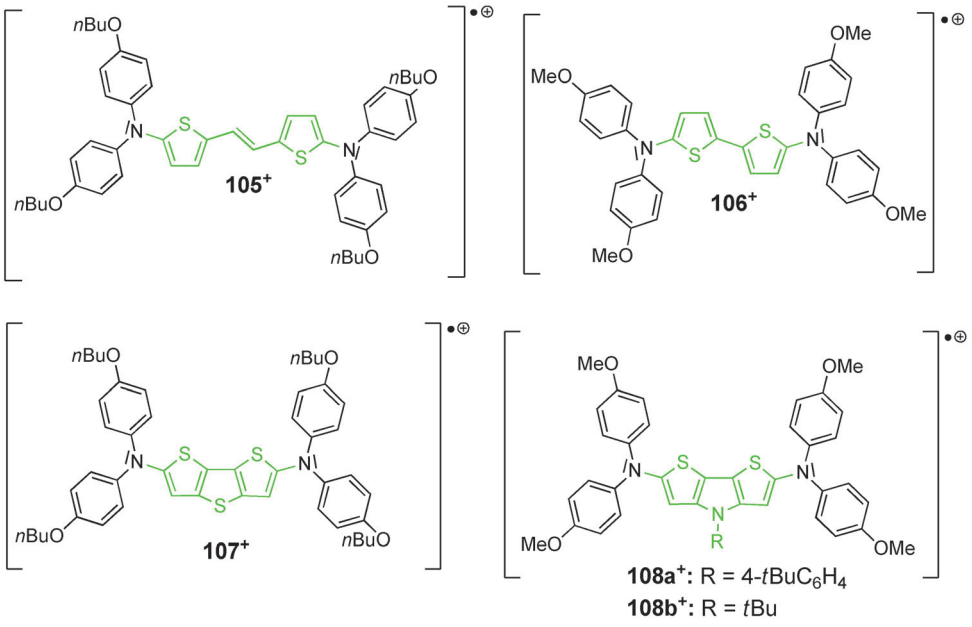

Scheme 38. Bis(diarylamine) radical cations with thiophene-based spacer moieties **105**$^+$–**108**$^+$.

ization energies λ_v, the situation is intrinsically different for MV compounds with phenothiazine and dihydrodimethylphenazine redox centers. Kochi and co-workers studied the ET process in a series of bis(phenothiazine) radical cations (**111**$^+$–**113**$^+$; Scheme 40). The structure of both the neutral

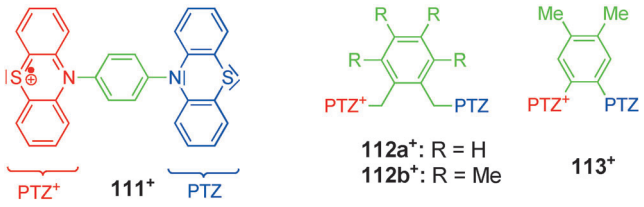

Scheme 40. Bis(phenothiazine) radical cations **111**$^+$–**113**$^+$.

and oxidized phenothiazine redox centers in the MV compounds **111**$^+$ and **112a**$^+$ were determined by X-ray crystal-structure analyses.[215] In these compounds the relatively large reorganization energies upon ET can be traced back to a planarization of the phenothiazine redox center upon oxidation (Scheme 41).

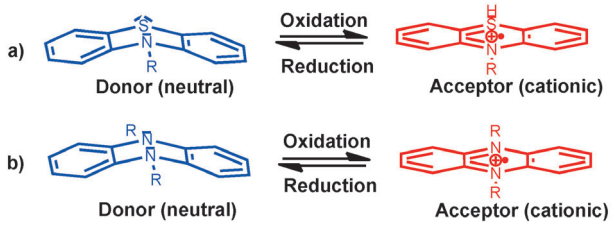

Scheme 41. Planarization upon oxidation of a) phenothiazine and b) dihydrodimethylphenazine redox centers.

Kochi and co-workers assigned MV compounds **111**$^+$–**113**$^+$ to Robin–Day class II, although optical analysis, ESR measurements, and crystallographic data suggest both class II and class III character. Some of the results of these studies are summarized in Table 22. This assignment is particularly questionable for compound **113**$^+$. One argument of the authors for a localization of the charge is the solvatochromism of the IV-CT band, while the large redox potential splitting ΔE, the narrow band shape, and dynamic ESR spectroscopy support delocalization in **113**$^+$.[215] Nevertheless, it is apparent

Table 22: IV-CT band data, electronic coupling determined by Mulliken–Hush analysis, ET rates from temperature-dependent ESR measurements, and redox potentials of **111**$^+$–**113**$^+$ in dichloromethane.[215]

	$\tilde{\nu}_{max}$ [cm^{-1}][a]	ε [M^{-1} cm^{-1}]	V [cm^{-1}][b]	ΔE [mV][c]	k_{ET} [s^{-1}][d]
111$^+$	10300	860	400	0.17	2.0×10^7
112a$^+$	10600	360	530	0.14	2.0×10^7
113$^+$	5600	2500	1280	0.34	$>10^{9}$[e]

[a] In the context of the two-state model and the assumption of class II character, $\tilde{\nu}_{max}$ corresponds to λ. [b] Calculated by the Mulliken–Hush two-state one-mode model. [c] $\Delta E = |E_{1/2}\,(\mathrm{Ox1}) - E_{1/2}\,(\mathrm{Ox2})|$ in dichloromethane. [d] ET rates determined by temperature-dependent ESR measurements. [e] Delocalized on the ESR timescale.

by comparison of the bis(phenothiazine) radical cations with similar bridged bis(triarylamine) radical cations, such as **1**$^+$, that the high reorganization energy of the former MV compounds should yield a localized class II charge distribution.

Bis(dihydrodimethylphenazine) radical cations **114**$^+$–**117**$^+$ (Scheme 42) are closely related to (bis)phenothiazine radical

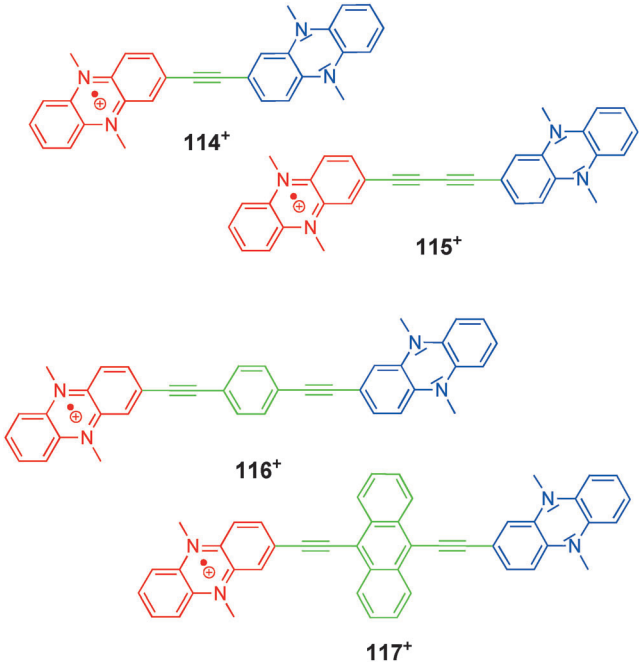

Scheme 42. Bis(dihydrodimethylphenazine) radical cations **114**$^+$–**117**$^+$ with various unsaturated spacers.

cations.[216] As shown in Scheme 41, the distinctive characteristics of this class of MV compounds are the large reorganization energy, which to some extent results from the planarization of the phenazine moiety upon oxidation, but is mainly due to changes in the C–C and C–N bonds, as shown by X-ray crystal data and density functional computations.[216] The optical band shape analysis of **114**$^+$–**117**$^+$ shows a decrease in the electronic communication with increasing spacer length, whereupon the values for V are on the same order of magnitude as for analogous bis(triarylamine) radical cations with identical spacer moieties (**3**$^+$, **4**$^+$, **63**$^+$, and **73a**$^+$). Unfortunately, optical analysis of **116**$^+$ was not possible due to strong overlap of the IV-CT band with higher energy transitions. It is remarkable that a plot of $\ln V$ versus the number of bonds of the spacer unit $n-1$ yields a linear correlation with an almost identical β value (0.17) as that determined for the corresponding (bis)triarylamine MV compounds (0.16). Despite similar electronic couplings, bis(dihydrodimethylphenazine) radical cations are class II compounds due to the higher inner reorganization energy and, therefore, have larger thermal ET barriers ΔG^* than the triarylamine analogues. These findings clearly demonstrate that the electronic coupling V is dominated by the type of the spacer but the localized/delocalized nature depends on both the spacer (which influences primarily V) and the redox

Table 23: Electron-transfer parameters derived from Mulliken–Hush analysis of the IV-CT bands of bis(dihydrophenazine) radical cations **114**$^+$, **115**$^+$, and **117**$^+$ in benzonitrile as well as of bis(triarylamine) radical cation **3**$^+$ (with the same spacer as **114**$^+$) in benzonitrile.[216]

	λ [cm^{-1}][a]	ε [M^{-1} cm^{-1}]	ΔG^* [cm^{-1}]	V [cm^{-1}][a]	ΔE [mV][b]
114$^+$	8500	4960	910	870	92
115$^+$	9200	3130	1310	600	82
117$^+$	8700	2240	1880	310	59
3$^+$	6600	10100	740	980	–[c]

[a] Determined by Mulliken–Hush two-state model with quartic augmentation of the diabatic potentials; $\tilde{\nu}_{max}$ is similar to λ. [b] $\Delta E = |E_{1/2}\,(Ox1) - E_{1/2}\,(Ox2)|$ in a benzonitrile/0.2 M tetrabutylammonium tetrafluoroborate solution, scan rate = 50 mV s^{-1}. [c] Not determined in benzonitrile.

centers (which primarily influence λ). The main results of these studies on MV compounds **114**$^+$–**117**$^+$ are listed in Table 23.

3.1.8. MV Compounds with Dialkylamine Redox Centers

MV compounds with dialkylamine redox centers have been investigated much less intensively than their aromatic analogues because of the instability of dialkylanilines upon oxidation. The main interest in this series of organic MV compounds is the comparison of its ET behavior with that of bis(triarylamine) radical cations to ascertain the influence of the redox centers on the ET. Brédas and co-workers showed that the electronic couplings in bis(dimethylamine) radical cations **33**$^+$, **118**$^+$, and **119**$^+$ (Scheme 43) are about 30–70 % larger than those in the corresponding bis(dianisylamine) radical cations **1**$^+$–**3**$^+$.[217] This increased coupling is due to the decreased delocalization of the charge and spin into the peripheral methyl groups in the bis(dimethylamine) MV compounds. Hence, the diabatic ET distances are presumably smaller, which directly yields an increased electronic coupling [see Eqs. (8) and (10)] compared to that of **1**$^+$–**3**$^+$, where the charge can additionally be delocalized over the peripheral anisyl substituents. The increased electronic coupling of bis(dimethylamine) radical cations **33**$^+$, **118**$^+$, and **119**$^+$ compared to their bis(dianisyl) analogues is also reflected by larger ΔE values.[217]

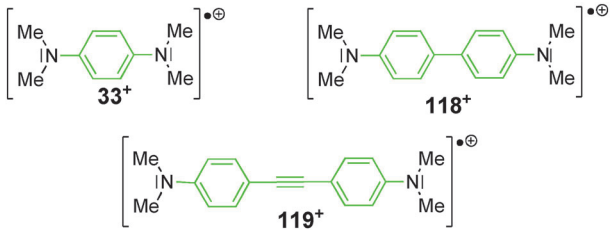

Scheme 43. Dialkylamine radical cations **33**$^+$, **118**$^+$, and **119**$^+$ with unsaturated spacers.

A second distinctive feature of bis(dimethylamine) MV compounds is the appearance of a significant vibrational fine structure of the CT band when the anisyl substituents are replaced by alkyl groups (here methyl). For a comparison of CT bands with vibrational fine structure of different MV systems, see Figure 14 (Section 3.4). Brédas and co-workers suggested that additional low-frequency modes are coupled to the ET process in the triarylamine MV systems and, hence, the vibrational fine structure is not resolved.[217] In particular for the bis(triarylamines), it could be shown that symmetric modes lead to line-broadening effects and have to be included (in addition to the commonly used asymmetric vibrations) to perform quantitative analyses of the CT bands.[117,134,217,218]

As indicated above, one problem when studying bis(dialkylamine) radical cations is the instability of these compounds because of α-H abstraction. This problem can be circumvented by protecting the amine redox centers with bicyclo[3.3.1]nonan-3-one substituents, which show kinetic stability according to Bredt's rule.[219] Nelsen, Zink et al. investigated the vibrational fine structure of the CT bands of a series of bicyclo[3.3.1]nonan-3-one-protected bis(dialkylamine) radical cations (**120**$^+$–**123**$^+$; Scheme 44).[220,221] Raman spectroscopy of **120**$^+$ elucidates the importance of symmetric vibrational modes, which are also coupled to the intervalence transition. Both the resonance Raman intensities of the modes as well as the electronic spectrum could be calculated successfully by time-dependent quantum-chemical approaches.[220] A good agreement between the experimental (optical) data and $\tilde{\nu}_{max}$ calculated by the NICG method (see Section 2.3) was found for the CT bands of **121**$^+$–**123**$^+$.[221]

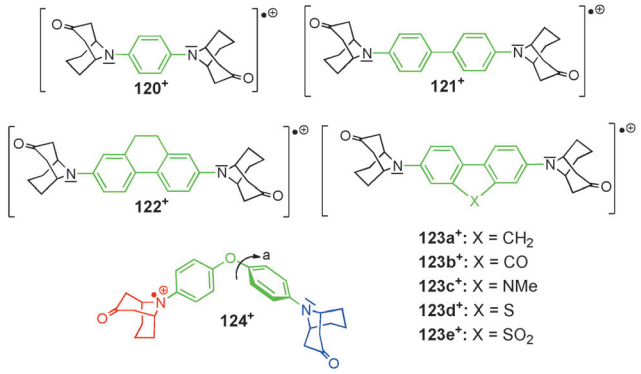

Scheme 44. Dialkylamine radical cations **120**$^+$–**124**$^+$ protected by bicyclo[3.3.1]nonan-3-one substituents.

Although the bis(dialkylamine) radical cations **121**$^+$–**123**$^+$ are all clearly delocalized class III MV compounds with rather intense vibrationally resolved CT bands, compound **124**$^+$ (Scheme 44) with a diphenylether spacer moiety is a weakly coupled localized class II compound with a weak but broad and symmetric IV-CT band at $\tilde{\nu}_{max} = 10600$ cm^{-1} with $\varepsilon = 720$ M^{-1} cm^{-1}[222] (for comparison, the CT bands of all the delocalized radical cations **121**$^+$–**123**$^+$ have extinction coefficients of at least $\varepsilon > 40000$ cm^{-1} at comparable energies).[221] The decoupling in **124**$^+$ mainly results from a twist around the C–O bond between the neutral dialkylaniline moiety and the oxygen lone pairs of electrons. A Mulliken–Hush treatment of the optical data using AM1 calculated dipole moments yielded an electronic coupling of $V = 810$ cm^{-1} in dichloromethane.[222] The experimental determined electronic coupling is surprisingly large considering the fact that AM1

calculations predict a twist angle of $\alpha = 82°$ in the optimized structure and assuming the usual cosα-dependence of V. This can be explained by the low-frequency character of the twist mode and a relatively flat energy surface for the twist. This permits the system to reduce the twist angle very easily for ET processes and, hence, increases the electronic coupling dramatically as a result of the cosine relationship (e.g. $\cos 82° = 0.14$; $\cos 70° = 0.34$).[222]

Diamine radical cations bridged by piperazine units may also be conceived to be bis(dialkylaniline) MV compounds, albeit bridged by alkyl spacers. In the series of MV compounds **125**$^+$–**128**$^+$ (Scheme 45), a switch-over from class III (**125**$^+$ and **126**$^+$) to class II (**127**$^+$ and **128**$^+$) can be

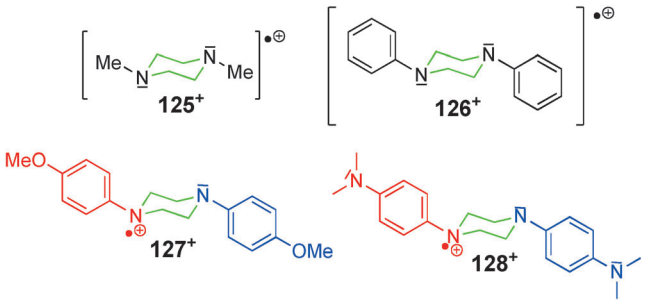

Scheme 45. Diamine radical cations **125**$^+$–**128**$^+$ bridged by piperazine spacers.

observed in acetonitrile.[223,224] Brouwer et al. showed by resonance Raman spectroscopy and ab initio calculations that the piperazine spacer unit has a symmetric chair conformation both in the neutral and in the oxidized state, while the nitrogen atoms are strongly pyramidalized in the neutral form, but almost planar coordinate in the cation.[225] Thus, electron transfer is associated with a large reorganization energy. The type of substituents on the piperazine spacer unit controls the localized/delocalized character of the radical cations: electron-donating aromatic substituents such as dimethylaniline or anisol on the piperazine nitrogen atom stabilize the positive charge and lead to a localization on one redox center. Hence, there is a crossover from class III to class II when electron-donating substituents such as OMe (**127**$^+$) or NMe_2 (**128**$^+$) are attached to the phenyl rings in **126**$^+$.

Unfortunately, the ET behavior of **125**$^+$–**128**$^+$ has not been studied in detail and only rather qualitative assessments were possible based on the study of the absorption spectra. A typical optical transition for dialkylsubstituted radical cations at about 500 nm in the UV/Vis spectrum served as the main criterion for the classification of the compounds as either delocalized or localized.[224] Furthermore, temperature-dependent ESR measurements of the absorption band in dichloromethane support the classification of at least **128**$^+$ as a localized class II MV compound.[223]

A carbonyl group acts as a decoupling linker in the bis(hydroxylamine) radical cation **129**$^+$ (Scheme 46) because of its cross-conjugated nature.[223,226] Although the distance between the redox centers is very small, Nelsen et al. found criteria to classify **129**$^+$ as a localized class II MV compound.

Scheme 46. Bis(hydroxylamine) radical cation **129**$^+$ with a carbonyl bridge unit.

Two reasons may account for this behavior: first, several investigations on other radical cations of urea derivatives[227] as well as semiempirical MO calculations predict that the neutral hydroxylamine–carbonyl conjugation is very strong while the oxidized hydroxylamine bears the whole spin density and is twisted out of plane by nearly 90°, which leads to a weak resonance interaction. Second, solvatochromic studies on the IV-CT band of **129**$^+$ indicate a relatively high inner reorganization energy as a consequence of enormous structural changes upon charge transfer.[226] Furthermore, the localized character of **129**$^+$ was confirmed experimentally by temperature-dependent ESR measurements.[226]

3.2. Organic MV Compounds with Carbon-Based Redox Centers

3.2.1. Bis(perchlorotriphenylmethyl) Radical Anions

The open-shell character of organic MV compounds limits the choice of redox centers to a few atomic groups that can form stable radicals. Even though the most important element

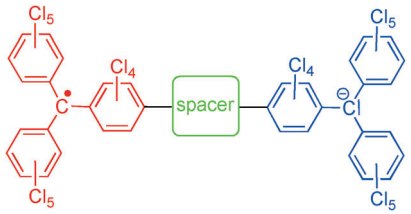

in this respect is nitrogen, there are some other non-metals that can form relatively stable radical species. Among them are organic redox centers where the charge or spin are mainly located at carbon centers, although some "tricks" have to be used to stabilize the radicals in these cases. One of these "tricks" is to introduce substituents which make these carbon radical centers persistent. Impressive examples are perchlorinated triphenylmethyl (PCTM) radicals which are inert towards many chemical reactions and reaction conditions.[228–231] Their inertness towards oxygen and moisture, with an estimated life-time of about 100 years, is due to the six *ortho*-chloro substituents which perfectly shield the radical center. Furthermore, the π-orbital overlap of the perchlorinated phenyl rings and the central carbon p orbital is reduced due to large torsional angles and, hence, most of the spin density is located at the central carbon atom. Ballester et al. developed a straightforward and regioselective chlorination reagent in the 1960s, and since then PCTM radicals have been frequently used as redox centers in MV compounds or other donor–acceptor compounds. PCTM radicals are ideal components for the design of polyradicals and high-spin systems with interesting magnetic properties. The key steps in the synthesis of PCTM radicals are the perchlorination reaction with the so-called BMC reagent,[92,232] which selectively chlorinates unsaturated carbon atoms. A subsequent radical-

ization of the in situ formed anion is achieved with an oxidant such as iodine or *p*-chloranil (Scheme 47). PCTM radical **130** can be further functionalized at the methyl substituent, and is an example of an important building block for the synthesis of

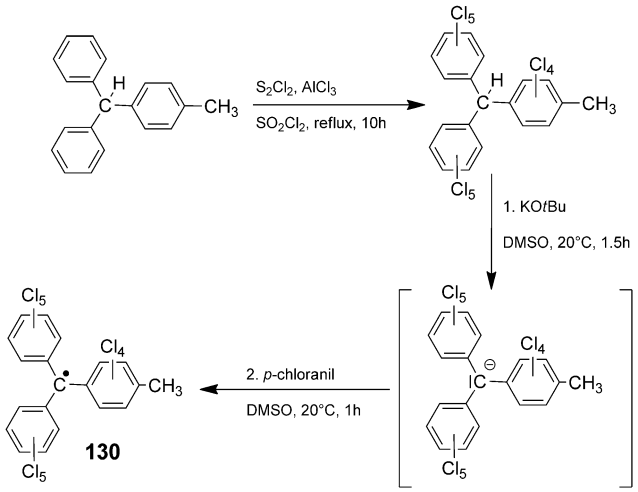

Scheme 47. Key steps in the synthesis of the PCTM radical **130**: Selective perchlorination of all unsaturated C–H atoms with the BMC reagent and formation of the radical by deprotonation of the α-H atom with KO*t*Bu in DMSO and subsequent oxidation of the in situ generated carbanion with *p*-chloranil.

bis(PCTM) radical anions. The problems with characterizing radicals by NMR spectroscopy usually result in the radicalization being made in the final synthetic step.

Veciana and co-workers synthesized three bis(PCTM) radical anions (**10**$^-$, **11**$^-$, and **131**$^-$; Scheme 48) and studied the ET behavior of these MV compounds by optical analyses of their IV-CT bands as well as by ESR experiments, with a focus on the influence of the topology (*para* versus *meta*).[3,233,234] The radical anions for the optical studies were generated by spectroelectrochemistry in a solution of dichloromethane and 0.1M tetrabutylammonium hexafluorophosphate. A weak IV-CT band is observable in the NIR region of the absorption spectrum of MV compounds **10**$^-$ and **131**$^-$, while such a band is missing in the case of the *meta*-substituted (non-Kekulè) MV species **11**$^-$, which is clear evidence for a very weak electronic coupling. In addition, this interpretation is confirmed by temperature-dependent ESR measurements, where no evidence for an electronic coupling was found for **11**$^-$ whereas weak electronic couplings could be identified for compounds **10**$^-$ ($V = 121$ cm^{-1}) and **131**$^-$ ($V = 100$ cm^{-1}). The attachement of the electron-donating octyloxy substituents had only a weak influence on the electronic coupling. This contrasts with the behavior of triarylamine radical cation **63**$^+$, where methyl donor groups attached to the bridge enhance the electronic coupling by raising the HOMO energy of the bridge. This difference can be understood if one assumes that the ET in the **131**$^-$ radical anion is mediated by the bridge LUMO, which should be influenced to a lesser degree by donor substituents than the HOMO. Quite recently, a series of bis(perchlorotriphenylmethyl) radicals with oligo(phenylenevinylene) bridges of various lengths was investigated by variable-temperature ESR spectroscopy. A transition from superexchange to hopping for longer bridges was concluded from this study.[235]

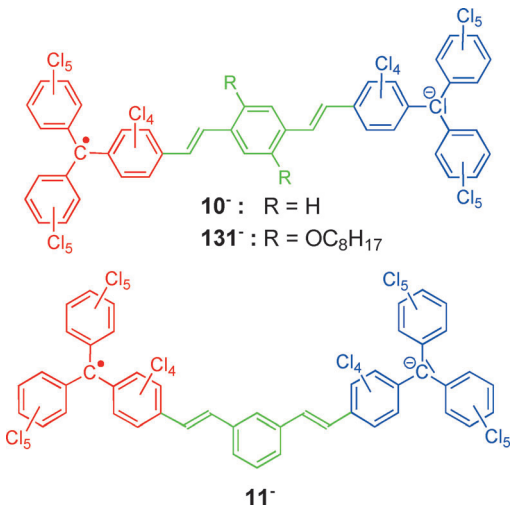

Scheme 48. Bis(PCTM) radical anions **10**$^-$, **11**$^-$, and **131**$^-$.

PCTM radicals are also used as acceptor centers in neutral organic MV compounds, but these will be treated separately in Section 3.5 because of the special characteristics of this class of compounds.

3.2.2. *Bis(1,4-dimethoxybenzene) Radical Cations*

Bis(1,4-dimethoxybenzene) radical cations are the most intensely studied organic MV compounds with carbon redox centers. The classification of 1,4-dimethoxybenzene as a

"carbon redox center" is made because of the fact that the whole redox center is dominated by the carbon ring system where the charge is delocalized. Oxidation of the 1,4-dimethoxybenzene redox centers is associated with large changes in the bond lengths as a result of the crossover from a benzenoid to a quinonoid structure and, hence, a relatively large inner reorganization energy is expected for this class of MV compounds. Kochi and co-workers synthesized many bis(2,5-dimethoxy-4-methylphenyl) radical cations, such as **132**$^+$–**144**$^+$ (Schemes 49–52) and studied the ET processes of these compounds by optical, electrochemical, and temperature-dependent ESR measurements.[192]

The distance between the redox centers in MV radical cations **132**$^+$–**135**$^+$ is identical. The influence of the bridge conformation has been probed by a step by step increase in the dihedral angle between the donor and the bridge π system through increasing the number of methyl substituents. A decreasing electronic coupling V in **132**$^+$–**135**$^+$ (Table 24) as determined by a Mulliken–Hush analysis of the correspond-

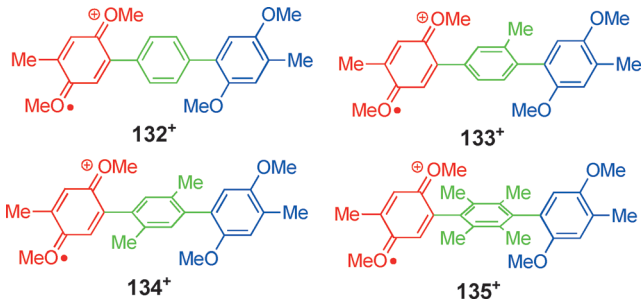

Scheme 49. Bis(2,5-dimethoxy-4-methylphenyl) radical cations **132**$^+$–**135**$^+$ with different substituted phenylene spacer units.

Table 24: IV-CT band data, electronic coupling values determined by Mulliken–Hush analyses, ET rate constants determined by ESR and calculated by Mulliken–Hush derived electronic coupling values, and differences in the redox potentials.[192,236,237]

	$\tilde{\nu}_{max}$ [cm^{-1}][a]	ε [M^{-1} cm^{-1}]	V [cm^{-1}]	k_{ET}(MH) [s^{-1}]	k_{ET}(ESR) [s^{-1}][a]	ΔE [mV][b]
132$^+$	6370	3900	760	1×10^{10}	$>10^{10}$	110
133$^+$	7870	780	377	4×10^{8}	10^{8}–10^{9}	90
134$^+$	8000	490	325	3×10^{8}	10^{8}	–[c]
135$^+$	8260	220	170	9×10^{7}	10^{8}	–[c]
136$^+$	6800	4200	430	2×10^{9}	3×10^{9}	–[c]
137$^+$	6710	1900	217	8×10^{8}	1×10^{8}	–[c]
138$^+$	–[d]	–[d]	–[d]	–[d]	3×10^{7}	–[c]
139$^+$	7040	2600	327	9×10^{8}	10^{8}	–[c]
140$^+$	5290	17200	618	2×10^{10}	10^{8}–10^{9}	–[c]
141$^+$	–[d]	–[d]	–[d]	–[d]	5×10^{7}	–[c]
142$^+$	7520	2300	270	4×10^{8}	10^{8}–10^{9}	–[c]
143$^+$	5620	10700	630	2×10^{10}	10^{8}–10^{9}	65
144$^+$	4660	4800	2330[e]	–[f]	–	290
145$^+$	6700	1200	400	–[f]	$>10^{8}$	–[c]

[a] Radical cations generated by chemical oxidation with $OMNSbCl_6$[238] in dichloromethane.[192] (OMN = 2,3,8,9-tetrahydro-1,1,4,4,7,7,10,10-octamethyltetracene.) [b] $\Delta E = |E_{1/2}(Ox1) - E_{1/2}(Ox2)|$ in a dichloromethane/0.1 M tetrabutylammonium hexafluorophosphate solution.[192,236] [c] No redox splitting observed.[192,236,237] [d] No band analysis possible because of band overlap.[192] [e] Determined by $V = \tilde{\nu}_{max}/2$. [f] Not calculated.

ing IV-CT bands accompanies this diminished conjugation of the donor, acceptor, and bridge π systems.[192] As the coupling decreases, the reorganization energies increase in the order **132**$^+$ < **133**$^+$ < **134**$^+$ < **135**$^+$. This is an interesting point, as in this series of compounds the distance between the redox centers is kept constant, which should lead to a constant solvent reorganization energy [see Eq. (1)]. Thus, one can conclude that the inner reorganization energy rises which might be due to a different dihedral angle between dimethoxybenzene moiety and the bridge in the charged and neutral state. This class of compounds is one of the rare cases where rate constants for ET were determined by both temperature-dependent ESR measurements and optical analysis of the IV-CT bands.[192] As can be seen from Table 24, the rate constants estimated by both methods are in qualitative agreement and run parallel with the electronic coupling in **132**$^+$–**135**$^+$.

The distance dependence in bis(2,5-dimethoxy-4-methylphenyl) radical cations was investigated in the series **132**$^+$ and **136**$^+$–**138**$^+$ (Scheme 50), where the bridge is extended stepwise by one phenylene moiety.[192] Unfortunately, an optical

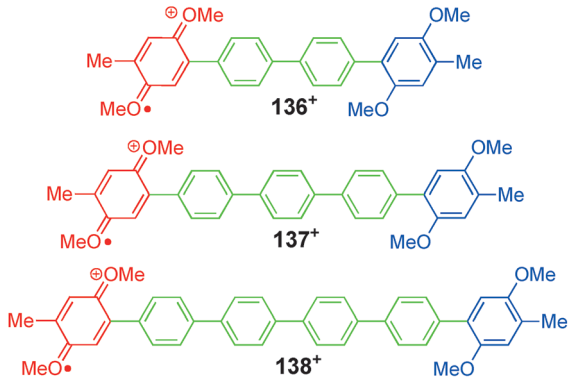

Scheme 50. Bis(2,5-dimethoxy-4-methylphenyl) radical cations **136**$^+$–**138**$^+$ with increasing length of the phenylene spacer.

analysis of the IV-CT band of **138**$^+$ with four phenylene spacer units is not possible due to too strong band overlap. The electronic coupling decreases as the bridge length increases and, consequently, the rate constants decrease in the same way (see Table 24). All the phenylene-bridged MV compounds have considerably smaller reorganization energies than their analogues with tolyl (**133**$^+$), xylyl (**134**$^+$), and duryl (**135**$^+$) spacer units because **132**$^+$ and **136**$^+$–**138**$^+$ may form planar conformations more easily. The type of connectivity of the spacer subunits has been varied in MV radical cations **139**$^+$–**143**$^+$ (Scheme 51) to probe its influence on ET. Compounds **139**$^+$–**143**$^+$ are all class II MV compounds and show IV-CT bands in the NIR region. Unfortunately, this band is masked by a higher energy transition in **141**$^+$ which precludes a band analysis. As can be seen from the optical data in Table 24, the reorganization energy λ ($=\tilde{\nu}_{max}$) strongly depends on the type of spacer. In particular, a significantly smaller reorganization energy is found for the stilbene-bridged MV compound **140**$^+$ than for the tolan-bridged **139**$^+$, and the electronic coupling in **140**$^+$ is nearly twice that of **139**$^+$. This finding agrees with the results of the Mulliken–Hush analysis by Barlow et al.[152,158] for the corresponding bis(triarylamine) radical cations **3**$^+$ and **12**$^+$ (see Section 3.1.5). Accordingly, the ET rate for **140**$^+$ determined by temperature-dependent ESR measurements is significantly larger than that of **139**$^+$ (Table 24).

Furthermore, the IV-CT band of **143**$^+$ is shifted to lower energy than that of **136**$^+$ because of the fluorene spacer which enforces planarization of the biphenyl bridge moiety, thus decreasing the inner reorganization energy in **143**$^+$. As can be seen from the results of the Mulliken–Hush analyses in Table 24, the electronic coupling in **143**$^+$ is clearly larger than for the corresponding biphenyl-bridged radical cation **136**$^+$. The observation of two separated oxidation waves by cyclovoltammetric measurements ($\Delta E = 65$ mV) is another indication of the stronger coupling in **143**$^+$. In contrast, the IV-CT band of the diphenyl ether bridged MV compound **142**$^+$ is

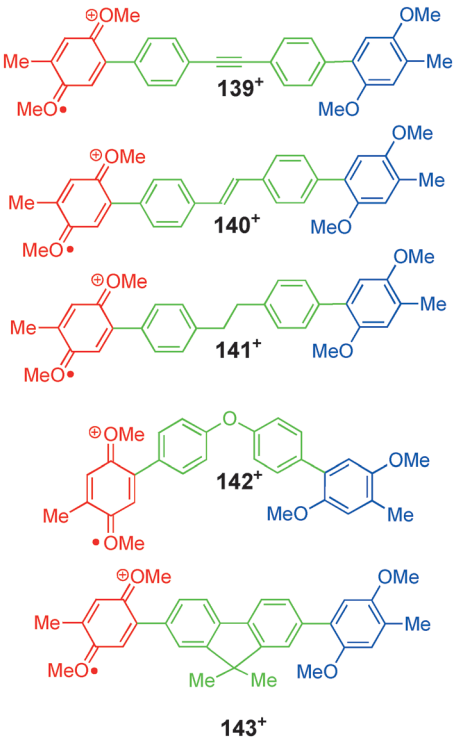

Scheme 51. Bis(2,5-dimethoxy-4-methylphenyl) radical cations **139**$^+$–**143**$^+$ with various bridge units.

shifted to higher energy (= higher total reorganization energy λ) and has a quite small electronic coupling V. Both effects are likely due to a twist around the oxygen–phenyl bond at the reduced redox site, similar to the twist found in the corresponding bis(dialkylaminophenylether) radical cation **124**$^+$ (Section 3.1.8).[222] Even though an optical analysis of **141**$^+$ was not possible, the ET rate constant determined by ESR measurements is relatively small and, consequently, a small electronic coupling can be assumed.

Kochi and co-workers employed X-ray crystallography to estimate the extent of localization or delocalization of the positive charge in a series of bis(2,5-dimethoxy-4-methylphenyl) radical cations **132**$^+$, **136**$^+$, and **143**$^+$–**145**$^+$ (Scheme 49–Scheme 52).[236,237] As a consequence of their large inner reorganization energy, 1,4-dimethoxybenzene redox centers are perfect candidates for this analytical method as they show large structural changes in the bond lengths upon oxidation The structural parameters for the neutral benzenoid as well as for the radical cation quinonoid structure of the redox center were determined by X-ray crystallography of appropriate model compounds. By assuming that the change in both the lengths and angles correlates linearly with the percentage of positive charge, the charge distribution in the MV systems can be calculated from structural parameters. This procedure clearly yields a delocalization of charge in **144**$^+$ with 50% charge distribution on each redox center. This class III character could also be supported by the large redox potential splitting $\Delta E =$ 290 mV[157] and by temperature-dependent ESR measurements. Furthermore, radical cation **144**$^+$ shows a low-energy non-Gaussian-shaped CT band, typical of delocalized systems.[237]

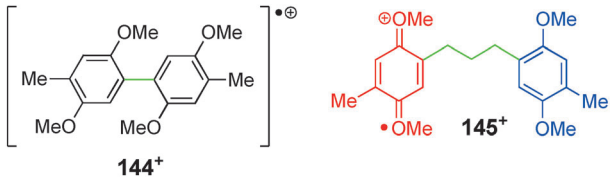

Scheme 52. Bis(2,5-dimethoxy-4-methylphenyl) radical cations **144**$^+$ and **145**$^+$.

Although X-ray crystallography predicts class III character for **144**$^+$, it assigns **136**$^+$ and **145**$^+$ as being class II systems with one redox center bearing the full charge and one remaining neutral.[237] This classification is also supported by optical, ESR, and cyclovoltammetric data (Table 24). The comparatively high value for the electronic coupling of **145**$^+$ with a saturated propylene spacer unit might be due to contributions of conformers where a significant through-space ET is provided by a "face to face" arrangement of the aromatic redox centers; however, this assumption was not proved experimentally. X-ray crystallographic investigations on compounds **132**$^+$ and **143**$^+$ clearly yielded an asymmetric charge distribution. According to these analyses, **132**$^+$ shows a 20%:80% charge distribution for the two redox centers.[237] Therefore, **132**$^+$ can be defined as a borderline class II/III compound. The X-ray crystallographic data for **143**$^+$ also clearly show an asymmetric charge distribution, but a quantitative analysis yielded the charge as not only being localized at the redox centers (20%:35%) but also significantly localized on the fluorene bridge (45%).[236] Therefore, **143**$^+$ is very close to the class II/III boundary, and a very small effective ET distance can be assumed.

Since 1,4-dimethoxybenzene redox centers are planar π systems, they are good candidates for studying intramolecular through-space interactions provided a conformation with cofacial arrangement of the redox centers is possible. In this context Kochi and co-workers investigated the ET process of a series of bis(1,4-dimethoxybenzene) radical cations **146**$^+$–**151**$^+$ (Scheme 53).[239] While MV compounds **146**$^+$ and **147**$^+$ are connected by a rigid spacer which inhibits a "face to face"

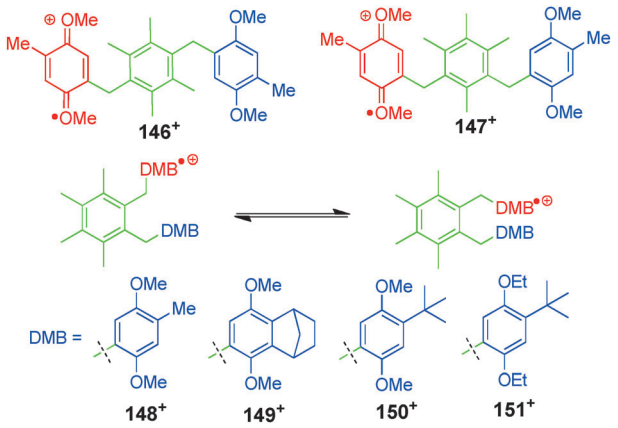

Scheme 53. Bis(1,4-dimethoxybenzene) radical cations **146**$^+$–**151**$^+$ with *ortho*-, *meta*-, and *para*-linked phenylene spacers.

conformation of the redox centers, such a cofacial conformation is possible in the *ortho*-bridged radical cations **148**$^+$–**151**$^+$. The *tert*-butyl substituent in **150**$^+$ and **151**$^+$ as well as the bicyclic substituent in **149**$^+$ increase the steric hindrance at the redox centers and, therefore, hamper good π–π interactions and, consequently, through-space ET.

The absorption spectra of the MV compounds with an *ortho*-substituted spacer unit (**148**$^+$–**151**$^+$) all show an IV-CT band in the NIR region, while no such band can be observed for the *para*- and *meta*-bridged compounds **146**$^+$ and **147**$^+$ (Table 25). Thus, the electronic coupling in **146**$^+$ and **147**$^+$ is

Table 25: IV-CT band data, electronic coupling values determined by Mulliken–Hush analyses, ET rate constants determined by ESR (k_{ET}(ESR)) and calculated by the Mulliken–Hush derived electronic coupling values (k_{ET}(MH)), as well as redox potential splittings of radical cations **148**$^+$–**151**$^+$.[239]

	$\tilde{\nu}_{max}$ [cm^{-1}]	ε [M^{-1} cm^{-1}]	V [cm^{-1}]	k_{ET}(MH) [s^{-1}]	k_{ET}(ESR) [s^{-1}]	ΔE [mV][f]
148$^+$	6250	1100	760	4×10^{9}[c]	$>10^{9}$[c]	160
149$^+$	8930	320	400	2×10^{7}[d]	4×10^{7}[d]	–[g]
150$^+$	10950[a]	360	–[b]	–[b]	–[e]	80
151$^+$	10720[a]	170	–[b]	–[b]	–[e]	90

[a] Absorption band with the lowest energy. It is a matter of debate if this band is an IV-CT band or a bridge band.[239] [b] Not determined (see [a]). [c] $T=+30$ °C. [d] $T=-20$ °C. [e] Not determined. [f] $\Delta E=|E_{1/2}$ (Ox1) $-E_{1/2}$ (Ox2)| in a dichloromethane/0.2 M tetrabutylammonium hexachlorophosphate solution. Scan rate: 2000 mV s^{-1}.[239] [g] No redox potential splitting observed.

assumed to be very small at best, and these compounds can be assigned as class I compounds or to be at the class I/II boundary. These findings were confirmed by the results of temperature-dependent ESR measurements, where no line-broadening effects could be observed and an ET process, if existing, is too slow to be measurable. Furthermore, **146**$^+$ and **147**$^+$ show no redox potential splitting ΔE. The lack of electronic coupling in these compounds can be explained by the two saturated methylene spacer units, which strongly attenuate the electronic communication. In contrast, the *ortho*-bridged radical cations **148**$^+$–**151**$^+$ display a significant electronic coupling which cannot be due to a through-bond interaction but rather to a through-space (π–π) interaction of the redox centers. Mulliken–Hush analysis of the IV-CT band of **148**$^+$ in dichloromethane yields an electronic coupling of 760 cm^{-1}.[239] This value is comparable to that of **132**$^+$, a MV compound approaching the boundary of class II/III compounds. Further evidence for through-space interaction being the origin for this large electronic communication is the decreased electronic coupling in **149**$^+$–**151**$^+$, where large bicyclic or *tert*-butyl substituents hamper the face to face interaction of the redox centers. Temperature-dependent ESR measurements on **148**$^+$ and **149**$^+$ also confirm these findings, as ET in **148**$^+$ is too fast to be resolved on the ESR time scale down to −90 °C. On the other hand, the ESR spectra of **149**$^+$ show line-broadening effects and simulation of the spectra yielded a significantly lower ET rate than for **148**$^+$ (see Table 25). Furthermore, the lack of a redox potential splitting in **149**$^+$ and the much smaller ΔE values of **150**$^+$ and **151**$^+$ compared to **148**$^+$ confirm a through-space ET process (Table 25).

Kochi and co-workers characterized crystalline salts of **148**$^+$ with $SbCl_6^-$ and PF_6^- counterions by X-ray crystallography.[239] Although a symmetric delocalization of the charge over both redox centers (50 %:50 %) was found for **148**$^+$-$SbCl_6^-$, the charge is asymmetrically distributed (90 %:10 %) in **148**$^+$-PF_6^-. Even though both counterions are relatively large, these results demonstrate the prononced influence of counterions on the (electronic) structure of MV salts. Despite X-ray crystallographic data suggesting **148**$^+$ to be a borderline class II/III compound, the symmetric band shape of the IV-CT band argues for class II character. A class II treatment of the IV-CT bands in the context of the Mulliken–Hush model yielded ET rates k_{ET}(MH) which are in agreement with the rates k_{ET}(ESR) derived by time-dependent ESR spectroscopy (Table 25).

The ideal model systems to probe direct through-space interactions are [*n.n*]paracyclophanes. Information gained by investigating such cyclophanes will also be helpful for understanding intermolecular charge transfer between π systems in solid-state organic materials, as they are employed in, for example, field-effect transistors. Neugebauer and co-workers studied the ET behavior of a series of bis(1,4-dimethoxybenzene) radical cations (**152**$^+$–**160**$^+$; Scheme 54) by ESR/

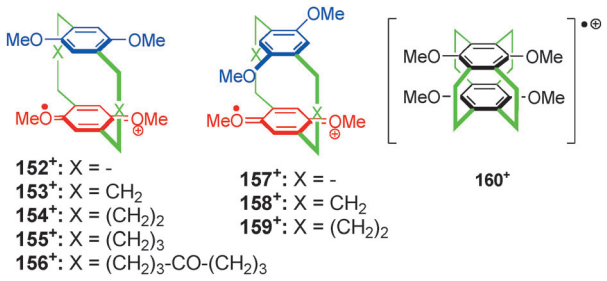

Scheme 54. Bis(1,4-dimethoxybenzene)paracyclophane MV compounds **152**$^+$–**160**$^+$ studied by ESR/ENDOR spectroscopy as well as by cyclic voltammetry.

ENDOR spectroscopy and cyclic voltammetry.[240] The main advantage of these systems is the increased persistence of the corresponding radical cations and the weaker susceptibility to ion-pairing effects compared to the radical anions of unsubstituted paracyclophanes.[45,241]

Unfortunately, MV systems **152**$^+$–**160**$^+$ have not been investigated by optical methods, and the ESR/ENDOR spectroscopic measurements yielded only qualitative information about the electronic coupling or rate constants. These investigations showed that the electronic communication between the redox centers is very strong in [2.2]-, [3.3]-, and [2.2.2.2]paracyclophane radical cations **152**$^+$, **153**$^+$, **157**$^+$, **158**$^+$, and **160**$^+$ with relatively short interplanar distances, and a delocalization of spin and charge over both 1,4-dimethoxybenzene systems was found. The large redox potential splitting ΔE confirms these findings (Table 26). In contrast, in compounds **155**$^+$ and **156**$^+$, with long interplanar distances (>5 Å), the charge is localized on one redox center at low temperatures (220 K) but there is still an electronic commu-

Table 26: Redox potential splittings and interplanar distances determined by X-ray crystal structure investigations of bis(1,4-dimethoxybenzene) radical cations **152**$^+$–**160**$^+$.[240]

	ΔE [mV][a]	Interplanar distance d [Å][c]
152$^+$	350	3.07
153$^+$	340	3.32
154$^+$	210	4.01
155$^+$	80	5.11
156$^+$	–[b]	7.38
157$^+$	290	3.05
158$^+$	360	3.25
159$^+$	210	–
160$^+$	200	–

[a] $\Delta E = \lvert E_{1/2}\ (\mathrm{Ox1}) - E_{1/2}\ (\mathrm{Ox2}) \rvert$ in an acetonitrile/0.1 M tetrabutylammonium hexafluorophosphate solution. Scan rate: 100 mV s^{-1}.[240] [b] No redox potential splitting observed. [c] Interplanar distances determined from X-ray crystal structure investigations of analogous derivatives (see Ref. [240] and references cited therein).

nication at higher temperatures (300 K). An intermediate ET behavior was found for [4.4]paracyclophane radical cations **154**$^+$ and **159**$^+$, where the ET process is fast over a broad temperature range. Although a large electronic coupling can be assumed in these compounds, they are localized (class II) systems, presumably because of the large reorganization energy typical of these bis(1,4-dimethoxybenzene) systems.

In addition to the paracyclophane radical cations, methoxy-substituted [2.2]naphthalenophane radical cations **161**$^+$ and **162**$^+$ (Scheme 55) as well as the corresponding anthracenophane radical cation **163**$^+$ were also investigated by ESR/ENDOR spectroscopy and cyclic voltammetry.[242]

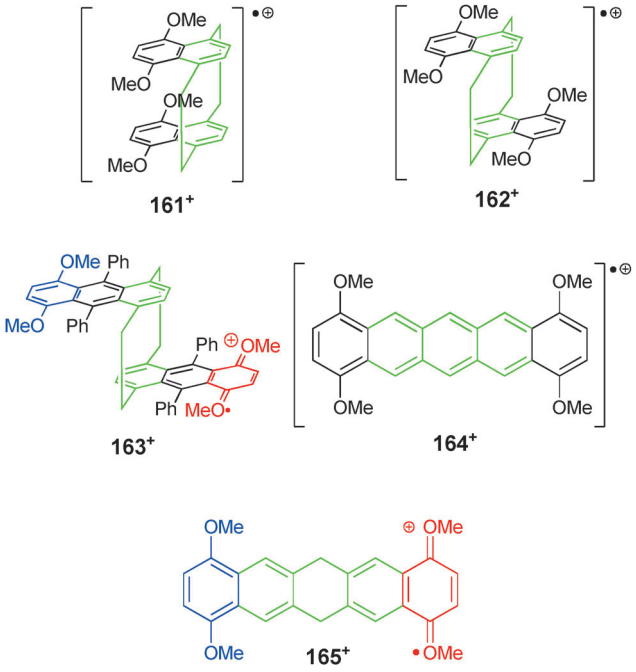

Scheme 55. Methoxy-substituted naphthalenophane (**161**$^+$ and **162**$^+$), anthracenophane (**163**$^+$), and pentacene (**164**$^+$ and **165**$^+$) radical cations.

These measurements yield a very fast electron-transfer process in both isomeric naphthalenophane radical cations **161**$^+$ and **162**$^+$. The measurements show that the odd electron is delocalized over both redox centers on the ESR time scale. The large electronic communications are also supported by the large redox potential splittings ΔE (Table 27). It is

Table 27: Redox potential splittings of bis(1,4-dimethoxybenzene) radical cations **161**$^+$–**165**$^+$.[242]

	ΔE [mV][a]
161$^+$	390
162$^+$	270
163$^+$	100
164$^+$	410
165$^+$	90

[a] $\Delta E = \lvert E_{1/2}\ (\mathrm{Ox1}) - E_{1/2}\ (\mathrm{Ox2}) \rvert$ in a dichloromethane/0.1 M tetrabutylammonium hexafluorophosphate solution. Scan rate: 100 mV s^{-1}.[242]

remarkable that the electronic coupling in **162**$^+$ is estimated to be nearly the same as for **161**$^+$, although the distance between the redox centers is much larger in the former. Thus, in these systems the ET rate-limiting effect is the direct π–π interaction in the paracyclophane moiety rather than the interaction of the methoxy-substituted redox centers. As indicated by the smaller redox potential splitting, the ET process in anthracenophane **163**$^+$ is slow enough to be measurable by ESR spectroscopy even at temperatures up to 360 K and this compound can thus be classified as a localized class II MV system.

In MV compounds where no through-space interaction of π systems is possible, the existence of a conjugated unsaturated spacer system is crucial for a significant electronic coupling. Thus, an ESR investigation of bis(1,4-dimethoxybenzene) radical cations shows a large coupling for **164**$^+$ (Scheme 55) with a pentacene skeleton (delocalized system on the ESR time scale) and a very small coupling for **165**$^+$ (Scheme 55) with a partially saturated spacer moiety.[242]

3.2.3. *MV Compounds with Quinone and Imide Redox Centers*

Quinones are certainly an important class of organic redox system that is widely used both in synthesis as oxidizing reagents and in nature in redox coenzymes. Here, we focus our attention on organic MV compounds comprising of two quinone redox centers where one quinone moiety is reduced to a so-called semiquinone. While the spin density in these radical anions is mostly located on the oxygen atoms,[243] the

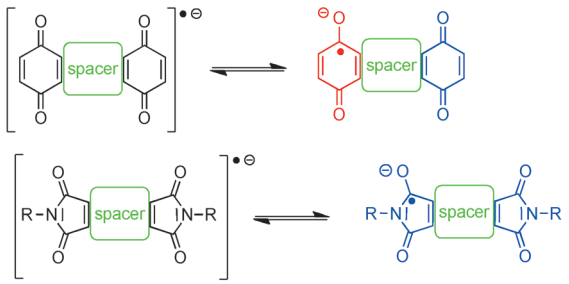

negative charge is delocalized over the whole system.[244] A large number of such diquinones were synthesized and their radical anions generated mostly by electrochemical methods, but unfortunately in most cases the ET behavior has not been investigated in detail. In particular, the IV-CT bands of these MV systems have not been discussed in the context of a band-shape model (e.g. Mulliken–Hush model) and, thus, no quantitative electronic couplings or other ET parameters have been evaluated.

As in the case of structurally related 1,4-dimethoxybenzene radical cations, the most important question is the assignmenet of diquinone radical anions to class II or III MV systems. This aspect was studied extensively for diquinones **166**$^-$–**169**$^-$ (Scheme 56).[241,245–248] The radical anions were

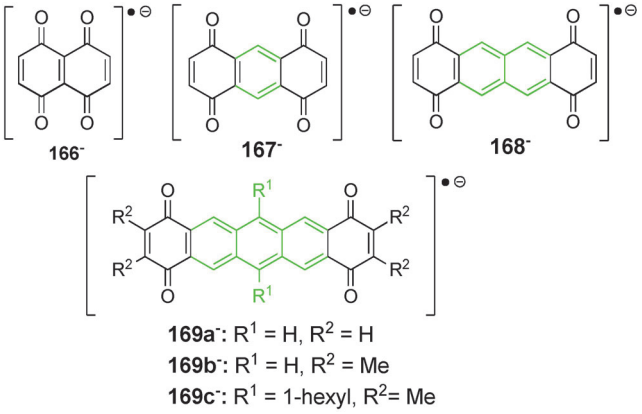

Scheme 56. Class III diquinone radical anions **166**$^-$–**169**$^-$, where the redox centers are annulated directly or to benzene, naphthalene, or anthracene spacers.

generated electrochemically in a DMF/tetrabutylammonium tetrafluoroborate solution. Compounds **166**$^-$–**168**$^-$ and **169a**$^-$ show significant CT bands in the NIR region, but the shape and intensities of these bands are different. While sharp CT bands with vibrational fine structure can be observed for **166**$^-$ and **167**$^-$, the CT bands of **168**$^-$ and **169a**$^-$ are extremely broad. Furthermore, analysis of the IR spectra of **168**$^-$ argues for a localization of the charge on one quinone redox moiety.[245] These findings lead to the assumption that **166**$^-$ and **167**$^-$ are delocalized class III compounds and the diquinone radical anions **168**$^-$ and **169a**$^-$ are localized class II species.[245] Temperature-dependent ESR measurements confirmed these results, but also clearly showed that the ET rate in **169a**$^-$ strongly depends on the counterion of the supporting electrolyte: ET is much faster for Li^+ counterions than for bulky tetraalkylammonium cations.[248] By temperature-dependent ESR measuremets Neugebauer and co-workers showed that the odd electron in **169b**$^-$ and **169c**$^-$ is delocalized over the whole pentacenetetrone system when the radical anions are generated with potassium in the presence of an appropriate cryptand, which inhibits ion pairing of the then shielded cation with the quinone radical anion.[241] From these experiments it can be deduced that ion-pairing effects play a much more important role in diquinone radical anions than in the corresponding cationic bis(1,4-dimethoxybenzene) radical cations. A large number of other diquinone radical anions have been synthesized and investigated, among them asymmetric systems such as **170**$^-$ (Scheme 57)[246] and radical anions with three quinone redox

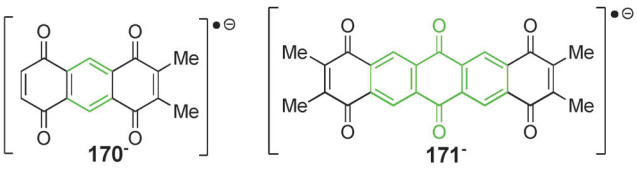

Scheme 57. Diquinone radical anion **170**$^-$ with nondegenerate redox centers and radical anion **171**$^-$ with three quinone redox centers.

centers linearily connected, as in **171**$^-$ (Scheme 57).[247] In these systems, CT processes between the peripheral quinone moieties and the bridge (central quinone moiety) must also be considered. Unfortunately, as mentioned above, no detailed analysis of the ET behavior in these systems was performed.

Diimide radical anions such as **172**$^-$ and **173**$^-$ (Scheme 58) are structurally and electronically related to diquinones and were also studied by ESR spectroscopy.[247,248] It appears that

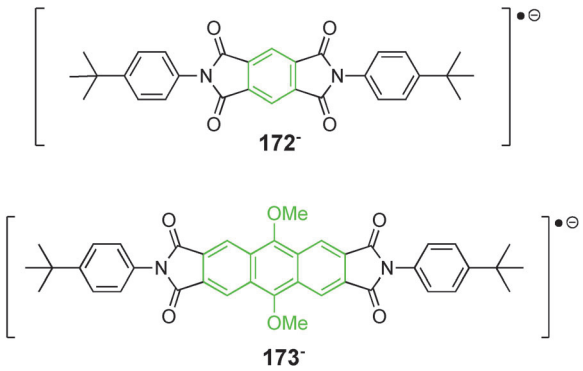

Scheme 58. Diimide radical anions **172**$^-$ and **173**$^-$ that are doubly linked to a benzene and an anthracene spacer unit.

diimide radical anions do not tend to stabilize the charge by ion-pairing to the same extent as the corresponding diquinone radical anions do.[249] Apperently, it is by far less favorable to localize a negative charge on an imide than on a quinone redox center. Hence, the diimide MV compounds show faster ET rates under the same experimental conditions than the related diquinone MV systems.

Diquinone radical anions were used to investigate through-space ET processes analoguous to the corrsponding MV systems **152**$^+$–**163**$^+$ containing 1,4-dimethoxybenzene redox centers (see Section 3.2.2). Temperature-dependent ESR measurements showed that the unpaired electron in radical anions **175**$^-$–**178**$^-$ (Scheme 59) is delocalized over both redox centers.[241] In these cases, the radical cations were generated in situ by chemical reduction with potassium in the presence of [2.2.2]cryptand and, hence, ion-pairing effects are surpressed. Cyclovoltammetric measurements of the redox potential splittings ΔE indicate that the electronic coupling in

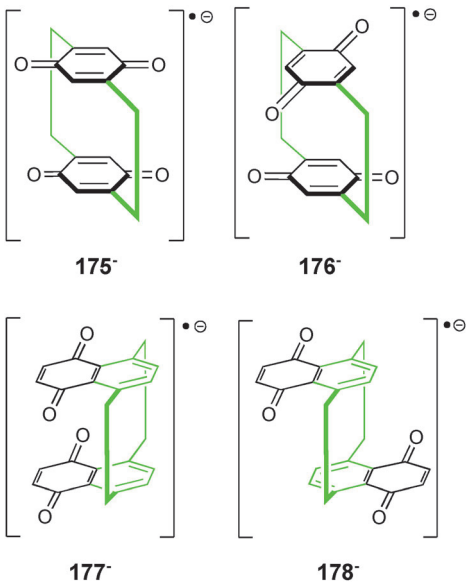

Scheme 59. Diquinone radical anions with [2.2]paracyclophane spacer units.

paracyclophane radical anions **175**$^-$ and **176**$^-$ is markedly larger than in naphthalenophane radical anions **177**$^-$ and **178**$^-$ (Table 28). Radical anions **175**$^-$ and **177**$^-$ show large differences in their redox splitting. However, this contrasts with the trends observed for the corresponding bis(1,4-dimethoxybenzene) radical cations **152**$^+$ and **161**$^+$ (see Tables 26 and 27) which show similar splittings. These findings are evidence that electronic coupling in the diquinone radical anions **177**$^-$ and **178**$^-$ is to a large extent influenced by the direct interaction of the two cyclophane benzene moieties of the spacer. This is also supported by the fact that the redox splittings of **177**$^-$ and **178**$^-$ do not differ significantly although the direct (through-space) distance of the quinone redox centers in **177**$^-$ is much smaller than in **178**$^-$.[157] In contrast, in the corresponding bis(1,4-dimethoxybenzene) radical cations the ΔE value in the *anti* isomer **162**$^+$ is 120 mV smaller than that of the *syn* isomer **161**$^+$ (Table 27). This behavior can be explained by an increased distance between the quinone redox centers in naphthalenophane **177**$^-$ compared to the paracyclophane **175**$^-$ as a consequence of a boat conformation. Crystallographic studies showed that the interplane distance between the quinones in **177**$^-$ is about 0.4 Å larger than that of the phenylene rings and, hence, the dominating π–π interaction is that of the phenylene ring systems, which should be similar for both isomers **177**$^-$ and **178**$^-$.[241]

Table 28: Redox potential splittings of diquinone radical anions **175**$^-$–**178**$^-$.[241]

	ΔE [mV][a]
175$^-$	420[a]
176$^-$	320[a]
177$^-$	230[b]
178$^-$	200[b]

[a] $\Delta E = \lvert E_{1/2}\ (\text{Red1}) - E_{1/2}\ (\text{Red2}) \rvert$ in an acetonitrile/0.1 M tetrabutylammonium hexafluorophosphate solution. Scan rate: 100 mV s^{-1}.
[b] $\Delta E = \lvert E_{1/2}\ (\text{Red1}) - E_{1/2}\ (\text{Red2}) \rvert$ in a dichloromethane/0.1 M tetrabutylammonium hexafluorophosphate solution. Scan rate: 100 mV s^{-1}.

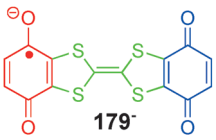

Scheme 60. Diquinone radical anion **179**$^-$ with a tetrathiafulvalene (TTF) bridge.

Recently, the ET process in a diquinone radical anion **179**$^-$ (Scheme 60) with a tetrathiafulvalene (TTF) bridge was investigated.[250] The ET rate constant could be determined by temperature-dependent ESR measurements in different solvents. The rate constant k_{ET} in dichloromethane is $2.58 \times 10^8\ s^{-1}$ at 300 K and the measurements yield a localization of the charge on one quinone redox center. The small redox potential splitting $\Delta E = 80$ mV between the first and second reduction implies a relatively small electronic communication compared to the diquinone radical anions discussed above. Unfortunately, a quantitative optical investigation of this compound was not performed because of insolubility of the charged species generated by spectroelectrochemistry or chemical reduction with copper.[250]

At this point we stress that assignment to the Robin–Day classification is very difficult and is often ambigous, especially in the case of diquinone radical anions. This is due to the fact that an assignment can only be done within the time domain of a given analytical method. Furthermore, ion pairing is particularly a problem with radical anions and may lead to localization of charge. Compound **179**$^-$, for example, is classified as a localized system, but **171**$^-$ as a delocalized one, although the distance between the redox centers is larger in the latter. In these cases, one has to keep in mind that the classification of **171**$^-$ is based upon measurements where ion-pairing effects were suppressed by the addition of cryptands, while the investigations which suggest a class II character for **179**$^-$ do not consider possible ion-pair effects.

While all the diquinone radical anions discussed so far can be viewed as MV compounds where the charge is mainly located on the carbon atoms, Nelsen et al. investigated a series of vinyloguous distonic quinone radical anions (**180**$^-$–**186**$^-$; Scheme 61) where the spin and charge is formally located at different oxygen atoms of the vinylogous quinone redox system.[251] In this way, **180**$^-$–**186**$^-$ might be viewed as MV systems with oxygen redox centers. However, because one can savely assume that both charge and spin will also be significantly localized at carbon, we will treat these compounds in this section.

As a consequence of the instability of quinones in the neutral as well as in the reduced oxidation states, *ortho*-substituents have been attached to **180**$^-$–**186**$^-$. The corresponding radical anions were generated by chemical reduction with Na-Hg amalgam in dimethylformamide in the presence of [2.2.2]cryptand to inhibit ion-pairing effects. Since the π systems are isoelectronic with the paraphenylenediamine or benzidine radical cations, such as **120**$^+$ and **121**$^+$, it is reasonable to compare the ET behavior of both series. The radical anions **182**$^-$–**185**$^-$ all show rather strong CT bands in the NIR region and have striking vibrational fine structures. A comparison of these bands clearly demonstrates the

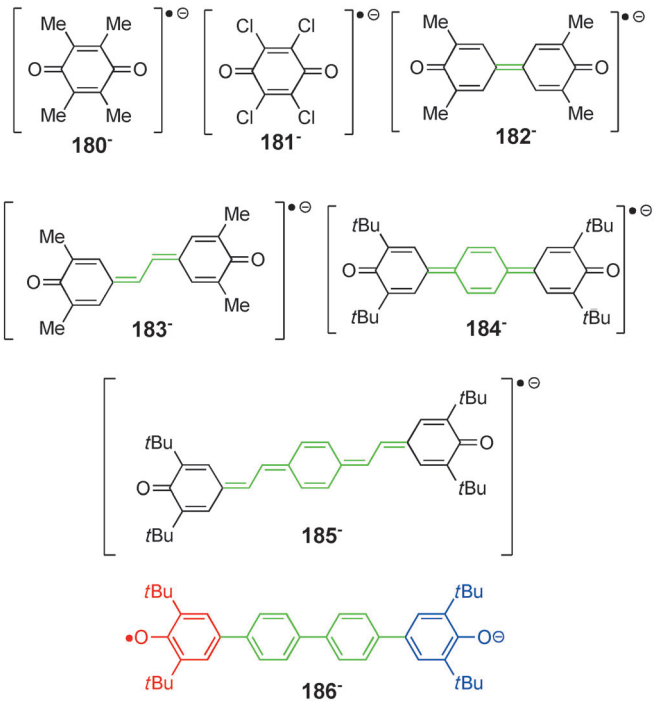

Scheme 61. Vinologuos distonic quinone radical anions **180**$^-$–**186**$^-$.

similarity to the corresponding paraphenylendiamine and benzidine radical cations **120**$^+$ and **121**$^+$.[251] For compounds **180**$^-$ and **181**$^-$ with only five bonds separating the charge- and spin-bearing oxygen atoms, the CT transitions are blue-shifted to the visible region (Table 29) due to the very strong

Table 29: Number of bonds separating the oxygen atoms *n*, absorption maxima of the CT bands, as well as electronic couplings $V = \tilde{\nu}_{max}/2$ for quinone radical anions **180**$^-$–**186**$^-$ in dimethylformamide.[251]

	n	$\tilde{\nu}_{max}$ [cm^{-1}]	*V* [cm^{-1}]
180$^-$	5	(22 700)[a]	(11 350)[a]
181$^-$	5	(22 200)[a]	(11 100)[a]
182$^-$	9	11 630	5820
183$^-$	11	9710	4860
184$^-$	13	6570	3290
185$^-$	17	4960	2480
186$^-$	17	6200	–[b]

[a] It is a matter of debate as to whether to these transitions can be defined as CT bands and the electronic coupling values extracted from these bands (see Ref. [251]). [b] Not determined.

electronic coupling in such small systems. It seems unusual to view compounds **180**$^-$ and **181**$^-$ as class III MV systems because the concept of mixed-valency loses its meaning for systems where even a formal separation of redox moieties is impossible. Nonetheless, a plot of ln *V* versus the number of bonds *n* between the quinone oxygen atoms for compounds **180**$^-$–**185**$^-$ yields a linear correlation, with a β value of 0.30.[251] This shows that the electronic properties of **180**$^-$–**185**$^-$ may be well described within one theoretical concept. In contrast to **180**$^-$–**185**$^-$, the CT band of **186**$^-$ shows no vibrational fine structure, but is broad and symmetric. This fact together with the existence of a significant solvatochromism proves **186**$^-$ to be a class II MV compound. Unfortunately, the electronic coupling for **186**$^-$ was not determined by a band-shape analysis, but DFT calculations also predict a smaller electronic coupling for **186**$^-$ than for the stilbene-bridged analogue **185**$^-$.[251] The reason for the decreased coupling in **186**$^-$ compared to **185**$^-$ might be due to the "biphenyl twist" in the former, which yields a decoupling compared to the more planar distilbene spacer in **185**$^-$.

3.2.4. Miscellaneous Organic MV Compounds Containing Carbon Redox Centers

There are some organic MV compounds in which the odd electron is formally located predominantly on carbon atoms but which do not belong to the main classes discussed above. One of those is the bis(indanone) radical anion **187**$^-$ (Scheme 62) investigated by Mazur et al.[49,252,253] as well as Hosoi and Masuda.[254] The ET behavior of this MV compound was studied by means of temperature-dependent ESR spectroscopy as well as IR spectroscopy. The unusual IR spectrum, which shows no characteristic absorptions that could be either directly attributed to vibrations of monoketyls or to monoketones, was analyzed by vibronic models which yield an electronic coupling $V =$ 450 cm^{-1} in dimethylsulfoxide and acetonitrile.[252,253] Furthermore, it could be shown that vibronic coupling is responsible for the unexpected IR spectrum. Temperature-dependent ESR measurements clearly proved class II character, while the ET rate is strongly influenced by both the counterion and the solvent.[49,254]

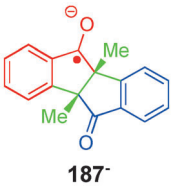

Scheme 62. Class II MV compound **187**$^-$ consisting of two indanone redox centers.

Compound **187**$^-$ shows an IV-CT band in the NIR region which, when analyzed by a Mulliken–Hush treatment, gave an electronic coupling of approximately 1000 cm^{-1} in acetronitrile or dimethylformamide. This coupling is significantly higher than that obtained from analysis of the IR spectra. Furthermore, the inner- and outersphere reorganization parameters λ_v and λ_o could be determined separetely by calculation of λ_v from the vibrational force constants, which in turn were extracted from the corresponding vibrational spectra.[253] As can be seen from the data collected in Table 30, the reorganization energy is dominated by the solvent part. The ratio of electronic coupling and total reorganization energy also classifies **187**$^-$ as a localized class II compound.

Quite recently, the ET process in a bis(dioxaborine) radical anion **188**$^-$ (Scheme 63) was investigated.[255] This radical anion was generated by chemical reduction with cobaltocene. A CT band ($\tilde{\nu}_{max} = 10\,870$ cm^{-1}; $\varepsilon =$ ca. 10 000 M^{-1} cm^{-1}; in acetonitrile) with a well-resolved vibrational fine structure is observable in the absorbtion spectrum. This fact in addition to the weak solvatochromic behavior of the CT band and relatively large redox potential splitting $\Delta E = 210$ mV between the first and second reversible reduc-

Table 30: Optical data, electronic coupling determined by Mulliken–Hush analyses, inner reorganization energy calculated from force constants extracted from IR spectra, as well as ET rates determined by temperature-dependent ESR spectroscopy of **187**$^-$ in different solvents.[254]

Solvent	$\tilde{\nu}_{max}=\lambda$ [cm^{-1}]	ε [M^{-1} cm^{-1}]	λ_o [cm^{-1}]	λ_v [cm^{-1}]	V [cm^{-1}]	k_{ESR} [s^{-1}]
acetonitrile[a]	5900	4030	5200	700	1060	$>10^{10}$[b]
DMF[c]	5700	4000	5000	700	1010	1.5×10^{10}[b]
THF[c]	5500	4000	4800	700	990	8.0×10^{8}[b]

[a] The radical anion was generated by electrochemical reduction with 0.1 M tetramethylammonium tetrafluorophosphate as the supporting electrolyte.[254] [b] Rate constants at 253 K.[254] [c] The radical anion was generated by chemical reduction with sodium amalgam in the presence of [2.2.2]cryptand.[254]

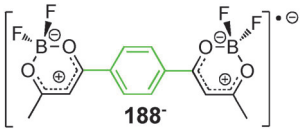

Scheme 63. Bis(dioxaborine) radical anion **188**$^-$.

tion process assigns **188**$^-$ to a delocalized class III compound with an electronic coupling of $V=\tilde{\nu}_{max}/2=5440\ cm^{-1}$ in acetonitrile.[255] Both ZINDO and DFT calculations confirmed the class III character and estimate the negative charge to be symmetrically distributed on the dioxaborine redox centers. Although DFT usually overestimates charge delocalization, the computed IV-CT band energy is in reasonable agreement with experiment. Furthermore, the CT band could be simulated by a vibronic model where only totally symmetric vibrations are considered.[255] The modes that contribute to the vibrational structure of the CT band could be identified, and the total Marcus reorganization energy $\lambda=1450\ cm^{-1}$ was calculated.[255] This relatively small reorganization energy might be due to the small geometrical changes that are predicted by DFT computations upon charge transfer.[255]

3.3. Organic MV compounds with Redox Centers Containing Sulfur

Organic MV compounds with redox centers containing sulfur atoms are much less common than their nitrogen or carbon analogues. Among these, MV compounds with tetrathiafulvalene (TTF) redox centers are the most important. Unfortunately, the number of compounds for which the ET behavior has been investigated in detail is small, although there are numerous compounds which should show a significant electronic coupling. In this Review we restrict ourselves to compounds where the ET behavior is reasonably well studied.

Tetrathiafulvalenes (TTFs) are common donor centers in organic chemistry and can easily be oxidized to the corresponding radical cations, where the charge and spin is delocalized over the whole TTF system. Lahlil et al. synthesized a series of bis(TTF) radical cations (**189**$^+$–**192**$^+$; Scheme 64) where two TTF redox centers are connected by various aromatic spacer units.[256] As expected, the electronic coupling V strongly depends on the bridge linkage. Thus, radical cation **189**$^+$ is a class I compound with two non-

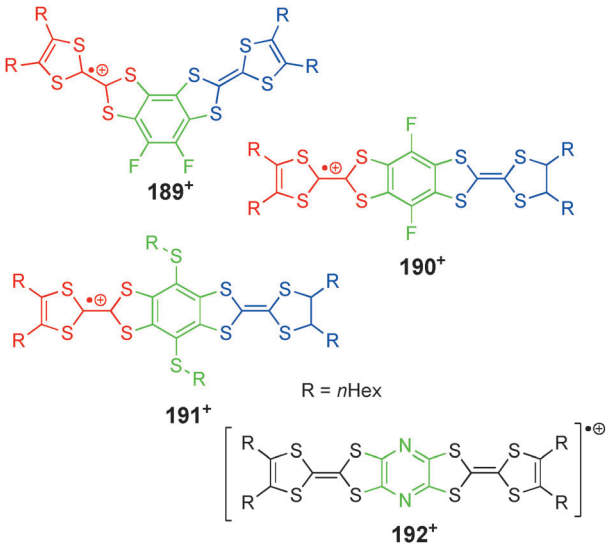

Scheme 64. Bis(tetrathiafulvalene) radical cations **189**$^+$–**192**$^+$ bridged by different aromatic spacers.

interacting redox centers, and no IV-CT band could be observed in the absorption spectrum. This absence of electronic communication is due to the *meta*-linkage, as was also observed for the bis(PCTM) radical anion **11**$^-$ (see Section 3.2.1). In contrast, the *para*-bridged bis(TTF) radical cations **190**$^+$–**192**$^+$ all show intense absorption bands in the NIR region in dichloromethane, which can be attributed to a CT process from one TTF unit to the other. Lahlil et al. classified these radical cations as localized class II MV compounds. This classification seems to be reasonable for **190**$^+$ and **191**$^+$ because of the broad and symmetrical band shape of the IV-CT bands, which are typical of localized MV compounds. However, the classification of **192**$^+$ as class II is questionable because the IV-CT band is strongly asymmetric and shows rudimental vibrational fine structure.[101,256] Furthermore, the extinction coefficient of the CT band is increased by a factor of 2.5 compared to **190**$^+$ and **191**$^+$ (see Table 31). By assuming **192**$^+$ is a class II system, band analysis yielded a similar coupling as **190**$^+$. However, Nelsen reanalyzed the data of compound **192**$^+$ and found evidence for a

Table 31: Optical parameters of the IV-CT bands of **190**$^+$–**192**$^+$ generated by spectroelectrochemistry in a dichloromethane/0.1 M tetrabutylammonium hexafluorophosphate solution as well as electronic coupling values determined by Mulliken–Hush analysis.[101,256]

	$\tilde{\nu}_{max}$ [cm^{-1}]	ε [M^{-1} cm^{-1}]	V [cm^{-1}]
190$^+$	6000	4600	1000[a]
192$^+$	5750	4300	800[a]
192$^+$	4000	12000	2000[b]

[a] Determined by treatment as a class II compound. [b] Determined by treatment as a class III compound ($V=\tilde{\nu}_{max}/2$).

class III arrangement.[101] Here, a significantly higher electronic coupling $V = 2000\ cm^{-1}$ was calculated for **192**$^+$ when treated as a delocalized system (Table 31).

The reason why the electronic coupling in **192**$^+$ is much larger than for **190**$^+$ and **191**$^+$ is still unclear. The substitution of the relatively electron-rich bridge moieties in **190**$^+$ and **191**$^+$ by the electron-withdrawing pyrazine spacer unit should stabilize the bridge HOMO and, therefore, a decreased electron coupling for this cationic systems is expected, as described in Section 2.8.

There is a number of bis(TTF) systems closely related to **192**$^+$ where the nitrogen atoms are replaced by other heteroatoms, such as S,[257] Te,[258,259] or PPh,[260] but most of these systems have not been investigated in the context of mixed valency. However, Geoffroy and co-workers studied the MV character of radical cations **193**$^+$ and **194**$^+$ (Scheme 65) by ESR spectroscopy.[261] They found a symmetrical delocalization of charge and spin over both TTF redox centers for both compounds. This class III character was also confirmed by DFT calculations and X-ray structure analyses.

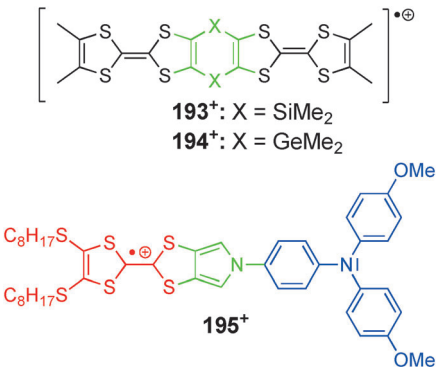

Scheme 65. TTF redox centers used in degenerate MV compounds **193**$^+$ and **194**$^+$ and as an acceptor redox center in a nondegenerate MV compound in combination with a triarylamine donor center **195**$^+$.

In our research group, a series of MV compounds were synthesized in which TTF redox centers are connected with triarylamine redox centers, such as in **195**$^+$ (Scheme 65).[262] Radical cation **195**$^+$ is a nondegenerate MV compound and, hence, a band-shape analysis is not straightforward. Electrochemical measurements clearly showed that the oxidized TTF redox center in these compounds acts as the electron acceptor and the triarylamine as the electron donor. Indeed, the absorption spectra of compounds such as **195**$^+$ show intense absorptions in the NIR region but a definite assignment and a quantitative analysis of the bands is impossible due to overlap of the CT bands with other bands, such as typical local NIR transitions of the TTF$^+$ system. IV-CT-like bands were also found in some partially oxidized π-stacked dimers of substituted TTFs, thus forming $[(TTF)_2]^+$, but as these TTF redox centers are not covalently linked to each other they are not MV compounds in the sense used here.[263,264]

Even though most of the MV compounds containing sulfur redox centers contain TTF, there is one series of MV compounds that contain anionic pentakis(thiophenyl)benzene redox centers (**196**$^-$–**198**$^-$; Scheme 66).[265] The degree of electronic communication between the redox centers strongly depends on the type of spacer unit. No electronic coupling between the redox centers was found for compound **196**$^-$ and, therefore, this system can be assigned to class I. This assignement is based on the lack of an IV-CT band and on the fact that no difference in the redox potential between the first and the second reduction processes could be observed.[265] In contrast, the diacetylene-bridged radical anion **198**$^-$ shows an intense and asymmetric absorption band in the NIR region (Table 32). This asymmetric line shape in addition with the presence of vibrational fine structure supports this radical anion as being a delocalized class III system, and the relatively large redox potential splitting ΔE also indicates a strong electronic communication between the redox centers (Table 32). The situation is ambigous for compound **197**$^-$ with an azo spacer group. A band in the NIR at 1250 nm appears upon electrochemical generation of the radical anion. According to the authors, this band is not assigned to an IV-CT process but rather to a transition between the redox center and the spacer unit.[265] Therefore, **197**$^-$ may be classified as a class I compound with two non-interacting

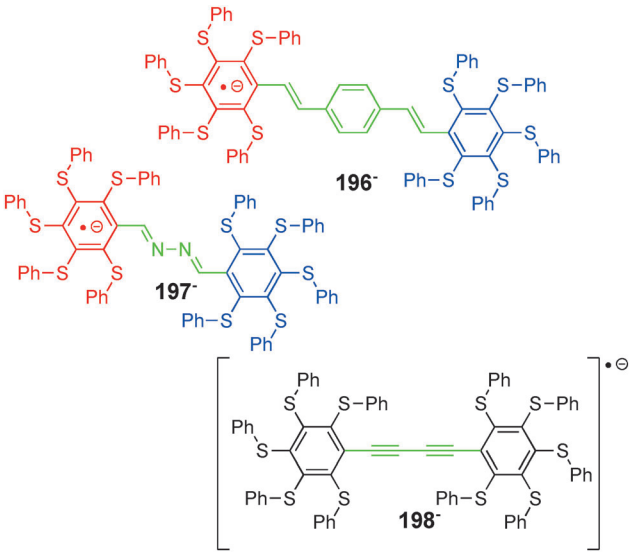

Scheme 66. Anionic organic MV compounds with pentakis(thiophenyl)benzene redox centers bridged by various unsaturated spacers **196**$^-$–**198**$^-$.

Table 32: Optical data of the lowest-energy transition in the absorption spectra in DMF and redox potential splittings derived from cyclic voltammetry in DMF for radical anions **197**$^-$–**198**$^-$.[265]

	$\tilde{\nu}_{max}$ [cm^{-1}]	ε [$M^{-1}cm^{-1}$]	ΔE [mV][c]
197$^-$	8000[a]	–[b]	–[d]
198$^-$	7630	19500	260

[a] Not assigned to an IV-CT process (see text and Ref. [265]). [b] Not determined. [c] $\Delta E = |E_{1/2}(\text{Red1}) - E_{1/2}(\text{Red2})|$ in a DMF/0.1 M tetrabutylammonium hexafluorophosphate solution. Scan rate: 100 $mV s^{-1}$. [d] No redox potential splitting ΔE observed.

redox centers. However, the electrochemical reduction of **197** is not completely reversible, and the observed transition could also be due to side products.

3.4. Organic MV Compounds with Boron Redox Centers

There are only a few MV compounds containing boron redox centers, which is due to their instability upon reduction.[266] At least one bulky substituent has to be introduced to guarantee a sufficient stability of the boron redox centers for electrochemical investigations. In compounds **199**$^-$ and **200**$^-$ (Scheme 67), stability is ensured by two bulky mesityl

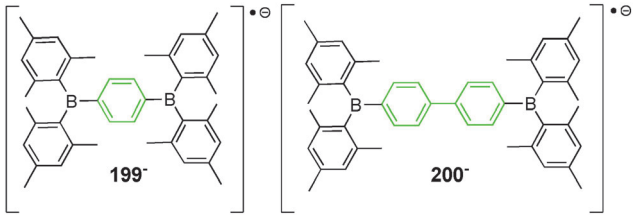

Scheme 67. Class III radical anions **199**$^-$ and **200**$^-$ with dimesitylboron redox centers.

substituents. The absorption spectra of both radical anions show an intense CT band with a distinctive vibrational fine structure in the NIR region (Figure 14), which makes them

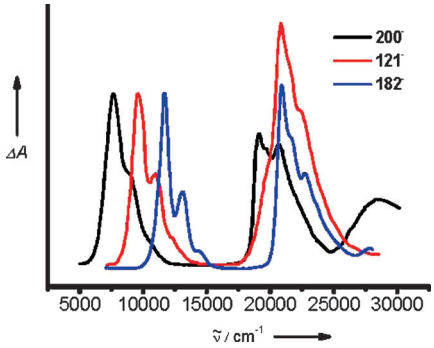

Figure 14. Normalized absorption spectra of bis(triarylboron) radical anion **200**$^-$ (black line) in DMF/0.1 M terabutylammoniumperchlorate solution (radical anion generated by spectroelectrochemistry),[267] bis(dialkylamine) radical cation **121**$^-$ (red line) in acetonitrile (generated by chemical oxidation with tri(*p*-bromophenyl)aminium hexachloroantimonate),[221] and quinone radical anion **182**$^-$ (blue line) in DMF (radical anion generated by chemical reduction with Na-Hg amalgam in the presence of an access of [2.2.2]cryptand).[251]

delocalized class III systems.[267] A comparison of the absorption spectra of bis(triarylboron) radical anion **200**$^-$, bis(dialkylamine) radical cation **121**$^+$, and quinone radical anion **182**$^-$ shows striking similarities in the intensity, band shape, and energy of the NIR bands (Figure 14). This similarity is impressive evidence for the fact that the lowest energy transitions in those compounds are mainly determined by the type of the π system between the redox centers, while the charge and type of the redox centers themselves are far less important, a clear indication for class III behavior.

3.5. Neutral Organic MV Compounds

All the MV compounds discussed so far are either radical cations or radical anions. Several disadvantages concerning the generation as well as the (optical) investigation of the ET behavior of these MV systems are associated with this charged character. For example, most of the charged MV compounds have to be generated in situ by chemical oxidation, chemical reduction, or by electrochemical methods. Additionally, as a consequence of the charged character, many compounds are quite unstable compared to uncharged compounds. These facts limit the use of solvents in which these systems can be generated and studied. The use of nonpolar solvents is often impossible because of the insolubility of the charged MV species. Furthermore, ion-pairing effects complicate the quantitative investigation of ET behavior as a result of its great influence on the solvent reorganization energy in particular.

Recently, a number of purely organic MV compounds were synthesized and investigated—a new class of organic compounds where the disadvantages described above were largely avoided.[4,92] The basic idea to generate these series of neutral MV compounds was to combine the concepts of bis(triarylamine) radical cations and perchlorinated bis(triarylmethyl) radical anions (Scheme 68). To understand the MV character of the neutral compounds it is helpful to keep in mind that the neutral triarylmethyl radical centers as well as the neutral triarylamine redox centers are isoelectronic with the corresponding donor and acceptor centers of the charged MV systems (Scheme 68). As a consequence of the different redox centers, these MV systems are all nondegenerate.

In our research group, we synthesized a series of neutral organic MV compounds containing perchlorinated triphenylmethyl radical acceptor centers and triarylamine **201**–**203** or dialkylamine **204**–**206** donor centers (Scheme 69). All of these MV compounds are sufficiently soluble in a large variety of solvents of different polarity ranging from very polar solvents such as acetonitrile or 2-propanol to very apolar solvents such as hexane or cyclohexane. Therefore, we characterized the absorption spectra of neutral MV compounds **201**–**206** in solvents of different polarity. An intense IV-CT band in the NIR region was observed for all of the compounds in all solvents. These IV-CT bands show a weak but nonsystematic solvatochromic behavior. While the IV-CT bands are broad and symmetrical in polar solvents such as acetonitrile, as expected for class II compounds, narrower bands with some evidence of a vibrational fine structure were observed in nonpolar solvents such as hexane. A band-shape analysis in context of Bixon–Jortner theory (Section 2.7.2) was performed to reveal this solvatochromic behavior. Least-squares fits of the IV-CT bands yielded all four ET parameters (solvent reorganization energy λ_o, inner reorganization energy λ_v, the difference of the diabatic free energy of the ground and the excited state ΔG^{00}, and the energy of the averaged vibrational mode $\tilde{\nu}_v$) in a wide range of solvents. A

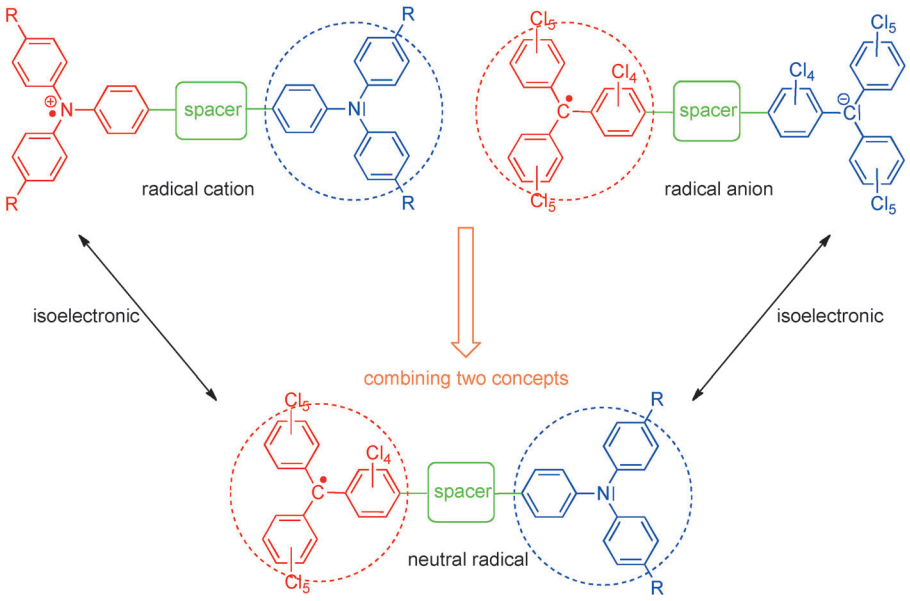

Scheme 68. Neutral organic MV systems may be formed by combinating the concepts of cationic and anionic MV systems. These neutral organic MV compounds consist of uncharged redox centers which are isoelectronic to the corresponding charged redox centers in radical cation and radical anion systems.

As described in detail in Section 2, the main problem in evaluating the electronic coupling V from optical data is the necessity to know the diabatic dipole moment difference $\Delta\mu_{12}$, which is not accessible by Mulliken–Hush analysis. We developed a new method which allows the calculation of $\Delta\mu_{12}$ by evaluation of the optical data derived from Bixon–Jortner fits of the IV-CT bands and applying Lippert–Mataga Equation (20)[92,268,269] (where $\Delta\mu_{ab}$ is the adiabatic dipole moment difference, ε_0 is the permittivity of vacuum, h is Planck's constant, c is the speed of light, a_0 is the radius of the compound, and D and n are the solvent permittivity and the index of refraction, respectively).

$$2(\lambda_v + \lambda_o) = \frac{(\Delta\mu_{ab})^2}{2\pi\varepsilon_0 hca_0^3}(f(D) - f(n^2))$$

$$\text{with} \quad f(D) = \frac{D-1}{2D+1} \text{ and } f(n^2) = \frac{n^2-1}{2n^2+1} \qquad (20)$$

plot of these parameters versus solvent polarity function revealed the reason for the weak and nonsystematic solvent behavior: as expected, the inner reorganization energy λ_v as well as the energy of the averaged vibrational mode $\tilde{\nu}_v$ is almost solvent-independent. However, both the solvent reorganization energy λ_o as well as the free energy difference ΔG^{00} show linear solvatochromic behavior. The solvent reorganization energy increases with increasing solvent polarity, but concomitantly ΔG^{00} decreases in the same direction. These opposite trends approximately compensate each other, which results in the weak and nonsystematic solvatochromic behavior as observed. The optical data as well as the values for all four ET parameters extracted by the Bixon–Jortner band shape analysis are listed in Table 33 for compounds **201**–**206** in two selected solvents (*n*-hexane and acetonitrile).

A plot of twice the total reorganization energy $2(\lambda_v+\lambda_o)$ derived from Bixon–Jortner fits of the IV-CT bands in various solvents versus the Onsager solvent parameter $(f(D)-f(n^2))$ [see Eq. (20)] gives a linear correlation. From the slope of the linear correlation, the adiabatic dipole moment difference $\Delta\mu_{ab}$ can be calculated by assuming a spherical chromophore geometry with radus a_0.[92] The diabatic dipole moment difference $\Delta\mu_{12}$ can then be calculated by Equation (10). The diabatic and adiabatic dipole moment differences as well as the electronic couplings [Eq. (8)] for neutral MV compounds **201**–**206** are listed in Table 34. The reliability of this new solvatochromic method for the determination of dipole moments was proved by electrooptical absorption measurements (EOAM). An adiabatic dipole moment difference of $\Delta\mu_{ab} = 19 \pm 1$ D was determined for **201** by EOAM,[4,92] which

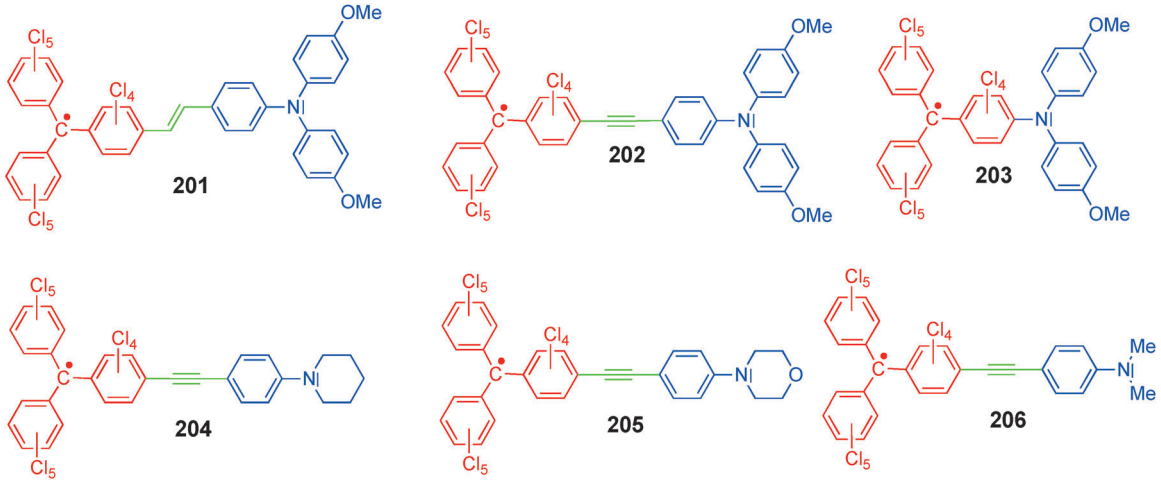

Scheme 69. Neutral organic MV compounds **201**–**206** with PCTM radical acceptor centers and various nitrogen donor centers.

Table 33: Optical data of the IV-CT bands of MV compounds **201**–**206** in *n*-hexane and acetonitrile and results of the band-shape analysis of these bands in the context of the Bixon–Jortner theory (free energy difference between the ground and the excited states ΔG^{00}, solvent reorganization energy λ_o, inner reorganization energy λ_v, and energy of the averaged vibrational mode $\tilde{\nu}_v$).[92]

	Solvent	$\tilde{\nu}_{max}$ [cm^{-1}]	ε [$M^{-1}cm^{-1}$]	ΔG^{00} [cm^{-1}]	λ_o [cm^{-1}]	λ_v [cm^{-1}]	$\tilde{\nu}_v$ [cm^{-1}]
201	*n*-hexane	12400	4750	10250	1000	1250	1150
	acetonitrile	12200	3400	7250	4150	1350	1750
202	*n*-hexane	12650	8150	10900	1050	650	1650
	acetonitrile	12450	5400	7900	4200	650	2800
203	*n*-hexane	12050	5050	9650	1650	800	1300
	acetone	11800	3400	7450	3450	900	1200
204	*n*-hexane	13550	5300	11550	1250	1050	1700
	acetonitrile	12750	4550	7900	4400	800	2500
205	*n*-hexane	14200	3800	12350	1050	1200	1650
	acetonitrile	13400	4050	9500	3450	1050	2300
206	*n*-hexane	13400	4600	11900	800	950	1600
	acetonitrile	12650	3700	8400	3700	900	2600

Table 34: Diabatic ($\Delta\mu_{12}$) and adiabatic ($\Delta\mu_{ab}$) dipole moment differences and electronic couplings determined by all-optical evaluation of the IV-CT bands in acetonitrile.[92]

	$\Delta\mu_{ab}$ [D]	$\Delta\mu_{12}$ [D]	V [cm^{-1}]
201	17.6	19.0	2310
202	17.9	19.7	2590
203	15.4	16.8	2340
204	15.4	17.3	2870
205	14.3	15.8	2880
206	14.6	16.2	2730

is in excellent agreement with the value determined by the solvatochromic method ($\Delta\mu_{ab} = 17.6$ D).

Closely related to the above mentioned neutral MV compounds are **207**–**213**[270] (Scheme 70). The special feature of this series is that these compounds are all built up through directly linked triarylamine donor centers and PCTM acceptor centers, which thus share an identical biphenyl spacer moiety. They only differ in the *para*-substituents R^1 and R^2 of the triarylamine donor, which almost exclusively influences ΔG^{00} (see Figure 4b) in these nondegenerate MV systems, while all the other ET parameters—the reorganization parameters λ_o and λ_v, as well as the averaged vibrational mode—are kept constant. In this series, the donor strength of the triarylamine was decreased step by step by the substituents R^1 and R^2 on going from **207** to **213**. This trend was further proved by the oxidation potentials of these compounds measured by cyclic voltammetry.[270] As a consequence of the constant reduction potential of the PCTM acceptor moiety, ΔE continuously increases as the acceptor strength of substituents R^1 and R^2 increases in **207**–**213** (Table 35).

MV compounds **207**–**213** show IV-CT bands in the NIR/Vis region in various

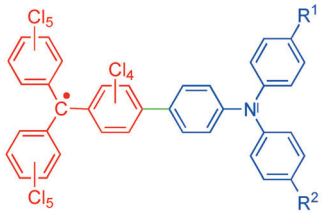

207: R^1 = OMe, R^2 = OMe
208: R^1 = Me, R^2 = Me
209: R^1 = Me, R^2 = Cl
210: R^1 = Cl, R^2 = Cl
211: R^1 = Cl, R^2 = CN
212: R^1 = CN, R^2 = CN
213: R^1 = NO_2, R^2 = NO_2

Scheme 70. Neutral organic MV compounds **207**–**213**.

solvents but, in contrast to compounds **201**–**206** with unsaturated spacers, a Bixon–Jortner band shape analysis of the IV-CT bands was only possible in nonpolar solvents such as cyclohexane. Two effects limited the band-shape analysis in more polar solvents: First, the IV-CT bands are too blue-shifted and, therefore, partially overlap with other transitions and, second, the bands are too symmetrical and a fit gives no definite results. The symmetry of the bands is a result of a much larger Huang–Rhys factor S [see Eq. (15)] for compounds **207**–**213** because of the smaller averaged vibrational mode caused by the lack of an unsaturated spacer moiety. In nonpolar solvents, such as cyclohexane, the small solvent reorganization energy induces asymmetry of the bands and the ET parameters could be determined at least for compounds **207**–**209** (Table 35).[270] Furthermore, we observed an unexpected intense fluorescence of all the compounds in nonpolar solvents. The emission spectra were all subjected to a Bixon–Jortner analysis. The results of the fits as well as the optical data of the absorption and emission bands are listed in Table 35.

As can be seen from the data in Table 35, the energy of the maxima of both the IV-CT absorption bands as well as of the emission bands increase with increasing acceptor strength of the substituents R^1 and R^2. The results of the Bixon–Jortner analysis of the absorption and of the emission bands are in an excellent agreement and show that the free energy difference of the ground and the excited state ΔG^{00} increases continuously as the strength of the triarylamine donor center decreases, while the other ET parameters are constant. These results are experimental evidence that the averaged

Table 35: Redox potential splittings ΔE determined by cyclic voltammetry,[271] maxima of the IV-CT absorption bands $\tilde{\nu}_{max}$(abs), and the emission bands $\tilde{\nu}_{max}$(em) as well as the ET parameters determined by Bixon–Jortner fits of the absorption (abs) and emission (em) bands in cyclohexane.[270]

	ΔE [mV][a]	$\tilde{\nu}_{max}$(abs) [cm^{-1}]	$\tilde{\nu}_{max}$(em) [cm^{-1}]	ΔG^{00} [cm^{-1}]	λ_o [cm^{-1}]	λ_v [cm^{-1}]	$\tilde{\nu}_v$ [cm^{-1}]
207	950	12700	–[c]	10600(abs)	1600(abs)	900(abs)	1250(abs)
208	1120	13150	11300	11900(abs)	1000(abs)	850(abs)	1200(abs)
				12100(em)	800(em)	800(em)	1150(em)
209	1270	14400	12250	12600(abs)	1400(abs)	950(abs)	1250(abs)
				13550(em)	1350(em)	600(em)	1350(em)
210	1390	15500	13100	14300(em)	1100(em)	800(em)	1250(em)
211	1480	17400	13800	14800(em)	1000(em)	850(em)	1350(em)
212	1600	–[b]	14350	15500(em)	1150(em)	1000(em)	1450(em)
213	1640	–[b]	14750	15750(em)	1050(em)	800(em)	1350(em)

[a] $\Delta E = E_{1/2}$ (Ox1) $- E_{1/2}$ (Red1) in dichloromethane/0.1 M tetrabutylammonium hexafluorophosphate solution, scan rate = 100 mVs^{-1}. [b] Not determined because of too strong overlap with energetically higher lying bands. [c] Not determined because the maximum is too strongly red shifted.

vibrational mode is mainly determined by vibrations along the ET direction. The solvent reorganization energy is constant and it can be seen from these data that the inner reorganization energy is also not significantly influenced by the substituents R^1 and R^2. The plots of the four ET parameters in cyclohexane are shown in Figure 15.

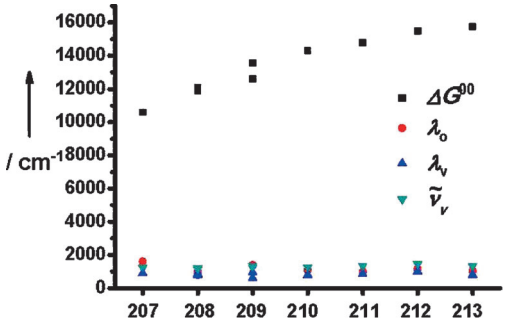

Figure 15. Plot of ΔG^{00}, λ_o, λ_v, and $\tilde{\nu}_v$ from Bixon–Jortner fits of MV compounds **207–213** in cyclohexane with decreasing strength of the triarylamine donor center.

The ET behavior of **207–213** was also characterized by transient absorption measurements in cyclohexane. The transient spectra are a superposition of the spectra of the reduced species and the oxidized species of the MV compounds as measured by spectroelectrochemistry.[270] The ground and the first excited (charge separated) state of neutral MV compounds **207–213** are outlined in Scheme 71. The characteristic radical anion transition and the well-known triarylamine radical cation band are both observed in the transient spectra with identical life-times, which is definite evidence for the zwitterionic character of the first excited state (see Scheme 71). Additionally, EOAM on compounds

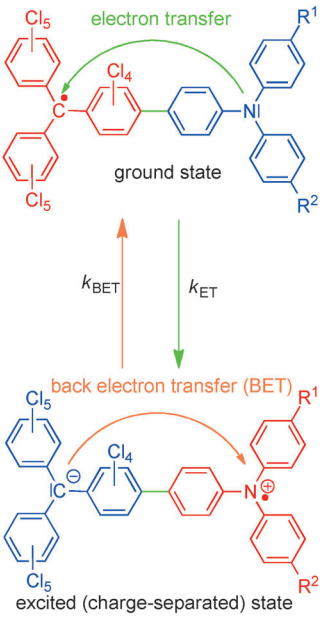

207: R^1 = OMe, R^2 = OMe

208: R^1 = Me, R^2 = Me

209: R^1 = Me, R^2 = Cl

210: R^1 = Cl, R^2 = Cl

211: R^1 = Cl, R^2 = CN

212: R^1 = CN, R^2 = CN

213: R^1 = NO_2, R^2 = NO_2

Scheme 71. Ground state and first excited state of neutral organic MV compounds **207–213**.

207–211 yielded large adiabatic dipole moment differences $\Delta\mu_{ab}$ (Table 36).[272] From these data and the corresponding transition moments μ_{ab} of the absorption and emission spectra, the adiabatic dipole moments $\Delta\mu_{12}$ was calculated

Table 36: Transition moments μ_{ab} extracted from the absorption (abs) or emission (em) spectra,[270] adiabatic dipole moment differences $\Delta\mu_{ab}$ determined by EAOM, as well as calculated diabatic dipole moment differences $\Delta\mu_{12}$ by Equation (10) and electronic couplings V by Equation (8) of neutral MV compounds **207–211**.[272]

	μ_{ab}(abs/em) [D]	$\Delta\mu_{ab}$(EAOM) [D]	$\Delta\mu_{12}$ [D]	V [cm^{-1}]
207	1.21 (abs)	30.7	30.8	500
208	1.23 (abs)	28.4	28.5	570
209	1.31 (abs)	28.5	28.6	660
210	1.16 (em)	28.8	28.9	620
211	1.17 (em)	26.5	26.6	770

by Equation (10) as was the electron coupling V by Equation (8). It is remarkable that the electronic coupling V slightly increases as the acceptor strength of the substituents R^1 and R^2 on the triarylamine donor center increases, an effect which might be a result of a decreasing effective diabatic ET distance r (Table 36). As mentioned above (Section 3.1.8), similar effects are responsible for larger electron couplings in bis(dialkylamine) radical cations compared to the corresponding bis(triarylamine) MV compounds. The electronic couplings of compounds **207–211** are significantly smaller than those of the corresponding neutral MV compounds with ethenyl (**201**) and ethynyl spacers (**202** and **204–206**) as a result of a twist around the biphenyl bridge moiety in **207–211**.

The back electron transfer (BET) after optical excitation of MV compounds **207–213** is in the so-called Marcus-inverted region (see also Section 2.1), which means that k_{BET} decreases as the exergonicity increases (ΔG^{00}, Tables 35 and 37). Moreover, fluorescence measurements of MV

Table 37: Fluorescence lifetimes τ_{fl}, quantum yields Φ_f, and rate constants for nonradiative back electron transfer k_{BET} of MV compounds **207–213** in cyclohexane.[270]

	τ_{fl} [ns]	Φ_f	k_{BET} [$\times 10^7$ s^{-1}]
207	0.29		340
208	4.8	0.03	20
209	12	0.15	6.9
210	20	0.33	3.4
211	20	0.37	3.1
212	20	0.35	3.2
213	23		2.9

compounds **207–213** revealed quantum yields of up to 37% (Table 37). This observation is very exciting because quantum yields on this order of magnitude are extremely remarkable for open-shell compounds, which generally do not fluoresce at room temperature.[270] The quantum yield strongly depends on the substituents R^1 and R^2 and, consequently, on the strength of the triarylamine donor center, that is, as ΔG^{00} increases, the quantum yield of the fluorescence increases.

This behavior can be explained by two competing deactivation mechanisms: fluorescence and nonradiative BET. Figure 16 shows that as ΔG^{00} increases, the activation energy (crossing point of the ground state and excited state

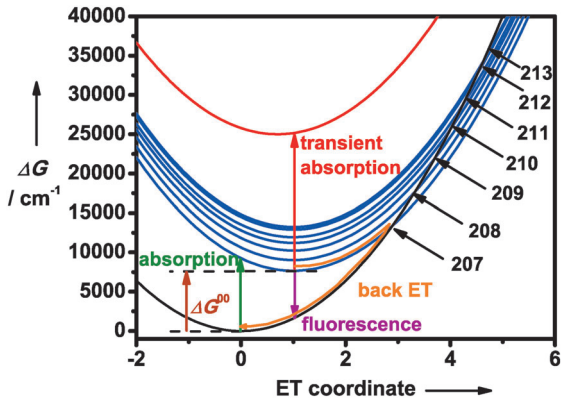

Figure 16. Diabatic FES of the ground (black) and first excited state (blue) of MV compounds **207**–**213**. The barrier for back electron transfer is given by the crossing point of the ground and excited state potentials, as indicated by the arrows for the different MV systems.

potentials) for a nonradiative deactivation increases and, as a direct consequence, the life time of the excited state increases. Thus, deactivation by fluorescence gets more and more likely. In this way, the high fluorescence quantum yields are a direct result of the Marcus-inverted region.

The ET dynamics of compound **207** was investigated in solvents of different polarity by time-resolved transient spectroscopy in the femtosecond time domain.[273] These studies yielded a BET rate constant in benzonitrile three orders of magnitude larger than in hexane. The increased rates with increasing solvent polarity was explained by a more effective stabilization of the strongly polar excited state compared to the ground state in polar solvents.

One of the few neutral MV compounds that has been studied in detail is composed of a tetrathiafulvalene (TTF) donor center directly linked to a 2,5-di-*tert*-butyl-6-oxophenalenoxy (6OP) radical acceptor (Scheme 72).[274] Indeed, this assignment is only correct in nonpolar and aprotic solvents such as toluene and dichloromethane, because then the electronic ground state consists of these redox motifs. It could

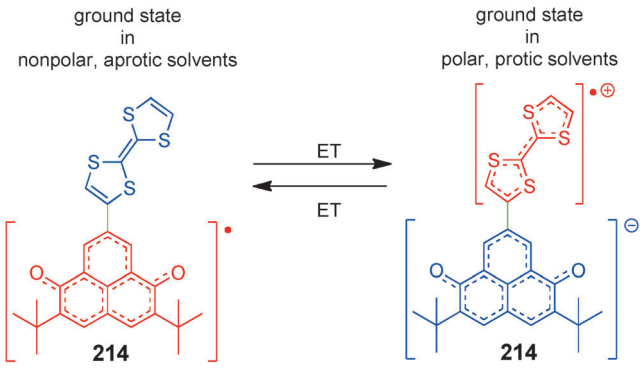

Scheme 72. Neutral organic MV compound **214**.

unequivocally be shown by ENDOR measurements in protic solvents, such as trifluoroethanol, that the ground state has zwitterionic character, with a TTF radical cation acceptor and a 6OP anion donor center, as shown in Scheme 72. Neutral radical **214** shows a broad IV-CT band centered at 1315 nm in dichloromethane which disappears on addition of small amounts of the protic solvent trifluoroethanol as a result of the stabilization of the zwitterionic ground state. Further evidence for this stabilization came from measurement of the redox potentials in benzonitrile solution in the presence of various amounts of trifluoroethanol. While the potential of the first oxidation remains at −0.01 V versus ferrocene, the first reduction potential continuously decreases from −0.29 V in pure benzonitrile to −0.11 V in a 4:1 mixture of benzonitrile/trifluoroethanol. Thus, the ground state **214** has an asymmetric double minimum potential, whose equilibrium can be shifted by solvent polarity. Some other related phenalenyl-based MV systems will be dealt with in Section 4.2.

3.6. Multidimensional MV Systems

In the last two decades, attention also focused on multidimensional MV systems. In particular, the use of GMH theory (see Section 2.6) on MV systems with any number of redox states allowed the investigation of the ET behavior of this special class of MV compounds. In most cases the MV compounds adopt symmetrical topologies in the neutral state with the redox centers arranged in trigonal, hexagonal, tetrahedral, and square or rectangular forms. These geometrical topologies are shown in Scheme 73, and we discuss the special features of multidimensional MV systems in terms

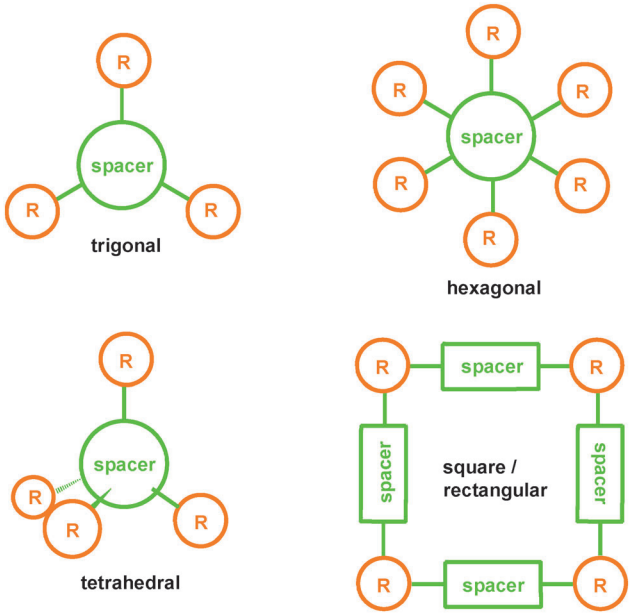

Scheme 73. The four main geometrical topologies of organic multidimensional MV systems. The redox centers R are equivalent and each MV systems may thus adopt different, multiply charged degenerate redox states.

of those arrangements. As a result of the many redox centers involved, multidimensional MV systems usually have more than one mixed-valence state.

3.6.1. Multidimensional MV Systems with Trigonal Topology

One of the first organic multidimensional MV systems investigated were the radical cations of triamines **215** and **216** (Scheme 74).[52,275] Both systems have MV character in the

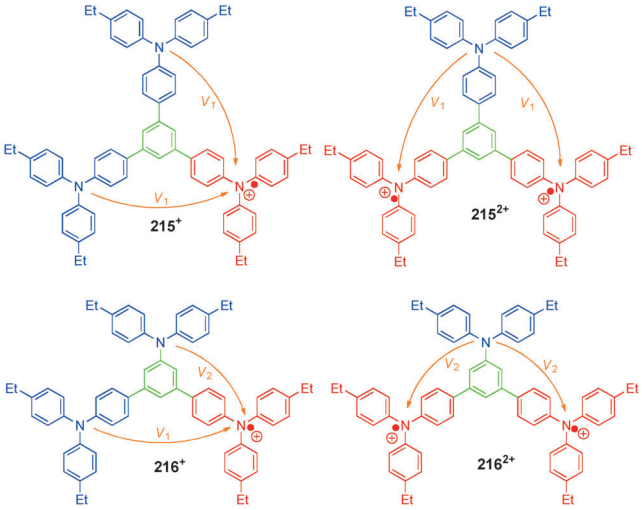

Scheme 74. Monocationic and dicationic MV compounds **215**$^{+}$, **215**$^{2+}$, **216**$^{+}$, and **216**$^{2+}$ investigated by Bonvoisin et al.[52,275]

singly and the doubly oxidized redox state. Symmetric tris(triarylamine) **215** shows one reversible oxidation wave, while the asymmetric analogue **216** shows two reversible oxidation waves with a 2:1 ratio. The fact that no redox potential splitting is detected for identical redox centers implies there is a very weak electronic communication between the MV states. The triarylamine redox centers at the periphery of **216** are oxidized at lower potential than the central triarylamine, which yields a defined dicationic state.

Electrochemical oxidation of compounds **215** and **216** results in a weak and broad band in the NIR region around 1400 cm^{-1}, which disappears in the absorption spectra of the trication. The proximity of the redox potentials results in the measured spectra at each electrical potential being a superposition of the spectra of the neutral, monocationic, dicationic, and tricationic species. Thus, the analysis of the spectra is—as for all multidimensional MV systems—not straightforward. Bonvoisin et al. described a generally appliciable method to obtain the comproportionation constants of the equilibria and thereby to obtain corrected absorption spectra of the compounds at each oxidation state.[52] In this way, a Mulliken–Hush analysis of the monocationic and dicationic MV compounds **215**$^{+}$, **215**$^{2+}$, and **216**$^{2+}$ was possible. The optical data as well as the electronic couplings derived by this procedure are listed in Table 38.

It was a particular challenge to extract the electronic couplings V_1 and V_2 of **216**$^{+}$ from the absorption spectra. The asymmetry of this MV compound means that two different

Table 38: Data of corrected IV-CT bands of mono- and dications of **215** and **216** in dichloromethane and electronic couplings V_1 and V_2 extracted by a modified Mulliken–Hush treatment for MV compounds with trigonal geometrical topology.[52,275]

	$\tilde{\nu}_{max}$ [cm^{-1}]	ε [M^{-1} cm^{-1}]	V_1 [cm^{-1}]	V_2 [cm^{-1}]
215^{+}	6935	797	205	–
215^{2+}	7734	675	227	—
216^{+}	5310	1483	230	387
216^{2+}	6135	1908	–	387

ET pathways exist and, hence, the observed IV-CT band can be seen as a result of two different ETs.[275]

Veciana et al. investigated the symmetrical trigonal tris-(PCTM) radical anion system **217** (Scheme 75) which has MV character in the singly reduced and doubly reduced redox

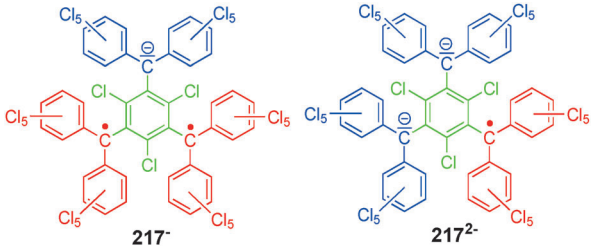

Scheme 75. Anionic MV states of trigonal tris(PCTM) radical **217**.

state **217**$^{-}$ and **217**$^{2-}$.[276–278] Spectroelectrochemical reduction of triradical **217** in dichloromethane led to a broad absorption band in the NIR region which disappeared when the trianion was generated. The corrected absorption spectra of MV compounds **217**$^{-}$ and **217**$^{2-}$ were evaluated using the comproportionation constants, which in turn were calculated from the reduction potentials.[276] The optical data of these IV-CT bands are listed in Table 39 together with the electronic couplings extracted by a similar method, as in the case of

Table 39: Optical data of the IV-CT bands of MV species **217**$^{-}$ and **217**$^{2-}$ generated by spectroelectrochemistry in dichloromethane and electronic coupling V.[277,278]

	$\tilde{\nu}_{max}$ [cm^{-1}]	ε [M^{-1} cm^{-1}]	V [cm^{-1}]
217^{-}	3470	2460	320
217^{2-}	3450	3600	392

216^{+}. The relatively low IV-CT band energies give evidence for a low inner reorganization energy of PCTM redox centers. As can be seen from the electronic coupling values, the electronic communication between the redox centers is relatively large despite the *meta*-linkage of the spacer. Even more remarkable is the observation of a high-spin triplet ground state in **217**$^{-}$. Therefore, this monoanion is one of the rare cases where ET prosseses are combined with high-spin states within one molecule. In this context, it is interesting that the energy difference between the singlet and triplet state

and, hence, the magnetic exchange interaction J correlates with the electronic coupling V in **217**$^{-}$.[279–283]

There are some other systems with a trigonal configuration of the redox centers connected through a central spacer unit. However, ET processes have not been evaluated quantitatively in these systems. Among these are tris(diarylamino)benzenes,[206,207,284] tris(diarylaminothiophenyl)benzenes,[285] and tris(triarylamio)truxenone compounds.[286]

The trigonal system **218** with tricyanovinyl redox centers connected to a central triphenylamine bridge unit was investigated regarding the mixed-valence behavior of the radical anion species **218**$^{-}$ and **218**$^{2-}$ (Scheme 76). These radical anions were generated in situ in acetonitrile by spectroelectrochemistry.[287]

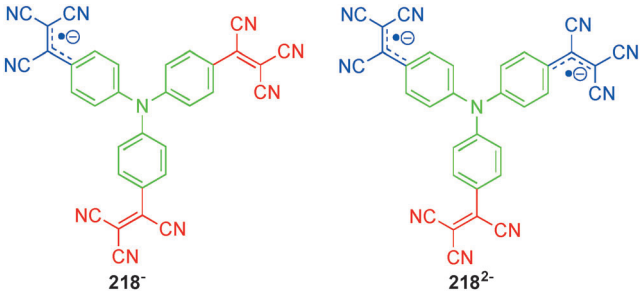

Scheme 76. MV states of tris(tricyanovinyl)triphenylamine **218**.

Surprisingly, no IV-CT band is observed in the absorption spectrum of the monoanion species **218**$^{-}$, while the dianion **218**$^{2-}$ shows a broad band in the NIR region centered around 8400 cm^{-1} ($\varepsilon = 420\,\text{M}^{-1}\,\text{cm}^{-1}$); this band disappears on further reduction to the trianion **218**$^{3-}$. Hush analysis of the IV-CT band (the effective ET distance of the redox centers was calculated by the AM1 method and taken as the distance between the first vinyl C atoms) gave an electronic coupling $V = 160$ cm^{-1}.[287]

3.6.2. *Multidimensional MV Systems with Hexagonal Topology*

All well-investigated hexagonal MV systems derive from the hexaphenylbenzene motif, not least because of the straightforward synthesis of such systems by a trimerization reaction of the corresponding tolan monomers (Scheme 77). Some of the first hexagonal organic systems studied in the context of mixed valency are those with dianisylamino and ditolylamino donor centers (**219**–**221**; Schemes 77 and 78).[2,288]

In principle, all of the cationic states **219**$^{+}$ to **219**$^{5+}$ of the hexagonal system **219** with dianisylamine redox centers are MV compounds, but because of the very close oxidation potentials (**219** shows six unresolved anodic processes in the cyclic voltammogram) it is nearly impossible to generate one species in a significantly higher concentration than the others. Thus, the IV-CT band observed could not be analyzed quantitatively to evaluate the electronic coupling. For this reason, a hexagonal MV compound **220** was synthesized in which three triarylamines possess methoxy groups and three have methyl groups, which makes the redox potentials of the

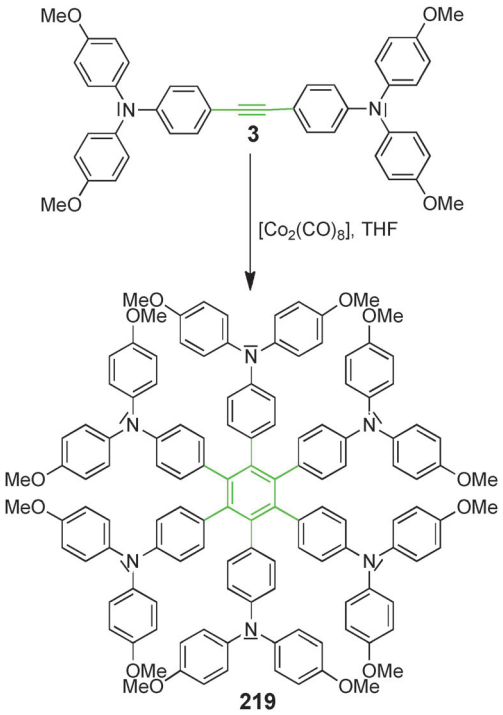

Scheme 77. Synthesis of a hexagonal dendrimer (e.g. **219**) from a tolan (e.g. **3**) by a cobalt-catalyzed trimerization reaction.

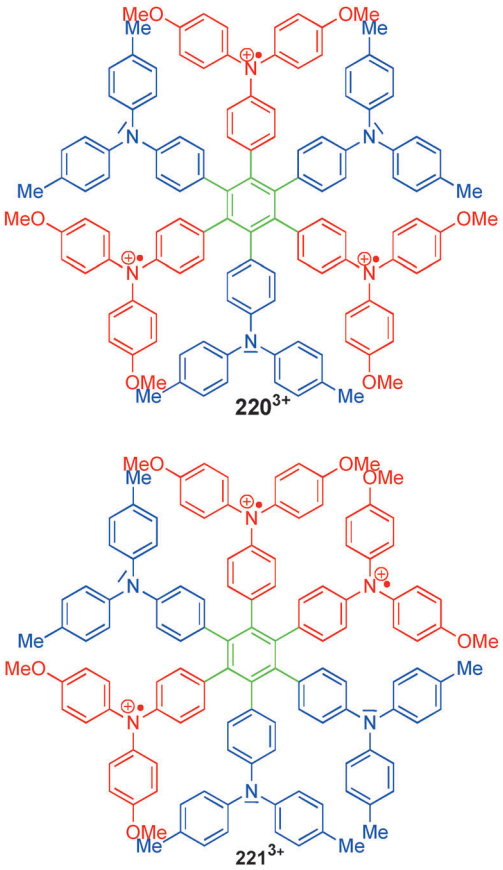

Scheme 78. Tricationic pseudohexagonal MV compounds.[2,288]

two sets of triarylamines slightly different. Again, this hexaarylabenzene was synthesized by trimerization of an appropriate tolan derivative. The trimerization mechanism results in two isomers being formed, one in which the methoxy-substituted triarylamines are in the 1- ,3-, and 5-position (**220**) of the central benzene ring, and one where they are in 1-, 2-, and 4-position (**221**). This makes these systems—strictly speaking—at best trigonal in topology. The different redox potentials of triarylamines allow the oxidation of, for example, **220** to yield the mixed-valence trication $\mathbf{220}^{3+}$ almost exclusively. Spectroelectrochemistry of this MV state shows a typical IV-CT band and an electronic coupling of 530 cm^{-1} in $\mathbf{220}^{3+}$. The interesting point with $\mathbf{220}^{3+}$ is whether all three positive charges can be optically or thermally transferred to the neutral redox centers in a concerted way. However, modeling studies on the FES and semiempirical AM1-CI calculations suggest that neither process is allowed and a stepwise transfer of three charges is preferred.[288]

Kochi and co-workers[289,290] investigated a number of hexakis(4-aminophenyl)benzene derivatives related to **220**. These authors demonstrated in a very detailed study that the thermal barrier for hole hopping in the case of hexakis(4-dialkylaminophenyl)benzene radical cation $\mathbf{222}^{+}$ is so low that, even at −20 °C, one approaches a toroidal delocalization of charge within the six phenyl rings attached to the central benzene ring.[291] One reason for that is the much stronger electronic coupling ($V = 1600\ cm^{-1}$) in $\mathbf{222}^{+}$ than in, for example, $\mathbf{220}^{3+}$. However, $\mathbf{222}^{+}$ may still be considered as a class II system.

Rathore et al.[292,293] also synthesized hexaarylbenzene systems, but with 2,5-dimethoxy-4-methyl redox centers (**223**) or triphenylvinyl redox centers (**224**; Scheme 79). For both species IV-CT bands were observed upon stepwise oxidation, but no quantitative evaluation of the electronic couplings etc. were done for the different MV states in either case.

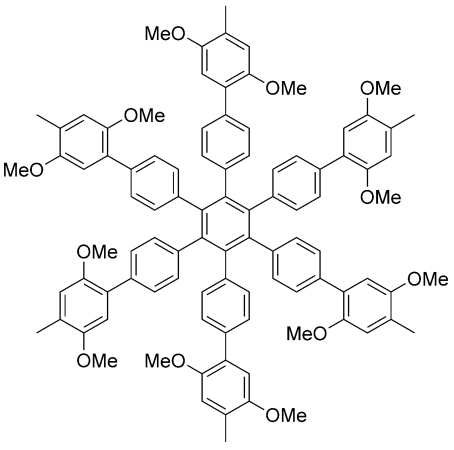

223

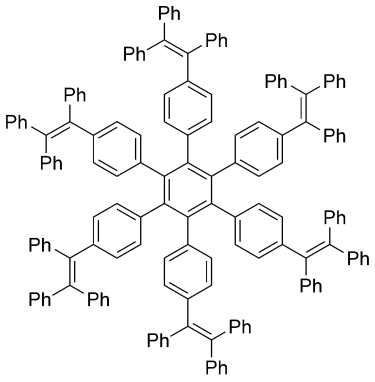

224

Scheme 79. Hexagonal MV compounds with 2,5-dimethoxy-4-methyl redox centers and triphenylvinyl redox centers, whose oxidized species show IV-CT bands.

3.6.3. *Multidimensional MV Systems with Tetrahedral and Square Topology*

The only MV system with tetrahedral topology that has been quantitatively characterized is tetrakis(dianisylamino-phenyl)phosphonium cation **225** (Scheme 80).[294] Here again, IV-CT bands were found upon oxidation of the triarylamines. Compound **225** may adopt three MV redox states ($\mathbf{225}^{+}$, $\mathbf{225}^{2+}$, and $\mathbf{225}^{3+}$). An averaged electronic coupling between the MV state of $V = 260\ cm^{-1}$ was evaluated form the IV-CT bands. Again, modeling studies of the FES led to the conclusion that the transfer of two charges in $\mathbf{225}^{2+}$ is stepwise rather than concerted. This raises the question of whether there are concerted electron-transfer processes in MV systems. A theoretical study[295] showed that this depends on the relative energies of the MV states involved as well as on the reorganization energy and the electronic coupling. There are indeed cases conceivable where a thermally activated concerted two-electron transfer may be favorable. These systems have a square (rectangular) topology such as $\mathbf{226}^{2+}$ and other similar cyclophanes.[296–299] In these systems two electrons may be transferred in a single step from a state in

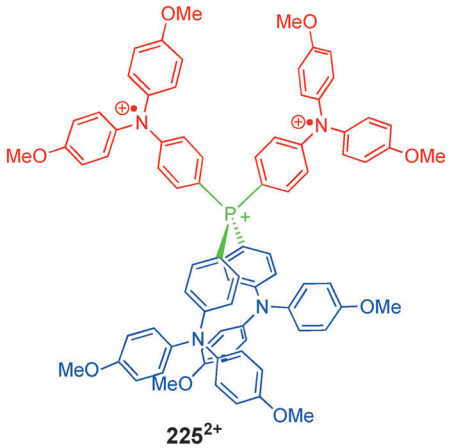

$\mathbf{225}^{2+}$

Scheme 80. MV compound with a tetrahedral topology.

which the charges are at the diagonal corners of the square to its symmetry equivalent without going via states where the charge is at adjacent redox centers (Scheme 81). This is due to the repulsion of charges in the latter states which makes these states higher in energy, even than the state where the positives

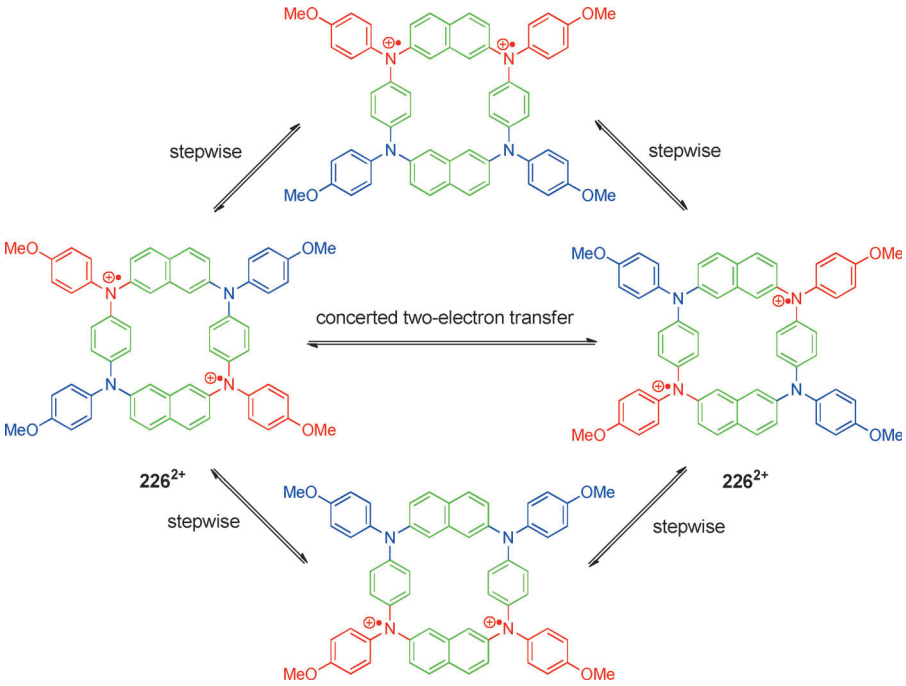

Scheme 81. MV compound with a square (rectangular) topology which possibly shows a concerted two-electron transfer pathway.

charges are delocalized within each phenylenediamine moiety. In fact, the formation of a FES that promotes concerted two-electron transfer depends on a delicate balance of state energies which might actually not be realized in the case of $\mathbf{226}^{2+}$, which thus serves more as a topological example. While this issue was addressed theoretically, there have been no attempts to prove or quantify this postulate, even though IV-CT bands were found for some of the square-type MV systems.[296,299]

4. Materials Aspects of Organic Mixed-Valence Compounds—An Outlook To Possible Applications

We close this Review with some examples of organic MV compounds that may be (or are) of practical use. All potential applications of MV compounds refer to the bulk solid state or films of MV compounds. The materials aspects are essentially restricted to either their optical properties or to their charge-transport properties. The former ones are usually associated with the NIR absorbance of the IV-CT band, the latter with the transport of a charge in an electric field.

The use of MV compounds as pigments is historically the first application of such compounds. Here, Prussian Blue is the most prominent example, but other inorganic MV compounds that serve as pigments are also known. Wurster's blue analogues (radical cation of *N*,*N*,*N*′,*N*′-tetraalkylphenylenediamine, **227**) may be considered to be the organic equivalent of Prussian Blue because of its intense blue colour. Although it is of no use as a pigment, it may be used in conjunction with *N*,*N*′-dialkyl-4,4′-bipyridylium ions (viologen dication, $\mathbf{228}^{2+}$) in electrochromic windows or mirrors. These devices are developed to prevent buildings with large window facades or cars from overheating on sunny days. Electrochromic rear-view mirrors are currently used to prevent the car driver from dazzling headlights at night.[300–302] A solution of compounds **227** and $\mathbf{228}^{2+}$ squeezed between two electrodes (both electrodes should be transparent for electrochromic windows, one transparent, and one reflecting for switchable mirrors) forms an electrochromic electrolyte system that can be switched between colorless (no voltage applied) and deep blue (voltage applied). Figure 17 illustrates the redox cycles that occur upon applying a voltage between the two electrode materials. While both $\mathbf{228}^{2+}$ and **227** are colorless, the oxidation of **227** at the anode and concomitant reduction of $\mathbf{228}^{2+}$ at the cathode yields $\mathbf{227}^{+}$ and $\mathbf{228}^{+}$, which are both deep blue. Both

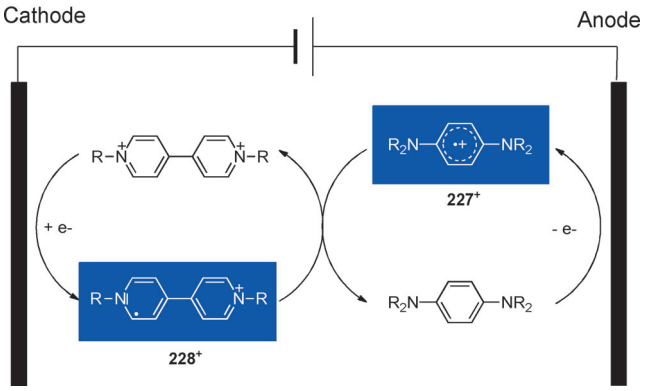

Figure 17. Principle of an electrochromic device based on viologen dication $\mathbf{228}^{2+}$ and *N*,*N*,*N*′,*N*′-tetraalkylphenylenediamine $\mathbf{227}^{2+}$. Upon current flow, the bluish viologen radical cation and *N*,*N*,*N*′,*N*′-tetraalkylphenylenediamine radical cation form, which recombine in the bulk solution to prevent overelectrolysis.

radical cations may be considered to be class III MV compounds, with the color being due to charge resonance in a single minimum system, as illustrated in Figure 6 f (Section 2.4). Back diffusion from the electrodes into the bulk electrolyte solution leads to charge recombination between $\mathbf{227}^{+}$ and $\mathbf{228}^{+}$. Thus, a constant current flow is necessary to maintain the colored state. On the other hand, the charge recombination in bulk solution prevents the system from overvoltage, which would otherwise damage the cell. Such a system operates in car rear-view mirrors developed by Gentex in the 1980s.[303]

Although the above-mentioned $\mathbf{227}^+$ and $\mathbf{228}^+$ MV systems display absorption bands around 600 nm, MV systems based on triarylamines may easily be designed so that their lowest energy absorption lies in the NIR region (see Section 3.1.5). Electropolymerization of compounds such as **229**, in which the phenyl groups are unprotected, leads to anodic C–C coupling and, thus, to the formation of benzidine units (Scheme 82).[304] Spectroelectrochemistry of the thus-

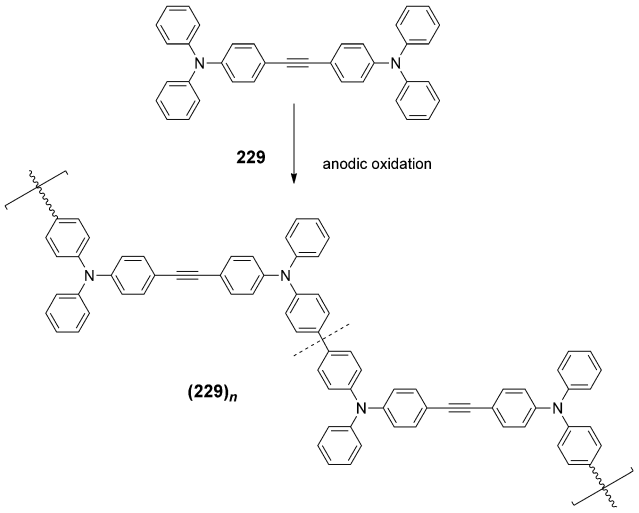

Scheme 82. Anodic oxidation of unprotected bis(triarylamine)s leads to polymers with benzidine units.[304]

formed films on a platinum electrode shows the formation of an IV-CT band at about 7000 cm^{-1} (ca. 1400 nm; Figure 18). This band has a maximum intensity when every second

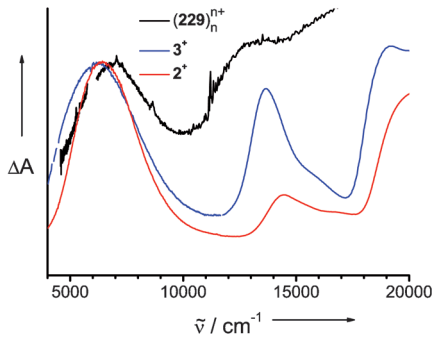

Figure 18. Absorption spectra of polymer $(\mathbf{229})_n$ at a 50% oxidation level, and of MV compounds $\mathbf{2}^+$ and $\mathbf{3}^+$ for comparison.[304]

triarylamine of the polymer is oxidized. Upon further oxidation, the IV-CT band disappears. This IV-CT band corresponds very well with that of tetraanisylbenzidine radical cation $\mathbf{2}^+$ and tetraanisyltolandiamine radical cation $\mathbf{3}^+$ (see Section 3.1.5).[79] Thus, unlike other conductive polymers, such as polythiophenes or polypyrroles, whose electronic structure are at least partially governed by band formation, polymers based on triarylamines show localized radical cation behavior (localized polarons in solid-state physics language) with typical optically induced charge-transfer bands (IV-CT).

Nishikitani et al.[305] synthesized polymers based on diaryldimethylbenzidine **230** and diaryldimethylphenylenediamine moieties **231** (Scheme 83). These polymers were attached to a transparent anode and used together with diheptylviologen and a solid electrolyte to build an electrochromic cell. After

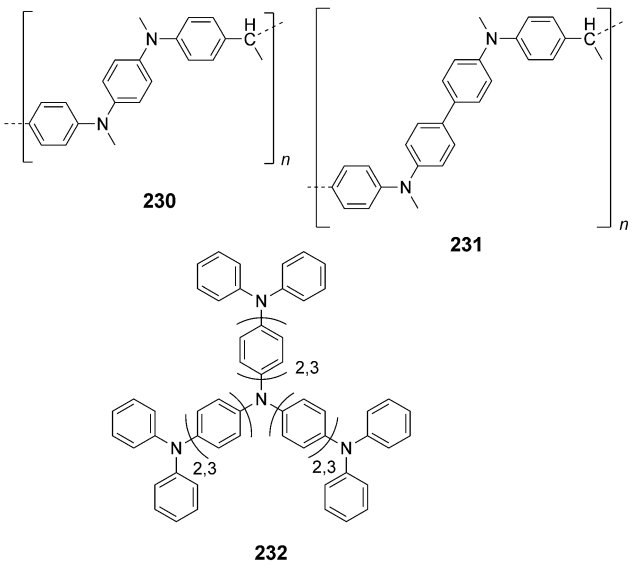

Scheme 83. Polymeric systems that form MV states upon charging in films.

application of a voltage, the cell shows absorption as a superposition of the spectra of $\mathbf{228}^+$ and of oxidized **230**, with a maximum at approximately 640 nm. For application as a device, not only are optimal optical properties required but complete reversibility of the redox processes within the lifetime of the device is also necessary. Although this has been demonstrated for electrochromic mirrors of the type shown in Figure 17, total reversibility of systems based on triarylamines remains to be proved.

In a first attempt, Leung and co-workers[306] prepared thin layers of electropolymerized starbust dendrimers **232** (Scheme 83). Upon oxidation, these films showed the characteristic broad and intense bands in the NIR region (1000 to >2000 nm) that are typical of IV-CT bands associated with triarylamine redox centers. The IV-CT band is significantly broader and at much lower energy than that of the tetraarylbenzidine radical cation (1570 nm), which indicates that the IV-CT process in the starbust dendrimer polymer is due to a class II situation. Consequently, full oxidation leads to the disappearance of these bands. Potential-step experiments proved the reversibility for at least a few cycles of the electrochromic process and showed a switching time of about 2–3 s.

Taken together, while class III compounds (or their derivatives) are currently used in electrochromic rear-view car mirrors in the visible region, the use of class II compounds

to move the electrochromic effect into the NIR region was demonstrated, but commercial devices have not yet entered the market. A possible explanation might be the long-term stability, which is generally better for class III systems, because of increased charge delocalization, than for class II MV compounds.

Besides their optical properties, an application of MV compounds might be for charge transport. While this application seems straightforward, it is in fact not because typical MV behavior requires localization of charge by vibronic coupling, that is, the charge is confined by structural distortions in the molecular framework. On the other hand, efficient charge transport requires the formation of electronic band structures in the solid state, in which polarons or bipolarons can move coherently.[214,307,308] This coherent charge transport can only be achieved in highly ordered materials. This is at least partially fulfilled in conjugated polymers or, much better, in crystalline organic materials provided that the molecular orientation is favorable for intermolecular charge transport. However, most organic MV compounds, and in particular those that are based on triarylamines, form amorphous, that is, disordered, materials.[309] In such materials, intermolecular charge transport can only be achieved by incoherent, thermally activated hopping. Thus, the rate-limiting step is not the charge transfer within the MV compound (which is a coherent superexchange in most cases) but the intermolecular charge transfer.[310] If organic MV compounds are incorporated into polymers through, for example, electropolymerization, materials result which usually show typical redox-polymer behavior, that is, charging leads to oxidized or reduced redox centers which may interact with neighboring uncharged redox centers in a MV-type interaction, but no electronic band structures are formed. This is the case for, for example, polymer **(229)$_n$** (see above).[304] The conductivity of such materials is usually very low,[311] but can in some cases display surprisingly high values (up to 1 S cm^{-1} in a polytriphenylamine).[312] However, whether electronic band structure or redox polymer behavior is formed depends strongly on the order of the material. Electropolymerization of ethylenedithiopyrrole **233** results in the formation of a typical, highly conducting polypyrrole.[313] The formation of electronic bands can be observed by spectroelectrochemistry, which shows different interband transitions at different levels of doping (Figure 19). In contrast, methylenedithiopyrrole **234**[314] shows the typical features of a redox polymer, that is, a broad and featureless absorption band in the NIR region which is due to IV-CT transitions, much in the same way as in the triarylamine polymer **(229)$_n$** (see Figure 18). The conductivity of the methylenedithiopyrrole polymer is less than half that of the ethylenedithiopyrrole polymer. The different behavior of both polymers can be explained by a different degree of order depending on the sulfur bridging group.[313]

In a similar way as **234**, polymer **235** (Scheme 84), which consists of alternating triarylamine and PCTM moieties, is a redox polymer that shows a localized IV-CT band much in the same way as its monomer analogue **201**. This polymer was used in a field-effect transistor device and shows nice ambipolar transport of both holes and electrons, albeit with

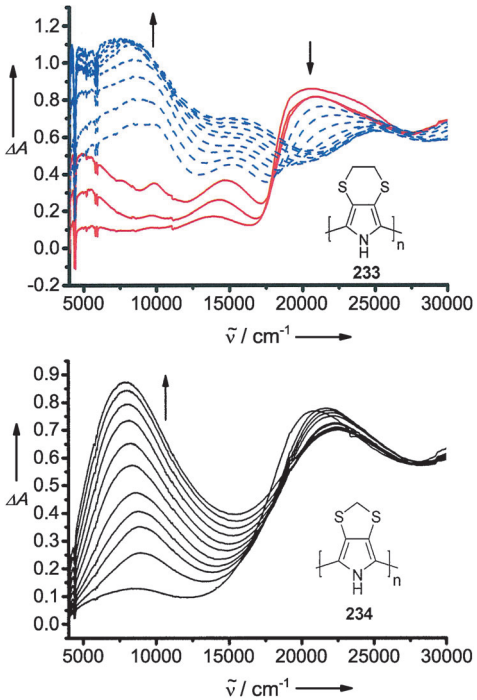

Figure 19. Changes in the Vis/NIR spectra upon anodic oxidation of poly(ethylenedithiopyrrole) **233** (red spectra: polaron transitions, blue spectra: bipolaron transitions) and poly(methylenedithiopyrrole) **234**.[313]

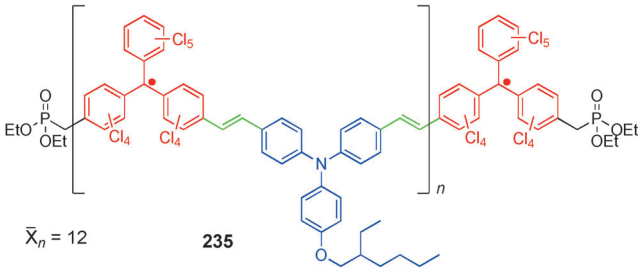

Scheme 84. Neutral polyradical **235** with alternating triarylamine and PCTM groups.

small charge carrier mobilities of about 10^{-5} cm^2 V^{-1} s^{-1}.[315] This is the consequence of the amorphous structure induced by the propeller-shaped triarylamine and PCTM groups.

Thus, on a molecular scale, the picture emerges that charge transport can be gradually changed from incoherent hopping to coherent band transport depending on the degree of order. While in conjugated polymers charge transport along the conjugated chain (within conjugation length) may be fast, it is the charge transfer between the polymer chains that is rate-determining.[310] This particular aspect of intermolecular (interpolymer) charge transfer in MV compounds has been addressed recently by using systems in which two π-redox systems are oriented in a fixed position through saturated bridges, that is, in cyclophane systems (Scheme 26).[129]

The benzene rings in the central [2.2]paracylophane of the bis(triarylamine) radical cation **6**$^+$ are separated by 3.1 Å, that is, their π faces approach less than twice the van der Waals

radius of a carbon atom (3.4 Å). The distance in [3.3]paracyclophane **70**$^+$ is similar to the van der Waals radius (3.3 Å) and, thus, mimics the closest distance π systems can approach in the solid state. Surprisingly, both bis(triarylamine) radical cations, which are class II MV systems, showed about the same electronic coupling (by analysis of the IV-CT band) and the same hole transfer rate constant (by dynamic ESR spectroscopy). Therefore, a decreased π distance does not necessarily lead to an increase in the interaction, at least not in terms of charge transfer. In contrast, resonance Raman investigations indicated [4.4]bis(quinquithiophene)-cyclophane radical cation **236**$^+$ to be a class III MV species that shows charge localization upon cooling (Scheme 85).[316]

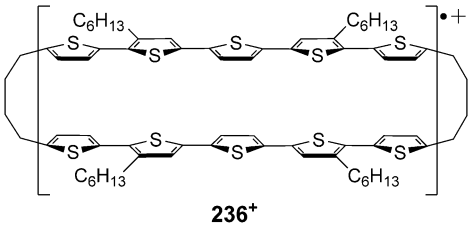

Scheme 85. Temperature-dependent class III/class II transition in [4.4]bis(quinquithiophene)-cyclophane radical cation **236**$^+$.

Mixed valency is also an issue in organic solid-state conductors of the CT type.[317] Since several review articles on the chemistry and physics of organic solid-state conductors have been published recently, we only refer to those aspects here which have a close relationship to MV systems.[318,319]

Electrical conductivity of organic crystalline solids requires partial charge transfer between segregated stacks of donor and acceptor molecules. This partial charge transfer state is often assigned as a MV state and is characterized by a NIR absorption. The well-known 1:1 mixture of tetrathiafulvalene (TTF) and tetracyanoquinodimethane (TCNQ) with a conductivity of about 10^2 S cm^{-1} at room temperature is such a CT complex.[319] While the interactions in these CT complexes are intermolecular, polymerization of **237** leads to a polymer with helix structure and partial stacking of the TTF moieties (Scheme 86).[320] Anodic oxidation then leads to a MV state which shows typical IV-CT band behavior in the NIR region, that is, the IV-CT band is maximal at 50% oxidation. A recently reported supramolecular arrangement of stacked TTF moieties within a xerogel also showed IV-CT bands and electrical conductivity upon doping.[321]

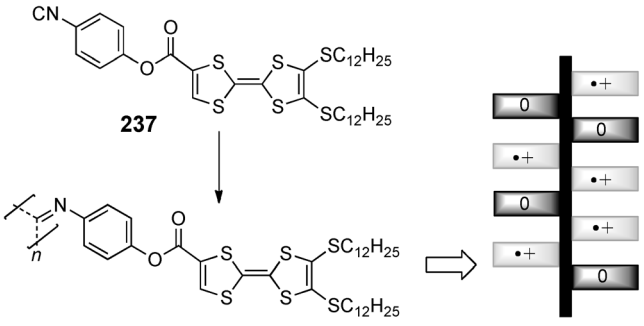

Scheme 86. Poly(isocyanide) helix (**237**)$_n$ with stacked TTF units that form MV strands at 50% oxidation.[320]

Phenalenyl-based spiro compounds such as **238**–**240** (Scheme 87) may be viewed as neutral MV species. EPR measurements and NIR absorption spectroscopy indicate these species to be delocalized by spiro conjugation.[322] The IV-CT band of **240** (R^1 = Me, R^2 = hexyl) in solution is at 4800 cm^{-1}.[323] In the solid state, **239** with R = hexyl shows a room-temperature conductivity of 0.05 S cm^{-1} although no favorable intermolecular interactions are evident.[324] However, compound **239** with R = ethyl forms a π dimer in the solid state which leads to symmetry breaking.[325] This symmetry breaking leads to a temperature-dependent bistability in three physical ways: magnetic, optical, and electrical. The reason is the spin pairing of two spin centers located at different molecular units within the π dimer upon lowering the temperature.

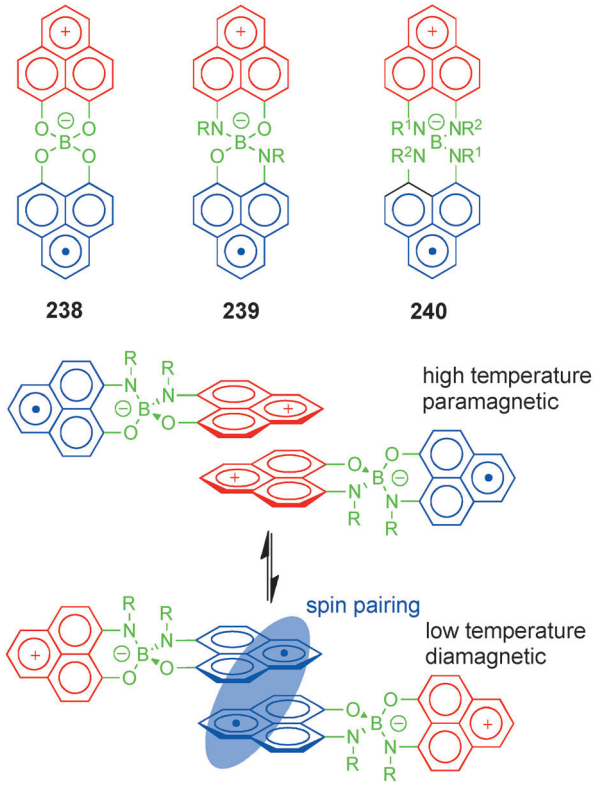

Scheme 87. Formation of dimers of phenalenyl spiro compounds with temperature-dependent spin pairing.

The last example in particular (compound **239**) shows that MV compounds bear a large treasure of possible applications, predominantly in the area of optoelectronic and/or magneto-optic materials. Up to now, the TMPD/viologen electrochromic system is the only case known to us in which MV species have gained commercial application. However, the importance of organic mixed-valence chemistry should not be seen in terms of the direct applicability of these species but in the wealth of knowledge about electron-transfer phenomena that has been gained through their study. Older (electrophotography) as well as recent technologies (OLEDs) are

based on compounds that form MV states during device operation, although this has hardly been recognized or even mentioned.

Our ongoing research on organic mixed-valence compounds has been supported by the Deutsche Forschungsgemeinschaft. C.L. wishes to express his gratitude to all co-workers who have contributed to this research and whose names are mentioned in the appropriate references. Furthermore, we are indebted to a referee who pointed out to us so many otherwise misleading statements, which led to a significant improvement of this Review.

Received: February 7, 2011
Published online: November 18, 2011

[1] In this Review, we use the term "charge transfer" (CT) if we want to stress that partial charge is transferred, as in the case of optically induced processes. In contrast "ET" is used as a more general term and in cases of photoinduced process where in practice a full charge is transferred. In cases where we want to point out that formally a positive charge (hole) is transferred we use the term "hole transfer" (HT).
[2] C. Lambert, G. Nöll, *Angew. Chem.* **1998**, *110*, 2239 – 2242; *Angew. Chem. Int. Ed.* **1998**, *37*, 2107 – 2110.
[3] C. Rovira, D. Ruiz-Molina, O. Elsner, J. Vidal-Gancedo, J. Bonvoisin, J.-P. Launay, J. Veciana, *Chem. Eur. J.* **2001**, *7*, 240 – 250.
[4] A. Heckmann, C. Lambert, M. Goebel, R. Wortmann, *Angew. Chem.* **2004**, *116*, 5976 – 5981; *Angew. Chem. Int. Ed.* **2004**, *43*, 5851 – 5856.
[5] R. Stahl, C. Lambert, C. Kaiser, R. Wortmann, R. Jakober, *Chem. Eur. J.* **2006**, *12*, 2358 – 2370.
[6] M. Hariharan, P. P. Neelakandan, D. Ramaiah, *J. Phys. Chem. B* **2007**, *111*, 11940 – 11947.
[7] P. V. Bernhardt, F. Bozoglian, B. P. Macpherson, M. Martinez, *Coord. Chem. Rev.* **2005**, *249*, 1902 – 1916.
[8] C. Creutz, H. Taube, *J. Am. Chem. Soc.* **1969**, *91*, 3988 – 3989.
[9] C. Creutz, H. Taube, *J. Am. Chem. Soc.* **1973**, *95*, 1086 – 1094.
[10] I. M. Klotz, H. Czerlinski, H. A. Fiess, *J. Am. Chem. Soc.* **1958**, *80*, 2920 – 2923.
[11] H. M. Powell, *Proc. Chem. Soc.* **1959**, 73 – 75.
[12] J. K. Beattie, N. S. Hush, P. R. Taylor, *Inorg. Chem.* **1976**, *15*, 992 – 993.
[13] N. S. Hush, A. Edgar, J. K. Beattie, *Chem. Phys. Lett.* **1980**, *69*, 128 – 133.
[14] S. B. Piepho, *J. Am. Chem. Soc.* **1990**, *112*, 4197 – 4206.
[15] A. Bencini, I. Ciofini, C. A. Daul, A. Ferretti, *J. Am. Chem. Soc.* **1999**, *121*, 11418 – 11424.
[16] J. R. Reimers, Z. L. Cai, N. S. Hush, *Chem. Phys.* **2005**, *319*, 39 – 51.
[17] K. D. Demadis, C. M. Hartshorn, T. J. Meyer, *Chem. Rev.* **2001**, *101*, 2655 – 2685.
[18] D. O. Cowan, F. Kaufman, *J. Am. Chem. Soc.* **1970**, *92*, 219 – 220.
[19] D. O. Cowan, C. Levanda, J. Park, F. Kaufman, *Acc. Chem. Res.* **1973**, *6*, 1 – 7.
[20] C. Levanda, K. Bechgaard, D. O. Cowan, M. D. Rausch, *J. Am. Chem. Soc.* **1977**, *99*, 2964 – 2968.
[21] C. Creutz, *Prog. Inorg. Chem.* **1983**, *30*, 1 – 73.
[22] M. D. Newton, N. Sutin, *Annu. Rev. Phys. Chem.* **1984**, *35*, 437 – 480.
[23] N. S. Hush, *Coord. Chem. Rev.* **1985**, *64*, 135 – 157.
[24] R. A. Marcus, N. Sutin, *Biochim. Biophys. Acta Rev. Bioenerg.* **1985**, *811*, 265 – 322.
[25] R. A. Marcus, N. Sutin, *Comments Inorg. Chem.* **1986**, *5*, 119 – 133.
[26] J. R. Reimers, N. S. Hush, *Chem. Phys.* **1989**, *134*, 323 – 354.
[27] C. G. Young, *Coord. Chem. Rev.* **1989**, *96*, 89 – 251.
[28] P. Chen, T. J. Meyer, *Chem. Rev.* **1998**, *98*, 1439 – 1478.
[29] J.-P. Launay, *Chem. Soc. Rev.* **2001**, *30*, 386 – 397.
[30] J. R. Reimers, N. S. Hush, *Inorg. Chem.* **1990**, *29*, 3686 – 3697.
[31] M. B. Robin, P. Day, *Adv. Inorg. Chem. Radiochem.* **1967**, *9*, 247 – 422.
[32] Almost at the same time as Wudl et al. other research groups also reported on the synthesis and on the redox behavior of tetrathiafulvalene, see S. Hünig, G. Kießlich, H. Quast, D. Scheutzow, *Justus Liebigs Ann. Chem.* **1973**, 310 – 323 and D. L. Coffen, J. Q. Chambers, D. R. Williams, P. E. Garrett, N. D. Canfield, *J. Am. Chem. Soc.* **1971**, *93*, 2258 – 2268.
[33] F. Wudl, G. M. Smith, E. J. Hufnagel, *J. Chem. Soc. Chem. Commun.* **1970**, 1453 – 1454.
[34] F. Wudl, D. Wobschal, E. J. Hufnagel, *J. Am. Chem. Soc.* **1972**, *94*, 670 – 671.
[35] S. Hünig, *Pure Appl. Chem.* **1967**, *15*, 109 – 122.
[36] L. Michaelis, E. S. Hill, *J. Am. Chem. Soc.* **1933**, *55*, 1481 – 1494.
[37] L. Michaelis, M. P. Schubert, S. Granick, *J. Am. Chem. Soc.* **1939**, *61*, 1981 – 1992.
[38] U. Nickel, *Chem. Unserer Zeit* **1978**, *12*, 89 – 98.
[39] B. Badger, B. Brocklehurst, *Trans. Faraday Soc.* **1970**, *66*, 2939 – 2947.
[40] J. E. Harriman, A. H. Maki, *J. Chem. Phys.* **1963**, *39*, 778 – 786.
[41] M. Itoh, *J. Am. Chem. Soc.* **1971**, *93*, 4750 – 4754.
[42] S. F. Nelsen, P. J. Hintz, J. M. Buschek, G. R. Weisman, *J. Am. Chem. Soc.* **1975**, *97*, 4933 – 4936.
[43] S. I. Weissman, *J. Am. Chem. Soc.* **1958**, *80*, 6462 – 6463.
[44] A. Ishitani, S. Nagakura, *Mol. Phys.* **1967**, *12*, 1 – 12.
[45] F. Gerson, W. B. Martin, *J. Am. Chem. Soc.* **1969**, *91*, 1883 – 1891.
[46] A. Carrington, R. E. Moss, P. F. Todd, *Mol. Phys.* **1967**, *12*, 95 – 96.
[47] F. Gerson, R. Gleiter, A. S. Dreiding, G. Moshuk, *J. Am. Chem. Soc.* **1972**, *94*, 2919 – 2923.
[48] H. E. Zimmerman, Y. A. Lapin, E. E. Nesterov, G. A. Sereda, *J. Org. Chem.* **2000**, *65*, 7740 – 7746.
[49] P. Fürderer, F. Gerson, J. Heinzer, S. Mazur, H. Ohyanishiguchi, A. H. Schroeder, *J. Am. Chem. Soc.* **1979**, *101*, 2275 – 2281.
[50] To the best of our knowledge the term "organic mixed-valence compound" was first used by Matsunaga in 1980; see Y. Matsunaga, K. Takayanagi, *Bull. Chem. Soc. Jpn.* **1980**, *53*, 2796 – 2799.
[51] S. F. Nelsen, H. Chang, J. J. Wolff, J. Adamus, *J. Am. Chem. Soc.* **1993**, *115*, 12276 – 12289.
[52] J. Bonvoisin, J.-P. Launay, M. Van der Auweraer, F. C. De Schryver, *J. Phys. Chem.* **1994**, *98*, 5052 – 5057, see also correction J. Bonvoisin, J.-P. Launay, M. Van der Auweraer, F. C. De Schryver, *J. Phys. Chem.* **1996**, *100*, 18006.
[53] M. R. Wasielewski, *Chem. Rev.* **1992**, *92*, 435 – 461.
[54] H. Kurreck, M. Huber, *Angew. Chem.* **1995**, *107*, 929 – 947; *Angew. Chem. Int. Ed.* **1995**, *34*, 849 – 866.
[55] J. R. Reimers, J. M. Hughes, N. S. Hush, *Biochemistry* **2000**, *39*, 16185 – 16189.
[56] J. M. Hughes, M. C. Hutter, J. R. Reimers, N. S. Hush, *J. Am. Chem. Soc.* **2001**, *123*, 8550 – 8563.
[57] J. R. Reimers, N. S. Hush, *J. Chem. Phys.* **2003**, *119*, 3262 – 3277.
[58] J. R. Reimers, W. A. Shapley, N. S. Hush, *J. Chem. Phys.* **2003**, *119*, 3240 – 3248.
[59] J. R. Reimers, W. A. Shapley, A. P. Rendell, N. S. Hush, *J. Chem. Phys.* **2003**, *119*, 3249 – 3261.

[60] J. R. Reimers, N. S. Hush, *J. Am. Chem. Soc.* **2004**, *126*, 4132 – 4144.
[61] D. B. Brown, *Mixed-Valence Compounds*, Reidel, Dordrecht, **1980**.
[62] A. Vogler, A. H. Osman, H. Kunkely, *Coord. Chem. Rev.* **1985**, *64*, 159 – 173.
[63] K. Y. Wong, P. N. Schatz, *Prog. Inorg. Chem.* **1981**, *28*, 369 – 449.
[64] D. E. Richardson, H. Taube, *Coord. Chem. Rev.* **1984**, *60*, 107 – 129.
[65] P. F. Barbara, T. J. Meyer, M. A. Ratner, *J. Phys. Chem.* **1996**, *100*, 13148 – 13168.
[66] B. S. Brunschwig, N. Sutin, *Coord. Chem. Rev.* **1999**, *187*, 233 – 254.
[67] B. S. Brunschwig, C. Creutz, N. Sutin, *Chem. Soc. Rev.* **2002**, *31*, 168 – 184.
[68] R. A. Marcus, *J. Chem. Phys.* **1956**, *24*, 966 – 978.
[69] R. A. Marcus, *Rev. Mod. Phys.* **1993**, *65*, 599 – 610.
[70] K. Wieghardt, *Chem. Unserer Zeit* **1979**, *13*, 118 – 125.
[71] R. A. Marcus, *Discuss. Faraday Soc.* **1960**, *29*, 21 – 31.
[72] R. A. Marcus, *J. Chem. Phys.* **1965**, *43*, 679 – 701.
[73] In reality, each state is a function of many nuclear and solvent modes and, hence is represented by a multidimensional potential-energy surface (PES). In the context of transition-state theory, a reaction coordinate can be introduced which results in a one-dimensional PES for each state. In a Gibbs energy space, these one-dimensional PESs which are a section along the reaction coordinate through the multidimensional PESs transform into a free-energy surface (FES) and can be approximated by parabolas, see Ref. [24].
[74] B. S. Brunschwig, S. Ehrenson, N. Sutin, *J. Phys. Chem.* **1986**, *90*, 3657 – 3668.
[75] P. Suppan, *Top. Curr. Chem.* **1992**, *163*, 95 – 130.
[76] G. Grampp, *Angew. Chem.* **1993**, *105*, 724 – 726; *Angew. Chem. Int. Ed.* **1993**, *32*, 691 – 693.
[77] N. S. Hush, *Electrochim. Acta* **1968**, *13*, 1005 – 1023.
[78] C. Creutz, M. D. Newton, N. Sutin, *J. Photochem. Photobiol. A* **1994**, *82*, 47 – 59.
[79] C. Lambert, G. Nöll, *J. Am. Chem. Soc.* **1999**, *121*, 8434 – 8442.
[80] S. F. Nelsen, R. F. Ismagilov, D. A. Trieber, *Science* **1997**, *278*, 846 – 849.
[81] S. F. Nelsen, R. F. Ismagilov, D. R. Powell, *J. Am. Chem. Soc.* **1997**, *119*, 10213 – 10222.
[82] R. J. Cave, M. D. Newton, *Chem. Phys. Lett.* **1996**, *249*, 15 – 19.
[83] R. J. Cave, M. D. Newton, *J. Chem. Phys.* **1997**, *106*, 9213 – 9226.
[84] M. D. Newton, R. J. Cave, *J. Mol. Electron.* **1997**, 73 – 118.
[85] S. F. Nelsen, M. D. Newton, *J. Phys. Chem. A* **2000**, *104*, 10023 – 10031.
[86] N. Q. Chako, *J. Chem. Phys.* **1934**, *2*, 644 – 653.
[87] I. R. Gould, R. H. Young, L. J. Mueller, A. C. Albrecht, S. Farid, *J. Am. Chem. Soc.* **1994**, *116*, 8188 – 8199.
[88] R. Wortmann, P. Krämer, C. Glania, S. Lebus, N. Detzer, *Chem. Phys.* **1993**, *173*, 99 – 108.
[89] B. S. Brunschwig, C. Creutz, N. Sutin, *Coord. Chem. Rev.* **1998**, *177*, 61 – 79.
[90] T. P. Treynor, S. G. Boxer, *J. Phys. Chem. A* **2004**, *108*, 1764 – 1778.
[91] S. F. Nelsen, D. A. Trieber, R. F. Ismagilov, Y. Teki, *J. Am. Chem. Soc.* **2001**, *123*, 5684 – 5694.
[92] A. Heckmann, C. Lambert, *J. Am. Chem. Soc.* **2007**, *129*, 5515 – 5527.
[93] L. Onsager, *J. Am. Chem. Soc.* **1936**, *58*, 1486 – 1493.
[94] J. Herbich, A. Kapturkiewicz, *J. Am. Chem. Soc.* **1998**, *120*, 1014 – 1029.
[95] S. F. Nelsen, R. F. Ismagilov, *J. Phys. Chem. A* **1999**, *103*, 5373 – 5378.
[96] S. F. Nelsen, S. C. Blackstock, Y. Kim, *J. Am. Chem. Soc.* **1987**, *109*, 677 – 682.
[97] F. Jensen, *Introduction to Computational Chemistry*, Wiley, New York, **1999**, pp. 64 – 65.
[98] A. Szabo, N. S. Ostlund, *Modern Quantum Chemistry*, McGraw-Hill, New York, **1989**, pp. 127 – 128.
[99] S. F. Nelsen, A. E. Konradsson, J. P. Telo, *J. Am. Chem. Soc.* **2005**, *127*, 920 – 925.
[100] S. F. Nelsen, M. N. Weaver, J. P. Telo, B. L. Lucht, S. Barlow, *J. Org. Chem.* **2005**, *70*, 9326 – 9333.
[101] S. F. Nelsen, *Chem. Eur. J.* **2000**, *6*, 581 – 588.
[102] O. Elsner, D. Ruiz-Molina, I. Ratera, J. Vidal-Gancedo, C. Rovira, J. Veciana, *J. Organomet. Chem.* **2001**, *637*, 251 – 257.
[103] S. F. Nelsen, K. P. Schultz, J. P. Telo, *J. Phys. Chem. A* **2008**, *112*, 12622 – 12628.
[104] S. B. Piepho, E. R. Krausz, P. N. Schatz, *J. Am. Chem. Soc.* **1978**, *100*, 2996 – 3005.
[105] "Electron Delocalization, Structure and Dynamics in Mixed-Valence Systems": N. S. Hush in *Mixed-Valence Compounds* (Ed.: D. B. Brown), Reidel, Dordrecht, **1980**, pp. 151 – 188.
[106] L. J. Root, M. J. Ondrechen, *Chem. Phys. Lett.* **1982**, *93*, 421 – 424.
[107] J. Ko, M. J. Ondrechen, *J. Am. Chem. Soc.* **1985**, *107*, 6161 – 6167.
[108] S. B. Piepho, *J. Am. Chem. Soc.* **1988**, *110*, 6319 – 6326.
[109] "Vibronic coupling models of mixed valency: relation of the PKS and MO models for one- and two-electron systems": P. N. Schatz in *Mixed Valency Systems: Applications in Chemistry, Physics and Biology* (Ed.: K. Prassides), Kluwer, **1991**, pp. 7 – 28.
[110] J. R. Reimers, N. S. Hush, *Chem. Phys.* **1996**, *208*, 177 – 193.
[111] D. S. Talaga, J. I. Zink, *J. Phys. Chem. A* **2001**, *105*, 10511 – 10519.
[112] C. Lambert, S. Amthor, J. Schelter, *J. Phys. Chem. A* **2004**, *108*, 6474 – 6486.
[113] J. R. Reimers, N. S. Hush, *Chem. Phys.* **2004**, *299*, 79 – 82.
[114] P. J. Low, M. A. J. Paterson, H. Puschmann, A. E. Goeta, J. A. K. Howard, C. Lambert, J. C. Cherryman, D. R. Tackley, S. Leeming, B. Brown, *Chem. Eur. J.* **2004**, *10*, 83 – 91.
[115] A. V. Szeghalmi, M. Erdmann, V. Engel, M. Schmitt, S. Amthor, V. Kriegisch, G. Nöll, R. Stahl, C. Lambert, D. Leusser, D. Stalke, M. Zabel, *J. Am. Chem. Soc.* **2004**, *126*, 7834 – 7845.
[116] C. Lambert, C. Risko, V. Coropceanu, J. Schelter, S. Amthor, N. E. Gruhn, J. C. Durivage, J.-L. Brédas, *J. Am. Chem. Soc.* **2005**, *127*, 8508 – 8516.
[117] V. Coropceanu, M. Malagoli, J. M. André, J. L. Brédas, *J. Am. Chem. Soc.* **2002**, *124*, 10519 – 10530.
[118] R. J. Cave, M. D. Newton, K. Kumar, M. B. Zimmt, *J. Phys. Chem.* **1995**, *99*, 17501 – 17504.
[119] M. D. Newton, *Adv. Chem. Phys.* **1999**, *106*, 303 – 375.
[120] Y.-G. K. Shin, M. D. Newton, S. S. Isied, *J. Am. Chem. Soc.* **2003**, *125*, 3722 – 3732.
[121] M. Rust, J. Lappe, R. J. Cave, *J. Phys. Chem. A* **2002**, *106*, 3930 – 3940.
[122] C. Lambert, G. Nöll, J. Schelter, *Nat. Mater.* **2002**, *1*, 69 – 73.
[123] S. Amthor, C. Lambert, *J. Phys. Chem. A* **2006**, *110*, 1177 – 1189.
[124] S. A. Borshch, I. N. Kotov, I. B. Bersuker, *Chem. Phys. Lett.* **1982**, *89*, 381 – 384.
[125] J. P. Launay, F. Babonneau, *Chem. Phys.* **1982**, *67*, 295 – 300.
[126] I. B. Bersuker, S. A. Borshch, L. F. Chibotaru, *Chem. Phys.* **1989**, *136*, 379 – 384.
[127] J.-P. Launay, C. Coudret, C. Hortholary, *J. Phys. Chem. B* **2007**, *111*, 6788 – 6797.
[128] J. Seibt, A. Schaumlöffel, C. Lambert, V. Engel, *J. Phys. Chem. A* **2008**, *112*, 10178 – 10184.
[129] D. R. Kattnig, B. Mladenova, G. Grampp, C. Kaiser, A. Heckmann, C. Lambert, *J. Phys. Chem. C* **2009**, *113*, 2983 – 2995.

[130] H. Sponer, E. Teller, *Rev. Mod. Phys.* **1941**, *13*, 75.
[131] J. N. Murrell, *J. Am. Chem. Soc.* **1959**, *81*, 5037 – 5043.
[132] G. Orlandi, W. Siebrand, *J. Chem. Phys.* **1973**, *58*, 4513 – 4523.
[133] V. Coropceanu, M. Malagoli, J. M. Andre, J. L. Brédas, *J. Chem. Phys.* **2001**, *115*, 10409 – 10416.
[134] V. Coropceanu, C. Lambert, G. Nöll, J.-L. Brédas, *Chem. Phys. Lett.* **2003**, *373*, 153 – 160.
[135] J. Jortner, M. Bixon, *J. Chem. Phys.* **1988**, *88*, 167 – 170.
[136] R. A. Marcus, *J. Phys. Chem.* **1989**, *93*, 3078 – 3086.
[137] I. R. Gould, D. Noukakis, L. Gomez-Jahn, R. H. Young, J. L. Goodman, S. Farid, *Chem. Phys.* **1993**, *176*, 439 – 456.
[138] J. Cortes, H. Heitele, J. Jortner, *J. Phys. Chem.* **1994**, *98*, 2527 – 2536.
[139] See also Ref. [73] in Ref. [92].
[140] S. F. Nelsen, M. T. Ramm, J. J. Wolff, D. R. Powell, *J. Am. Chem. Soc.* **1997**, *119*, 6863 – 6872.
[141] S. F. Nelsen, H. Q. Tran, M. A. Nagy, *J. Am. Chem. Soc.* **1998**, *120*, 298 – 304.
[142] S. F. Nelsen, F. Blomgren, *J. Org. Chem.* **2001**, *66*, 6551 – 6559.
[143] D. Dehareng, G. Dive, A. Moradpour, *Int. J. Quantum Chem.* **2000**, *76*, 552 – 573.
[144] E. Fernández, L. Blancafort, M. Olivucci, M. A. Robb, *J. Am. Chem. Soc.* **2000**, *122*, 7528 – 7533.
[145] W. Helal, S. Evangelisti, T. Leininger, D. Maynau, *J. Comput. Chem.* **2009**, *30*, 83 – 92.
[146] F. Blomgren, S. Larsson, S. F. Nelsen, *J. Comput. Chem.* **2001**, *22*, 655 – 664.
[147] M. Renz, K. Theilacker, C. Lambert, M. Kaupp, *J. Am. Chem. Soc.* **2009**, *131*, 16292 – 16302.
[148] P. Siddarth, R. A. Marcus, *J. Phys. Chem.* **1990**, *94*, 2985 – 2989.
[149] M. D. Newton, *Chem. Rev.* **1991**, *91*, 767 – 792.
[150] H. M. McConnell, *J. Chem. Phys.* **1961**, *35*, 508 – 515.
[151] D. M. Adams, L. Brus, C. E. D. Chidsey, S. Creager, C. Creutz, C. R. Kagan, P. V. Kamat, M. Lieberman, S. Lindsay, R. A. Marcus, R. M. Metzger, M. E. Michel-Beyerle, J. R. Miller, M. D. Newton, D. R. Rolison, O. Sankey, K. S. Schanze, J. Yardley, X. Zhu, *J. Phys. Chem. B* **2003**, *107*, 6668 – 6697.
[152] S. Barlow, C. Risko, S.-J. Chung, N. M. Tucker, V. Coropceanu, S. C. Jones, Z. Levi, J.-L. Brédas, S. R. Marder, *J. Am. Chem. Soc.* **2005**, *127*, 16900 – 16911.
[153] G. L. Closs, M. D. Johnson, J. R. Miller, P. Piotrowiak, *J. Am. Chem. Soc.* **1989**, *111*, 3751 – 3753.
[154] M. J. Shephard, M. N. Paddon-Row, K. D. Jordan, *Chem. Phys.* **1993**, *176*, 289 – 304.
[155] S. F. Nelsen, R. F. Ismagilov, D. R. Powell, *J. Am. Chem. Soc.* **1996**, *118*, 6313 – 6314.
[156] P. J. Low, M. A. J. Paterson, D. S. Yufit, J. A. K. Howard, J. C. Cherryman, D. R. Tackley, R. Brook, B. Brown, *J. Mater. Chem.* **2005**, *15*, 2304 – 2315.
[157] Here we stress that splitting of redox potentials can at best be used as a qualitative measure for the electronic coupling, for reasons discussed in Refs. [79,165,166] and F. Barrière, W. E. Geiger, *J. Am. Chem. Soc.* **2006**, *128*, 3980 – 3989.
[158] S. Barlow, C. Risko, V. Coropceanu, N. M. Tucker, S. C. Jones, Z. Levi, V. N. Khrustalev, M. Y. Antipin, T. L. Kinnibrugh, T. Timofeeva, S. R. Marder, J. L. Brédas, *Chem. Commun.* **2005**, 764 – 766.
[159] "Radical Ions: Generation, Characterization and Reactions": J. Gebicki, A. Marcinek in *General Aspects of the Chemistry of Radicals* (Ed.: Z. B. Alfassi), Wiley, New York, **1999**.
[160] J. P. Snyder, M. Heyman, M. Gundestrup, *J. Org. Chem.* **1978**, *43*, 2224 – 2231.
[161] S. F. Nelsen, J. J. Wolff, H. Chang, D. R. Powell, *J. Am. Chem. Soc.* **1991**, *113*, 7882 – 7886.
[162] S. F. Nelsen, D. A. Trieber II, J. J. Wolff, D. R. Powell, S. Rogers-Crowley, *J. Am. Chem. Soc.* **1997**, *119*, 6873 – 6882.
[163] D. Rehm, A. Weller, *Z. Phys. Chem.* **1970**, *69*, 183 – 200.
[164] J. B. Flanagan, S. Margel, A. J. Bard, F. C. Anson, *J. Am. Chem. Soc.* **1978**, *100*, 4248 – 4253.
[165] F. Barrière, N. Camire, W. E. Geiger, U. T. Mueller-Westerhoff, R. Sanders, *J. Am. Chem. Soc.* **2002**, *124*, 7262 – 7263.
[166] J. E. Sutton, H. Taube, *Inorg. Chem.* **1981**, *20*, 3125 – 3134.
[167] G. L. Closs, L. T. Calcaterra, N. J. Green, K. W. Penfield, J. R. Miller, *J. Phys. Chem.* **1986**, *90*, 3673 – 3683.
[168] M. D. Johnson, J. R. Miller, N. J. Green, G. L. Closs, *J. Phys. Chem.* **1989**, *93*, 1173 – 1176.
[169] J. F. Smalley, H. O. Finklea, C. E. D. Chidsey, M. R. Linford, S. E. Creager, J. P. Ferraris, K. Chalfant, T. Zawodzinsk, S. W. Feldberg, M. D. Newton, *J. Am. Chem. Soc.* **2003**, *125*, 2004 – 2013.
[170] E. A. Weiss, M. J. Ahrens, L. E. Sinks, A. V. Gusev, M. A. Ratner, M. R. Wasielewski, *J. Am. Chem. Soc.* **2004**, *126*, 5577 – 5584.
[171] R. D. Williams, J. T. Hupp, M. T. Ramm, S. F. Nelsen, *J. Phys. Chem. A* **1999**, *103*, 11172 – 11180.
[172] S. F. Nelsen, J. Adamus, J. J. Wolff, *J. Am. Chem. Soc.* **1994**, *116*, 1589 – 1590.
[173] S. F. Nelsen, R. F. Ismagilov, D. R. Powell, *J. Am. Chem. Soc.* **1998**, *120*, 1924 – 1925.
[174] S. F. Nelsen, R. F. Ismagilov, K. E. Gentile, D. R. Powell, *J. Am. Chem. Soc.* **1999**, *121*, 7108 – 7114.
[175] B. Ferrer, H. Garcia, K. P. Schultz, S. F. Nelsen, *J. Phys. Chem. B* **2007**, *111*, 13967 – 13970.
[176] S. F. Nelsen, A. E. Konradsson, Y. Teki, *J. Am. Chem. Soc.* **2006**, *128*, 2902 – 2910.
[177] S. F. Nelsen, K. P. Schultz, *J. Phys. Chem. A* **2009**, *113*, 5324 – 5332.
[178] S. F. Nelsen, K. P. Schultz, *J. Phys. Chem. A* **2009**, *113*, 5577 – 5584.
[179] The cryptand used is 4,7,13,16,21,24-hexaoxa-1,10-diazabicyclo[8.8.8]hexacosane.
[180] H. Hosoi, Y. Mori, Y. Masuda, *Chem. Lett.* **1998**, 177 – 178.
[181] S. F. Nelsen, M. N. Weaver, A. E. Konradsson, J. P. Telo, T. Clark, *J. Am. Chem. Soc.* **2004**, *126*, 15431 – 15438.
[182] S. F. Nelsen, A. E. Konradsson, M. N. Weaver, J. P. Telo, *J. Am. Chem. Soc.* **2003**, *125*, 12493 – 12501.
[183] S. F. Nelsen, M. N. Weaver, J. I. Zink, J. P. Telo, *J. Am. Chem. Soc.* **2005**, *127*, 10611 – 10622.
[184] The actual twist of the radical anion is not known and might be smaller than in the neutral biaryl compound as a result of some quinoidal character.
[185] S. F. Nelsen, M. N. Weaver, J. P. Telo, *J. Am. Chem. Soc.* **2007**, *129*, 7036 – 7043.
[186] J. P. Telo, S. F. Nelsen, Y. Zhao, *J. Phys. Chem. A* **2009**, *113*, 7730 – 7736.
[187] E. T. Seo, R. F. Nelson, J. M. Fritsch, L. S. Marcoux, D. W. Leedy, R. N. Adams, *J. Am. Chem. Soc.* **1966**, *88*, 3498 – 3503.
[188] L. Hagopian, G. Kohler, R. I. Walter, *J. Phys. Chem.* **1967**, *71*, 2290 – 2296.
[189] S. Dapperheld, E. Steckhan, K.-H. G. Brinkhaus, T. Esch, *Chem. Ber.* **1991**, *124*, 2557 – 2567.
[190] H. B. Goodbrand, N. X. Hu, *J. Org. Chem.* **1999**, *64*, 670 – 674.
[191] K. Lancaster, S. A. Odom, S. C. Jones, S. Thayumanavan, S. R. Marder, J.-L. Brédas, V. Coropceanu, S. Barlow, *J. Am. Chem. Soc.* **2009**, *131*, 1717 – 1723.
[192] S. V. Rosokha, D. L. Sun, J. K. Kochi, *J. Phys. Chem. A* **2002**, *106*, 2283 – 2292.
[193] A. Heckmann, C. Lambert, S. Amthor, *Chem. Commun.* **2006**, 2959 – 2961.
[194] C. Lambert, G. Nöll, *J. Chem. Soc. Perkin Trans. 2* **2002**, 2039 – 2043.
[195] G. Nöll, M. Avola, M. Lynch, J. Daub, *J. Phys. Chem. C* **2007**, *111*, 3197 – 3204.

[196] G. Nöll, S. Amthor, M. Avola, C. Lambert, J. Daub, *J. Phys. Chem. C* **2007**, *111*, 3512 – 3516.
[197] I. Tabakovic, Y. Kunugi, A. Canavesi, L. L. Miller, *Acta Chem. Scand.* **1998**, *52*, 131 – 136.
[198] G. Zhou, M. Baumgarten, K. Muellen, *J. Am. Chem. Soc.* **2007**, *129*, 12211 – 12221.
[199] S. C. Jones, V. Coropceanu, S. Barlow, T. Kinnibrugh, T. Timofeeva, J.-L. Brédas, S. R. Marder, *J. Am. Chem. Soc.* **2004**, *126*, 11782 – 11783.
[200] R. Sakamoto, S. Kume, H. Nishihara, *Chem. Eur. J.* **2008**, *14*, 6978 – 6986.
[201] P. J. Low, M. A. J. Paterson, A. E. Goeta, D. S. Yufit, J. A. K. Howard, J. C. Cherryman, D. R. Tackley, B. Brown, *J. Mater. Chem.* **2004**, *14*, 2516 – 2523.
[202] It is important to distinguish the reorganization energies for an intramolecular charge transfer within a bis(triarylamine)radical cation and the intermolecular charge transfer between a bis(triarylamine)radical cation and a neutral bis(triarylamine). For the intramolecular process, the reorganization energy refers to the energy difference associated with structural changes of charged versus neutral triarylamine moieties of the diabatic (=localized) states, while for the intermolecular process it refers to the analogous energy difference, but of the whole bis(triarylamine)system.
[203] M. Yano, Y. Ishida, K. Aoyama, M. Tatsumi, K. Sato, D. Shiomi, A. Ichimura, T. Takui, *Synth. Met.* **2003**, *137*, 1275 – 1276.
[204] K. Y. Chiu, T. H. Su, C. W. Huang, G. S. Liou, S. H. Cheng, *J. Electroanal. Chem.* **2005**, *578*, 283 – 287.
[205] M. Yano, K. Sato, D. Shiomi, A. Ichimura, K. Abe, T. Takui, K. Itoh, *Tetrahedron Lett.* **1996**, *37*, 9207 – 9210.
[206] K. Sato, M. Yano, M. Furuichi, D. Shiomi, T. Takui, K. Abe, K. Itoh, A. Higuchi, K. Katsuma, Y. Shirota, *J. Am. Chem. Soc.* **1997**, *119*, 6607 – 6613.
[207] M. J. Plater, T. Jackson, *J. Chem. Soc. Perkin Trans. 1* **2001**, 2548 – 2552.
[208] G. Nöll, M. Avola, *J. Phys. Org. Chem.* **2006**, *19*, 238 – 241.
[209] C. Lambert, G. Nöll, V. Kriegisch, M. Zabel, F. Hampel, E. Schmälzlin, C. Bräuchle, K. Meerholz, *Chem. Eur. J.* **2003**, *9*, 4232 – 4239.
[210] A. Ito, M. Urabe, K. Tanaka, *Angew. Chem.* **2003**, *115*, 951 – 954; *Angew. Chem. Int. Ed.* **2003**, *42*, 921 – 924.
[211] Y. Hirao, M. Urabe, A. Ito, K. Tanaka, *Angew. Chem.* **2007**, *119*, 3364 – 3367; *Angew. Chem. Int. Ed.* **2007**, *46*, 3300 – 3303.
[212] S. A. Odom, K. Lancaster, L. Beverina, K. M. Lefler, N. J. Thompson, V. Coropceanu, J. L. Brédas, S. R. Marder, S. Barlow, *Chem. Eur. J.* **2007**, *13*, 9637 – 9646.
[213] J. C. Lacroix, K. I. Chane-Ching, F. Maquere, F. Maurel, *J. Am. Chem. Soc.* **2006**, *128*, 7264 – 7276.
[214] J. L. Brédas, G. B. Street, *Acc. Chem. Res.* **1985**, *18*, 309 – 315.
[215] D. Sun, S. V. Rosokha, J. K. Kochi, *J. Am. Chem. Soc.* **2004**, *126*, 1388 – 1401.
[216] M. Holzapfel, C. Lambert, C. Selinka, D. Stalke, *J. Chem. Soc. Perkin Trans. 2* **2002**, 1553 – 1561.
[217] C. Risko, V. Coropceanu, S. Barlow, V. Geskin, K. Schmidt, N. E. Gruhn, S. R. Marder, J. L. Brédas, *J. Phys. Chem. C* **2008**, *112*, 7959 – 7967.
[218] V. Coropceanu, N. E. Gruhn, S. Barlow, C. Lambert, J. C. Durivage, T. G. Bill, G. Nöll, S. R. Marder, J.-L. Brédas, *J. Am. Chem. Soc.* **2004**, *126*, 2727 – 2731.
[219] S. F. Nelsen, C. R. Kessel, D. J. Brien, *J. Am. Chem. Soc.* **1980**, *102*, 702 – 711.
[220] S. E. Bailey, J. I. Zink, S. F. Nelsen, *J. Am. Chem. Soc.* **2003**, *125*, 5939 – 5947.
[221] S. F. Nelsen, Y. Luo, M. N. Weaver, J. V. Lockard, J. I. Zink, *J. Org. Chem.* **2006**, *71*, 4286 – 4295.
[222] S. F. Nelsen, G. Li, A. Konradsson, *Org. Lett.* **2001**, *3*, 1583 – 1586.
[223] S. F. Nelsen, M. J. R. Yunta, *J. Phys. Org. Chem.* **1994**, *7*, 55 – 62.
[224] A. M. Brouwer, P. G. Wiering, J. M. Zwier, F. W. Langkilde, R. Wilbrandt, *Acta Chem. Scand.* **1997**, *51*, 217 – 219.
[225] A. M. Brouwer, F. W. Langkilde, K. Bajdor, R. Wilbrandt, *Chem. Phys. Lett.* **1994**, *225*, 386 – 390.
[226] S. F. Nelsen, J. A. Thompson-Colon, M. Kaftory, *J. Am. Chem. Soc.* **1989**, *111*, 2809 – 2815.
[227] X. Z. Qin, T. C. Pentecost, J. T. Wang, F. Williams, *J. Chem. Soc. Chem. Commun.* **1987**, 450 – 453.
[228] M. Ballester, J. Riera, J. Castaner, C. Badia, J. M. Monso, *J. Am. Chem. Soc.* **1971**, *93*, 2215 – 2225.
[229] M. Ballester, *Acc. Chem. Res.* **1985**, *18*, 380 – 387.
[230] M. Ballester, *Adv. Phys. Org. Chem.* **1989**, *25*, 267 – 445.
[231] M. Ballester, I. Pascual, C. Carreras, J. Vidalgancedo, *J. Am. Chem. Soc.* **1994**, *116*, 4205 – 4210.
[232] M. Ballester, C. Molinet, J. Castaner, *J. Am. Chem. Soc.* **1960**, *82*, 4254 – 4258.
[233] J. Bonvoisin, J.-P. Launay, C. Rovira, J. Veciana, *Angew. Chem.* **1994**, *106*, 2190 – 2193; *Angew. Chem. Int. Ed.* **1994**, *33*, 2106 – 2109.
[234] V. Lloveras, J. Vidal-Gancedo, D. Ruiz-Molina, T. M. Figueira-Duarte, J.-F. Nierengarten, J. Veciana, C. Rovira, *Faraday Discuss.* **2006**, *131*, 291 – 305.
[235] V. Lloveras, J. Vidal-Gancedo, T. M. Figueira-Duarte, J.-F. Nierengarten, J. J. Novoa, F. Mota, N. Ventosa, C. Rovira, J. Veciana, *J. Am. Chem. Soc.* **2011**, *133*, 5818 – 5833.
[236] D. L. Sun, S. V. Lindeman, R. Rathore, J. K. Kochi, *J. Chem. Soc. Perkin Trans. 2* **2001**, 1585 – 1594.
[237] S. V. Lindeman, S. V. Rosokha, D. L. Sun, J. K. Kochi, *J. Am. Chem. Soc.* **2002**, *124*, 843 – 855.
[238] R. Rathore, A. S. Kumar, S. V. Lindeman, J. K. Kochi, *J. Org. Chem.* **1998**, *63*, 5847 – 5856.
[239] D.-L. Sun, S. V. Rosokha, S. V. Lindeman, J. K. Kochi, *J. Am. Chem. Soc.* **2003**, *125*, 15950 – 15963.
[240] A. R. Wartini, J. Valenzuela, H. A. Staab, F. A. Neugebauer, *Eur. J. Org. Chem.* **1998**, 139 – 148.
[241] A. R. Wartini, J. Valenzuela, H. A. Staab, F. A. Neugebauer, *Eur. J. Org. Chem.* **1998**, 221 – 227.
[242] A. R. Wartini, H. A. Staab, F. A. Neugebauer, *Eur. J. Org. Chem.* **1998**, 1161 – 1170.
[243] S. E. Boesch, R. A. Wheeler, *J. Phys. Chem. A* **1997**, *101*, 8351 – 8359.
[244] J. M. Lü, S. V. Rosokha, I. S. Neretin, J. K. Kochi, *J. Am. Chem. Soc.* **2006**, *128*, 16708 – 16719.
[245] T. H. Jozefiak, J. E. Almlof, M. W. Feyereisen, L. L. Miller, *J. Am. Chem. Soc.* **1989**, *111*, 4105 – 4106.
[246] J. E. Almlöf, M. W. Feyereisen, T. H. Jozefiak, L. L. Miller, *J. Am. Chem. Soc.* **1990**, *112*, 1206 – 1214.
[247] S. F. Rak, T. H. Jozefiak, L. L. Miller, *J. Org. Chem.* **1990**, *55*, 4794 – 4801.
[248] S. F. Rak, L. L. Miller, *J. Am. Chem. Soc.* **1992**, *114*, 1388 – 1394.
[249] We are currently investigating radical anions of differently linked di-perylenebisimides. Although the negative charge is delocalized within a perylenebisimide moiety, it depends on the kind of linkage whether the negative charge is localized or delocalized within a di-perylenebisimide; Z. Wang, F. Negri, H. Ceymann, C. Lambert, unpublished results.
[250] N. Gautier, F. Dumur, V. Lloveras, J. Vidal-Gancedo, J. Veciana, C. Rovira, P. Hudhomme, *Angew. Chem.* **2003**, *115*, 2871 – 2874; *Angew. Chem. Int. Ed.* **2003**, *42*, 2765 – 2768.
[251] S. F. Nelsen, M. N. Weaver, J. P. Telo, *J. Phys. Chem. A* **2007**, *111*, 10993 – 10997.
[252] S. Mazur, C. Streekumar, A. H. Schroeder, *J. Am. Chem. Soc.* **1976**, *98*, 6713 – 6714.
[253] A. H. Schroeder, S. Mazur, *J. Am. Chem. Soc.* **1978**, *100*, 7339 – 7346.
[254] H. Hosoi, Y. Masuda, *J. Mol. Liq.* **2005**, *119*, 89 – 96.

[255] C. Risko, S. Barlow, V. Coropceanu, M. Halik, J. L. Brédas, S. R. Marder, *Chem. Commun.* **2003**, 194 – 195.
[256] K. Lahlil, A. Moradpour, C. Bowlas, F. Menou, P. Cassoux, J. Bonvoisin, J.-P. Launay, G. Dive, D. Dehareng, *J. Am. Chem. Soc.* **1995**, *117*, 9995 – 10002.
[257] E. Aqad, J. Y. Becker, J. Bernstein, A. Ellern, V. Khodorkovsky, L. Shapiro, *J. Chem. Soc. Chem. Commun.* **1994**, 2775 – 2776.
[258] C. Wang, A. Ellern, J. Y. Becker, J. Bernstein, *Tetrahedron Lett.* **1994**, *35*, 8489 – 8492.
[259] C. Wang, A. Ellern, V. Khodorkovsky, J. Y. Becker, J. Bernstein, *J. Chem. Soc. Chem. Commun.* **1994**, 2115 – 2116.
[260] N. Avarvari, M. Fourmigue, *Chem. Commun.* **2004**, 2794 – 2795.
[261] F. Biaso, M. Geoffroy, E. Canadell, P. Auban-Senzier, E. Levillain, M. Fourmigue, N. Avarvari, *Chem. Eur. J.* **2007**, *13*, 5394 – 5400.
[262] H. Li, C. Lambert, *Chem. Eur. J.* **2006**, *12*, 1144 – 1155.
[263] A. Saad, F. Barriere, E. Levillain, N. Vanthuyne, O. Jeannin, M. Fourmigue, *Chem. Eur. J.* **2010**, *16*, 8020 – 8028.
[264] J. M. Spruell, A. Coskun, D. C. Friedman, R. S. Forgan, A. A. Sarjeant, A. Trabolsi, A. C. Fahrenbach, G. Barin, W. F. Paxton, S. K. Dey, M. A. Olson, D. Benitez, E. Tkatchouk, M. T. Colvin, R. Carmielli, S. T. Caldwell, G. M. Rosair, S. G. Hewage, F. Duclairoir, J. L. Seymour, A. M. Z. Slawin, W. A. Goddard, M. R. Wasielewski, G. Cooke, J. F. Stoddart, *Nat. Chem.* **2010**, *2*, 870 – 879.
[265] M. Mayor, M. Büschel, K. M. Fromm, J.-M. Lehn, J. Daub, *Chem. Eur. J.* **2001**, *7*, 1266 – 1272.
[266] W. Kaim, N. S. Hosmane, S. Zalis, J. A. Maguire, W. N. Lipscomb, *Angew. Chem.* **2009**, *121*, 5184 – 5193; *Angew. Chem. Int. Ed.* **2009**, *48*, 5082 – 5091.
[267] J. Fiedler, S. Zalis, A. Klein, F. M. Hornung, W. Kaim, *Inorg. Chem.* **1996**, *35*, 3039 – 3043.
[268] N. Mataga, Y. Kaifu, M. Koizumi, *Bull. Chem. Soc. Jpn.* **1956**, *29*, 465 – 470.
[269] E. Lippert, *Z. Elektrochem.* **1957**, *61*, 962 – 975.
[270] A. Heckmann, S. Dümmler, J. Pauli, M. Margraf, J. Köhler, D. Stich, C. Lambert, I. Fischer, U. Resch-Genger, *J. Phys. Chem. C* **2009**, *113*, 20958 – 20966.
[271] A. Heckmann, C. Lambert, unpublished results.
[272] M. Kaupp, M. Renz, M. Parthey, M. Stolte, F. Würthner, C. Lambert, *Phys. Chem. Chem. Phys.* **2011**, *13*, 16973 – 16986.
[273] R. Maksimenka, M. Margraf, J. Koehler, A. Heckmann, C. Lambert, I. Fischer, *Chem. Phys.* **2008**, *347*, 436 – 445.
[274] S. Nishida, Y. Morita, K. Fakui, K. Sato, D. Shiomi, T. Takui, K. Nakasuji, *Angew. Chem.* **2005**, *117*, 7443 – 7446; *Angew. Chem. Int. Ed.* **2005**, *44*, 7277 – 7280.
[275] J. Bonvoisin, J.-P. Launay, W. Verbouwe, M. Van der Auweraer, F. C. De Schryver, *J. Phys. Chem.* **1996**, *100*, 17079 – 17082.
[276] J. Veciana, C. Rovira, N. Ventosa, M. I. Crespo, F. Palacio, *J. Am. Chem. Soc.* **1993**, *115*, 57 – 64.
[277] J. Sedo, D. Ruiz, J. Vidal-Gancedo, C. Rovira, J. Bonvoisin, J. P. Launay, J. Veciana, *Adv. Mater.* **1996**, *8*, 748 – 752.
[278] J. Sedo, D. Ruiz, J. Vidal-Gancedo, C. Rovira, J. Bonvoisin, J.-P. Launay, J. Veciana, *Synth. Met.* **1997**, *85*, 1651 – 1654.
[279] M. Y. Okamura, R. A. Isaacson, G. Feher, *Biochim. Biophys. Acta Bioenerg.* **1979**, *546*, 394 – 417.
[280] S. F. Nelsen, R. F. Ismagilov, Y. Teki, *J. Am. Chem. Soc.* **1998**, *120*, 2200 – 2201.
[281] A. S. Lukas, P. J. Bushard, E. A. Weiss, M. R. Wasielewski, *J. Am. Chem. Soc.* **2003**, *125*, 3921 – 3930.
[282] E. A. Weiss, M. A. Ratner, M. R. Wasielewski, *J. Phys. Chem. A* **2003**, *107*, 3639 – 3647.
[283] M. Fabre, J. Bonvoisin, *J. Am. Chem. Soc.* **2007**, *129*, 1434 – 1444.
[284] K. R. Stickley, S. C. Blackstock, *J. Am. Chem. Soc.* **1994**, *116*, 11576 – 11577.
[285] P. Rapta, A. Tabet, H. Hartmann, L. Dunsch, *J. Mater. Chem.* **2007**, *17*, 4998 – 5007.
[286] C. Lambert, G. Nöll, E. Schmälzlin, K. Meerholz, C. Bräuchle, *Chem. Eur. J.* **1998**, *4*, 2129 – 2135.
[287] C. Lambert, W. Gaschler, E. Schmälzlin, K. Meerholz, C. Bräuchle, *J. Chem. Soc. Perkin Trans. 2* **1999**, 577 – 588.
[288] C. Lambert, G. Nöll, *Chem. Eur. J.* **2002**, *8*, 3467 – 3477.
[289] D. Sun, S. V. Rosokha, J. K. Kochi, *Angew. Chem.* **2005**, *117*, 5266; *Angew. Chem. Int. Ed.* **2005**, *44*, 5133 – 5136.
[290] S. V. Rosokha, I. S. Neretin, D. L. Sun, J. K. Kochi, *J. Am. Chem. Soc.* **2006**, *128*, 9394 – 9407.
[291] C. Lambert, *Angew. Chem.* **2005**, *117*, 7503 – 7505; *Angew. Chem. Int. Ed.* **2005**, *44*, 7337 – 7339.
[292] R. Rathore, C. L. Burns, M. I. Deselnicu, *Org. Lett.* **2001**, *3*, 2887 – 2890.
[293] R. Rathore, C. L. Burns, S. A. Abdelwahed, *Org. Lett.* **2004**, *6*, 1689 – 1692.
[294] C. Lambert, G. Nöll, F. Hampel, *J. Phys. Chem. A* **2001**, *105*, 7751 – 7758.
[295] C. Lambert, *ChemPhysChem* **2003**, *4*, 877 – 880.
[296] S. I. Hauck, K. V. Lakshmi, J. F. Hartwig, *Org. Lett.* **1999**, *1*, 2057 – 2060.
[297] A. Ito, Y. Ono, K. Tanaka, *Angew. Chem.* **2000**, *112*, 1114 – 1117; *Angew. Chem. Int. Ed.* **2000**, *39*, 1072 – 1075.
[298] T. D. Selby, S. C. Blackstock, *Org. Lett.* **1999**, *1*, 2053 – 2055.
[299] X. Z. Yan, J. Pawlas, T. Goodson III, J. F. Hartwig, *J. Am. Chem. Soc.* **2005**, *127*, 9105 – 9116.
[300] M. Green, *Chem. Ind.* **1996**, 641 – 644.
[301] R. J. Mortimer, *Electrochim. Acta* **1999**, *44*, 2971 – 2981.
[302] D. R. Rosseinsky, R. J. Mortimer, *Adv. Mater.* **2001**, *13*, 783 – 793.
[303] http://www.gentex.com.
[304] C. Lambert, G. Nöll, *Synth. Met.* **2003**, *139*, 57 – 62.
[305] Y. Nishikitani, M. Kobayashi, S. Uchida, T. Kubo, *Electrochim. Acta* **2001**, *46*, 2045 – 2040.
[306] M. Y. Chou, M. K. Leung, Y. L. O. Su, C. L. Chiang, C. C. Lin, J. H. Liu, C. K. Kuo, C. Y. Mou, *Chem. Mater.* **2004**, *16*, 654 – 661.
[307] J.-L. Brédas, D. Beljonne, V. Coropceanu, J. Cornil, *Chem. Rev.* **2004**, *104*, 4971 – 5003.
[308] V. Coropceanu, J. Cornil, D. A. da Silva, Y. Olivier, R. Silbey, J. L. Brédas, *Chem. Rev.* **2007**, *107*, 926 – 952.
[309] M. Thelakkat, *Macromol. Mater. Eng.* **2002**, *287*, 442 – 461.
[310] M. Jaiswal, R. Menon, *Polym. Int.* **2006**, *55*, 1371 – 1384.
[311] A. Petr, C. Kvarnström, L. Dunsch, A. Ivaska, *Synth. Met.* **2000**, *108*, 245 – 247.
[312] M. Ishikawa, M. Kawai, Y. Ohsawa, *Synth. Met.* **1991**, *40*, 231 – 238.
[313] H. Li, C. Lambert, R. Stahl, *Macromolecules* **2006**, *39*, 2049 – 2055.
[314] H. Li, C. Lambert, *J. Mater. Chem.* **2005**, *15*, 1235 – 1237.
[315] D. Reitzenstein, T. Quast, F. Kanal, M. Kullmann, S. Ruetzel, M. S. Hammer, C. Deibel, V. Dyakonov, T. Brixner, C. Lambert, *Chem. Mater.* **2010**, *22*, 6641 – 6655.
[316] J. Casado, K. Takimiya, T. Otsubo, F. J. Ramirez, J. J. Quirante, R. P. Ortiz, S. R. Gonzalez, M. M. Oliva, J. T. L. Navarrete, *J. Am. Chem. Soc.* **2008**, *130*, 14028 – 14029.
[317] G. Saito, T. Murata, *Philos. Trans. R. Soc. London Ser. A* **2008**, *366*, 139 – 150.
[318] See *Chem. Rev.* **2004**, *104*(11), 4887 – 5782.
[319] G. Saito, Y. Yoshida, *Bull. Chem. Soc. Jpn.* **2007**, *80*, 1 – 137.
[320] E. Gomar-Nadal, L. Mugica, J. Vidal-Gancedo, J. Casado, J. T. L. Navarrete, J. Veciana, C. Rovira, D. B. Amabilino, *Macromolecules* **2007**, *40*, 7521 – 7531.
[321] X. J. Wang, L. B. Xing, W. N. Cao, X. B. Li, B. Chen, C. H. Tung, L. Z. Wu, *Langmuir* **2011**, *27*, 774 – 781.

[322] R. C. Haddon, S. V. Chichester, J. H. Marshall, *Tetrahedron* **1986**, *42*, 6293 – 6300.
[323] S. K. Mandal, M. E. Itkis, X. L. Chi, S. Samanta, D. Lidsky, R. W. Reed, R. T. Oakley, F. S. Tham, R. C. Haddon, *J. Am. Chem. Soc.* **2005**, *127*, 8185 – 8196.
[324] X. Chi, M. E. Itkis, B. O. Patrick, T. M. Barclay, R. W. Reed, R. T. Oakley, A. W. Cordes, R. C. Haddon, *J. Am. Chem. Soc.* **1999**, *121*, 10395 – 10402.
[325] M. E. Itkis, X. Chi, A. W. Cordes, R. C. Haddon, *Science* **2002**, *296*, 1443 – 1445.
[326] While this manuscript was in press, a review dealing with organic MV compounds appeared in: J. Hankache, O. S. Wenger, *Chem. Rev.* **2011**, *111*, 5138 – 5178.

